National Prosperity and the Engineer

The Presidential Address of
Colonel G. W. RABY, C.B.E., M.I.Mech.E., M.I.E.R.E.

Delivered after the Annual General Meeting of the Institution on Wednesday, 9th December 1964

During our Annual General Meeting tonight, a statement was made that annual reports are a record of the administration of the Council of the Institution during the past year. Such reports are, in fact, designed to give members an opportunity to express agreement, or otherwise, with the decisions and actions of the Council during the year under review. This has led me to wonder whether the President of a learned Institution should not give an account of his stewardship at the end of his term of office, rather than a Presidential Address at the beginning.

Of course, one reason for the initial Presidential Address may well be that, having elected the President, members wish to know—indeed, they have a right to know as quickly as possible—how he is likely to influence the future policies of the Institution during his term of office.

I propose tonight, therefore, to indicate some of the more important policies which, in my view, will best serve both the national interest and the interest of this Institution. And I hope they will also meet with the approval of my colleagues on the Council and our members.

First let us consider our work and obligations as a Chartered Institution. For example, in the hard light of modern developments, are we as an Institution sufficiently realistic in our forward planning to take account of the 'winds of change' in international affairs and world economics?

Are we as an Institution doing enough to ensure the continuing development of our art by attracting the right kind of young men and women to our profession?

Are we, in the electronics field, content with the efforts we are making in our relatively small field of engineering activity?

Ought we not to be giving more assistance to others in the expansion and exploitation of developments in the broader fields of scientific research and technology?

I believe that our ultimate answers to those questions will largely determine the future for the electronic engineer and indeed the future prosperity of the electronics industry.

Working Together

It is a condition of a country's prosperity in these days that there must be wide blending of the skills of the people. And since the prosperity of the world, and particularly of our own country, affects our individual well-being, we surely cannot be content to confine our skills and knowledge to relatively small fields of activity. I believe we must, as an Institution, contribute to, and profit by, a wide blending of our national skills.

This is particularly so in the engineering profession as a whole, for the technologist who today works in isolation is largely an anachronism. In these days, scientists, engineers, chemists and metallurgists must work in combination, firstly to understand and analyse the problems, and secondly to fit the solution into the complex network of most modern-day requirements. And it surely must follow that learned Institutions such as ours cannot indefinitely hold aloof from the concept of 'team work with a wide blending

of skills'. I submit that we must not allow ourselves to drift into a policy of isolation.

Recently I heard an eminent metallurgist refer to a field of engineering which he called 'Materials Engineering'. When asked to explain he said that the metallurgist and the chemist could, and did, develop new materials when they knew the requirements, but without the engineer's close co-operation and understanding of these new materials, they would neither be used correctly nor exploited for use in wider fields.

The truth of this view can be assessed by remembering the advances made over the past ten years in the co-operative development and exploitation of both new and improved materials, such as piezo-electric, ferro-electric, magneto-strictive and magnetic materials; also microwave ferrites and associated components, semiconductor materials and, of course, entirely new materials for use in high temperature environments. These important developments and their subsequent exploitation have been possible by the 'wide blending of skills' and not so much by the brilliance of isolated technologists. Nor for that matter by the efforts of any one learned Institution.

Co-operation and collaboration between Chartered Engineering Institutions in this country is an ideal means (and I stress the word 'ideal') for securing this 'wide blending of skills' on a national scale, and, in fact, such a co-operation could play a vital role in ensuring that developments and progress in any one branch of technology can quickly be used and exploited by others. So often we start new ideas but others beat us to the development and exploitation of them.

As one of the Institution's representatives on the Council of Engineering Institutions (formerly the E.I.J.C.) I recommended that the Council should sponsor a Convention which would appeal to all branches of engineers. The purpose underlying this proposal was threefold.

First, it is only by knowing precisely what the other fellow wants, and why, that one's own skill can be employed to mutual advantage.

Second, only by demonstrating the possibility of a wide blending of skills on a national scale will close co-operation between qualified engineers and scientists be automatically encouraged on a national scale.

Third, the wholehearted co-operation and co-ordination at technical levels will be seen by the younger generation as a visible sign of the unity of the engineering profession as a whole, and will stimulate in them the excitement and attraction of joining what must be the largest creative industry in the world. It will also help to convince them that to become a professional engineer will provide not only a worthwhile career, but enable them to make an essential contribution to the well-being, the progress, and even the preservation of mankind.

The invaluable contribution made by the engineering industry as a whole to the national economy is undisputed. It is nevertheless a disturbing fact that throughout the country, and indeed throughout the world, there is a shortage of qualified men. Whilst I do not lay the blame entirely at the doors of the professional Institutions, few will dispute the need for all learned Institutions to take more active steps in securing recruits to the profession. They must also exercise their influence in ensuring that standards of training are suitable not only for professional status, but in accordance with increasing standards of knowledge demanded by modern technological progress.

It is, of course, an unfortunate fact that the Chartered Engineering Institutions are not wholly representative of all the qualified engineers in Great Britain, but according to figures produced by the Council of Engineering Institutions, the joint Corporate Membership of the thirteen Chartered Engineering Institutions is less than 130,000—and this includes members outside Great Britain!

I will not digress to discuss the desirability or otherwise of compulsory registration of professional engineers, other than to comment that insufficient statistics make it extremely difficult to plan for the future and enable our hard pressed universities and technical colleges to indicate to the younger generation the particular fields wherein the demand for their services is likely to be greatest in the future.

The significant point is this. The membership of all the Chartered Engineering Institutions in Great Britain of 130,000 is disconcertingly low when one remembers that the total working population of this country is 25 millions, and that the entire population of some 56 millions very largely depends upon technological progress in the engineering fields to maintain our standard of living at home, and to develop a healthy export business overseas. The awful truth is that even if we double the figure of 130,000 to include qualified engineers who are not members of a learned Institution—and I think this is a gross overestimate—then it means that we have in this country less than 260,000 qualified engineers to sustain a population of 56 millions! It also means that every qualified engineer in Great Britain carries a direct burden and responsibility for the well being of no fewer than 200 others of his countrymen, every day he goes to work!

And then we express surprise that the annual growth rate of our national economy is falling short of the predicted 4%.

But it will be of no use for the Council of Engineering Institutions to consider this national problem only in terms of Chartered Engineers. What it must surely

do is to look at the country's entire technological manpower requirements. Prosperity can only be won if the engineering technologists and engineering leaders are of the right calibre and are adequately supported by first-rate technicians and craftsmen. Clearly, we ought to be giving far more attention to technicians and craftsmen generally.

In our own Institution we have given a considerable lead in the production of first-rate technicians and craftsmen as a supporting force for the electronic engineers by creating a national examining body known as the Radio Trades Examination Board, and by encouraging the formation of a Society for technicians engaged in radio and electronic work. All engineers must welcome the foundation of the Engineering Industry Training Board. Let us be prepared to give that Board our support and, if required, our help through the Council of Engineering Institutions.

The Council of Engineering Institutions is the body which could promote the desired co-operation between Chartered Institutions so that some of the problems I have mentioned may be tackled from the national viewpoint. Indeed I thought that was the prime purpose behind its formation, although I regret to say that we have not seen much of it to date.

I feel that if the Council of Engineering Institutions does not soon put itself in a position to undertake the vital roles for which it was created, it will merely become another overhead expense for each individual member to bear, and any such additional financial burden for little or no return would certainly not be acceptable to this Institution.

I make a plea therefore for the Council of Engineering Institutions to show a much more determined and positive attitude toward the problem of how best to serve the engineering profession as a whole, and to take immediate action to convince all Chartered Engineers of the need for such a national engineering organization.

I truly believe that if our Chartered Institutions in the engineering profession as a whole fail to co-operate in the exploitation of technical advances made in Great Britain and elsewhere, then we will have failed to fulfil our purpose in life, and have failed to provide a satisfactory future for the generations of engineers to come.

Incidentally, another matter with which the Council of Engineering Institutions should deal is amply set out in this extract from the September issue of our *Journal*. I quote—slightly paraphrased—

"Although there are numerous channels for the international exchange of information and opinion, the engineer does not seem to play such an active role at international meetings in comparison with members of other professions. It is true that increasing numbers of engineers travel abroad, but in the main their journeys are for prescribed purposes only, with little time available for gaining understanding of other ways of living or even to have discussions with overseas members of the same profession. Shortage of qualified staff is often advanced as a reason for cutting down the time of engineers' trips to a minimum, with the result that he misses the opportunity of expanding his knowledge and understanding of matters essential for expansion of trade, and even for ultimate managerial responsibility."

In other words, we have too few engineers who can spare the time to play their full part in cultivating international understanding and goodwill. Considering the enormous amount of money and effort engineers have spent on developing communications, faster travel, computer aids, and many other devices to ease the daily burden of others, it is indeed an ominous sign when the same engineers allow themselves to get caught in a rat-race as a direct result of their own ingenuity!

The fact is that it would not add more than a day or two to an overseas trip if engineers were to give a little time to meet other engineers in the country they are visiting. I have been asked by a Government body to draw attention to the fact that a great deal of help is willingly given by the Scientific Attachés of the Embassies and High Commissioners' Offices in effecting introductions. In fact the British Council was set up in order to promote meetings between the representatives of various countries. The trouble is that the average engineer, or his employer, either does not know of these facilities, or pretends there is not the time to take advantage of them. How can we expand our export trade in such a combination of adverse circumstances?

I would like to see the Council of Engineering Institutions do positive work in this connection; it should have a staff officer whose job would be to encourage all Chartered Engineers to advise him of a forthcoming overseas visit and for him to contact the relevant bodies of those countries. Nor should such introductions be confined to members working in the same field of specialization. I have already referred to the need for cross-fertilization of ideas between the various specializations in the engineering industry. In the underdeveloped countries especially, this is of particular importance and I submit that this is a very real and positive action which the Council of Engineering Institutions can take in promoting co-operation between all engineers in all countries. I certainly expect this to be one of the functions of the C.E.I. for how else in Britain can we expect to open up new

ideas and new markets abroad ahead of other export-ing nations?

Our own Institution has offices in India and Canada and intends to reconstruct its membership activities in Commonwealth countries through the establishment of Divisions which will not only give autonomy to each Division, but will also strengthen the Institution as an international body for profes-sional radio and electronic engineers. We are adopting this course because we believe that we must play our part in the Commonwealth and elsewhere in the world on a two-way basis if we are to keep our Institution and our members abreast of world-wide requirements and developments in the future.

Whilst this may be regarded as a pilot plan for the future development of the Institution outside Great Britain, I firmly believe that such a scheme should be developed on a wider basis and in co-operation with other Institutions. In many countries of the Com-monwealth industrial development is limited and as you will know the number of qualified engineers, and engineers under training, is small indeed.

But are our Engineering Institutions to work in isolation abroad and thereby weaken the aid we can give toward Commonwealth co-operation? Surely, if for some outmoded or obscure reasons, Chartered Institutions cannot, or will not, get closer together at home then for heaven's sake let us at least show a national unity of purpose overseas, especially in the Commonwealth.

Let no one under-estimate the danger of technolo-gical isolation in these modern times, for Great Britain is a small island with few natural resources; we have only the products of our heads and our hands to rely upon and sell. We must expand our overseas trade, and we can only do that by supplying what is required ahead of all others. It is in this context that I believe our Chartered Engineering Institutions could and should play a vital role by stimulating a more aggressive policy of industrial research and development.

I believe the only way we in this country can hold our own in world progress in the future is to co-ordinate all our skills to match the formidable con-centration of skills in other competitive countries, such as the United States, Russia, Germany and Japan.

Our national prosperity depends heavily upon the professional engineer and his supporters. Let us see to it that they do not have to work in isolation but in a full and enthusiastic combination of all our national skills.

But I must emphasize, here, that in making this very strong plea for co-operation, I am not advocating the surrender of the Charter sovereignty of this or any other Institution. Our own Charter was earned because we were able successfully to demonstrate to Britain and the Commonwealth the importance of the contribution which can be made to the common good by engineers trained and specializing in radio and electronics. The same philosophy must apply to other Chartered Institutions.

We can make, and we are anxious to make, a valuable contribution to the Council of Engineering Institutions and help that Council to become a strong co-ordinating force in bringing the thirteen Institu-tions closer together. A great deal of collaboration already exists, and I am particularly pleased to refer to and pay tribute to the very close working arrange-ments which now exist between our Institution and the Institution of Electrical Engineers. In the last few years we have fully co-operated with each other in promoting meetings and symposia of interest to the joint memberships, and we look forward to the Council of Engineering Institutions promoting similar cross-fertilization of ideas between all the Engineering Institutions in Great Britain.

The International Role of the Radio and Electronic Engineer

It is our task as an Institution to ensure that we promote co-operation between radio and electronic engineers throughout the world—and particularly throughout the Commonwealth. In order to succeed in this task we must be sure of being able to make a worthwhile British contribution on a very wide range of technical matters.

Through the British Standards Institution we promulgate British views on standardization and I think that we ought to do more to promote the British views on standardization at international meetings; it is a field which calls for an increasing measure of international co-operation and under-standing.

And then, of course, we must be sure to make known throughout the world our achievements not only in research, but also in technology, and in the field of radio and electronics our own *Journal* is a very sub-stantial medium. You may be surprised to know that it circulates to over ninety countries, and the circulation is growing year by year; proof indeed of its influence and impact abroad.

But to sustain that huge demand requires at least the maintenance of the present high standard of the *Journal*. This in turn is dependent upon the help that is given by the individual member, and I want to use this opportunity to urge our members to do more in their contributions to the *Journal*, and also to the *Proceedings* of the Institution.

International co-operation is a very live issue in my own particular field of nuclear energy. We are, as yet, only on the fringe of harnessing atomic energy for the benefit of man. This very modern development is entirely dependent upon co-ordinating the efforts of all branches of engineering—civil, mechanical, chemical, electrical, electronics, and many other skills. Indeed, the building of the very first atomic power stations in Great Britain (Calder Hall and Chapel Cross) was to me an outstanding example of the team-work and wide blending of skills I have emphasized tonight.

The nuclear energy programme has not only been an example of the value of the blending of skills, but has also created a valuable feed-back to the electronics industry. The construction of atomic power stations at home and abroad has created a demand for new instruments and entirely new systems of instrumentation, which understandably could only be produced by the highly qualified electronic engineer.

Research Planning

The wide blending of skills I have mentioned starts, of course, with research. Our Institution has for very many years advocated greater collaboration between the research scientist and the engineer, but in practical terms, and on the larger scale, this requires a getting together of government interests, university activities, and industrial requirements, for it is only in one combination or another that it will be possible to translate original ideas into hardware. And it is only by selling hardware overseas that we will expand our exports and maintain our standard of living.

In the combination of all those interests (government, universities and industry) lies the potential impact and effectiveness of the National Electronics Research Council.

This imaginative concept of our Charter President, Lord Mountbatten, actually encourages team work and planning at the highest levels, so that engineers and scientists in government service, universities and industry, can now be brought together, if necessary on a massive scale, not only to promote research, but also to ensure frequent examination of security embargoes, thereby enabling industry to use, in advance of overseas competitors, the manufacturing ideas and techniques which have been developed in secrecy.

We badly need the imagination and drive which fostered N.E.R.C. in securing co-ordination between our Institutions, educational authorities and the Government, for we must seize upon every opportunity to improve the status of the engineering profession as a whole. In this respect we compare rather poorly with other professions, such as medicine, accountancy, and law.

Rationalization of Manufacturing Processes

The complexity of modern industry requires managerial ability to weld together associated skills. Automation has become a magic word. But technological co-operation, and rationalization of manufacturing techniques play just as important a part as the introduction of new machines. The application of new techniques and rationalization of productive effort are essential if we are, in fact, to afford shorter hours with increased pay. The part that the engineer has to play in this modernization of industry is enormous—and it will grow.

Possession of technical knowledge is increasingly required in the management of industry. Many engineers are, of course, content with the intellectual demands of doing a purely technical job. There must, however, be at least an equal number of engineers who could well deploy their skill and ability in management. They do, of course, require training over and above the requirements of a Chartered Engineer, and I suggest that the training or retraining of engineers for top management might well be a subject which the Council of Engineering Institutions should consider.

Let us therefore see whether the thirteen Chartered Engineering Institutions in Great Britain can, as a whole, make an effective contribution towards national, and indeed, international prosperity. Remember that we are all professional engineers, and that it is our job to convert the ideas of scientists and research workers into hardware which is of benefit to others.

Merely to be able to use the initials of an Institution to indicate personal achievement is not enough. We must work together and so conduct ourselves that people may know that an engineer, whatever his speciality, is as important to the community as the family doctor in the field of medicine. In fact engineers, by their combined efforts, can do a great deal to help to heal the illness which besets the world, through poverty and ignorance.

In conclusion may I say that this Institution has been fortunate in its choice of the past seventeen Presidents. Each in his way has given leadership. Our first Presidents were key figures in helping to establish the radio industry, out of which the whole business of electronics was developed. Subsequent Presidents were prominent in the development of new techniques such as radar, and the occupant of the first Chair of Electronics in a British University was another Past President.

I have already referred to the current work of our Charter President in the field of electronic research. In this, and in countless other ways, Lord

Mountbatten has made a major contribution to the development of our profession and our Institution.

My immediate predecessor, Mr. Thompson, brought to the office of President the benefits of his own successful career which has been entirely spent in the radio and electronics industry, and we shall remember him particularly for the time and help that he has given to promoting collaboration between the Institutions which has now led to the formation of the Council of Engineering Institutions. Moreover, many of the ideas he advanced in his Presidential Address regarding the role of the technician as a supporting force have since been adopted.

Living up to the contributions which have been made by all these eminent personalities will indeed be a difficult task, for as our technology advances and the Institution grows, so do the problems.

I am grateful for the honour accorded me by the election to this high office, thereby giving me the opportunity to repay some of the benefits and advantages I have enjoyed in my life as an engineer.

One final point. You and I and all our fellow professional engineers must contribute to the national prosperity, especially now when our economy needs all the strength and vitality we can give it. We can do so by harnessing our joint efforts and so create a dynamic driving force for our modern society.

Let us see to it that we are not found wanting, in national pride, in determination, in ideas—and above all—in our ideals.

(Address No. 35)

A Transistorized Rocket-borne Proton Magnetometer and associated Data Processing Equipment

By

K. BURROWS, Ph.D., M.Sc.

(*Associate Member*)†

Summary: The design and construction of a complete system for the accurate determination of the earth's magnetic field in a rocket vehicle are described. The flight equipment utilizes the principle of proton-free precession to produce a frequency analogue of the intensity of the geomagnetic field; this frequency is independent of the attitude of the rocket. Some special features of the instrument which are necessary to make it perform satisfactorily in the severe environmental conditions of a rocket flight are discussed in detail. During play-back of the telemetered and recorded precession signals the ground equipment described improves the quality of the data and converts them to a form more suitable for analysis and interpretation.

The results of the first instrument-proving flight are presented and briefly discussed.

1. Introduction

In a previous paper‡ the design of a prototype valve/transistor rocket-borne magnetometer using the principle of proton-free precession was described. The purpose of the present paper is to discuss a completely transistorized version of the previous rocket instrument together with its associated ground equipment for post-flight data processing. Since the new instrument is based on the same principle as the original prototype, only those design features which constitute a significant change will be discussed in detail. It will be assumed that the reader is familiar with the general geophysical and instrumental considerations which were discussed in the previous paper.

2. The Rocket Magnetometer

2.1. *The Sensing Head*

A cross-section through the sensing head is shown in Fig. 1. The coil consists of 1500 turns of 20 s.w.g. Simgold 'M' (high temperature) enamelled copper wire; this arrangement produces a coil with an inductance of 34·4 mH and a resistance of 6·5 ohms. Paraffin is used as the proton sample because, of the numerous materials which have been tried, it was found to provide the best compromise between an acceptable polarizing time and duration of the resulting precession signal. The fibreglass sheath protects the sensor during the rocket's ascent through the atmosphere.

In construction the coil is first vacuum impregnated with a high temperature resin and the end plates are attached. The 'bottle' thereby formed is then filled

with paraffin and sealed at a temperature of 100°C, the maximum expected temperature during the flight of a *Skylark* rocket. The whole assembly is then bonded together with epoxy resin. Finally the four brass screws are incorporated in the mounting platform to provide an extra key into the resin. The platform is attached to the nose cone by means of a 1-in o.d., 18 s.w.g. austenitic stainless steel tube, the base of which is further supported by a second tube of $1\frac{1}{4}$ in diameter.

The high temperature double-screened twin cable, used to connect the sensing head to the electronics unit, is embedded in resin inside the probe tube.

The complete fixed probe assembly is shown, mounted on the instrumented section of a *Skylark* rocket, in Fig. 2.
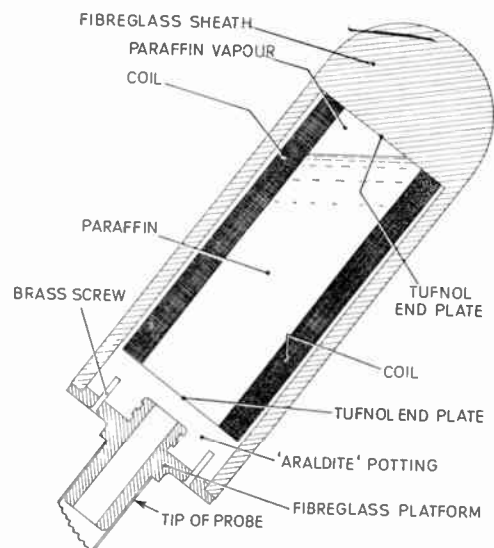

Fig. 1. Cross-section through sensing head.

† Geophysics Department, Imperial College of Science and Technology, London; now with the Fields and Plasmas Division, Goddard Space Flight Center, Greenbelt, Maryland, U.S.A.

‡ K. Burrows, "A rocket borne magnetometer", *J. Brit.I.R.E.*, **19**, No. 12, pp. 769–76, December 1959.
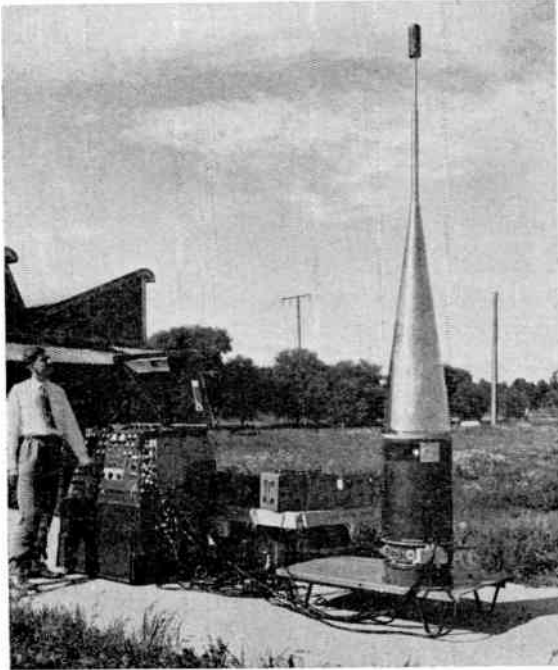
Fig. 2. *Skylark* SL40 showing fixed probe assembly.

Sometimes it is necessary for a rocket to carry other instruments which would produce intolerable magnetic fields in the vicinity of the sensing head as, for example, when it is required to fly the magnetron of the missile tracking system used with *Skylark* rockets. It is, therefore, essential to position the sensing head further away from the rocket than the 4 ft maximum length of a fixed probe. On these occasions an inflatable probe is used and the magnetometer is mounted at the aft end of the instrumented section of the rocket. During the ascent through the atmosphere the probe and sensing head are contained in the body of the rocket and then, after ejecting the spent motor tube, compressed air from gas bottles is allowed into the pneumatic tubing and the probe is deployed. By this means the sensing head can readily be positioned 20 ft away from the rocket, where it is outside the magnetic field perturbations caused by any normal rocket instrumentation. Figure 3 shows a typical instrumented *Skylark* rocket with the flexible pneumatic probe extended. Since the rigidity of the inflated probe is insufficient to carry the weight of the sensing head in the earth's gravitational field, the probe is here being supported from the top of the wooden tower for test purposes. (It should be noted that in this photograph the rocket is inverted, relative to its more usual attitude.) The use of a pneumatic probe has the further advantages that it is not necessary to protect the sensing head from aerodynamic heating and more space is available inside the rocket than could be

allowed at the tip of a fixed probe. The inside and outside diameters of the sensing coil are therefore both increased by $\frac{1}{2}$ in, resulting in a useful increase in signal amplitude. The deployment of the pneumatic probe does, however, involve the use of additional mechanical and electro-mechanical devices, with consequent reduction in the reliability of the system.

2.2. *Electronic Circuitry*

The circuit diagram of the instrument is shown in Fig. 4 and Fig. 5 shows the complete equipment mounted in a *Skylark* parallel section (for use with the pneumatic probe).

In flight the operations which lead to the detection of a proton precession signal are as follows.

(i) Relays RLA and RLB close and supply current to the sensing coil thereby creating a strong polarizing field through the proton sample.
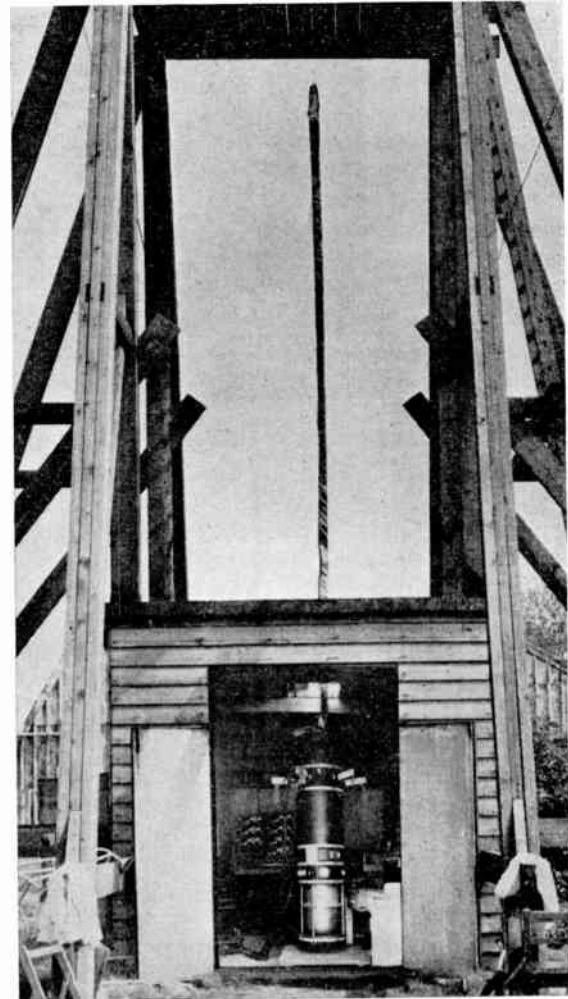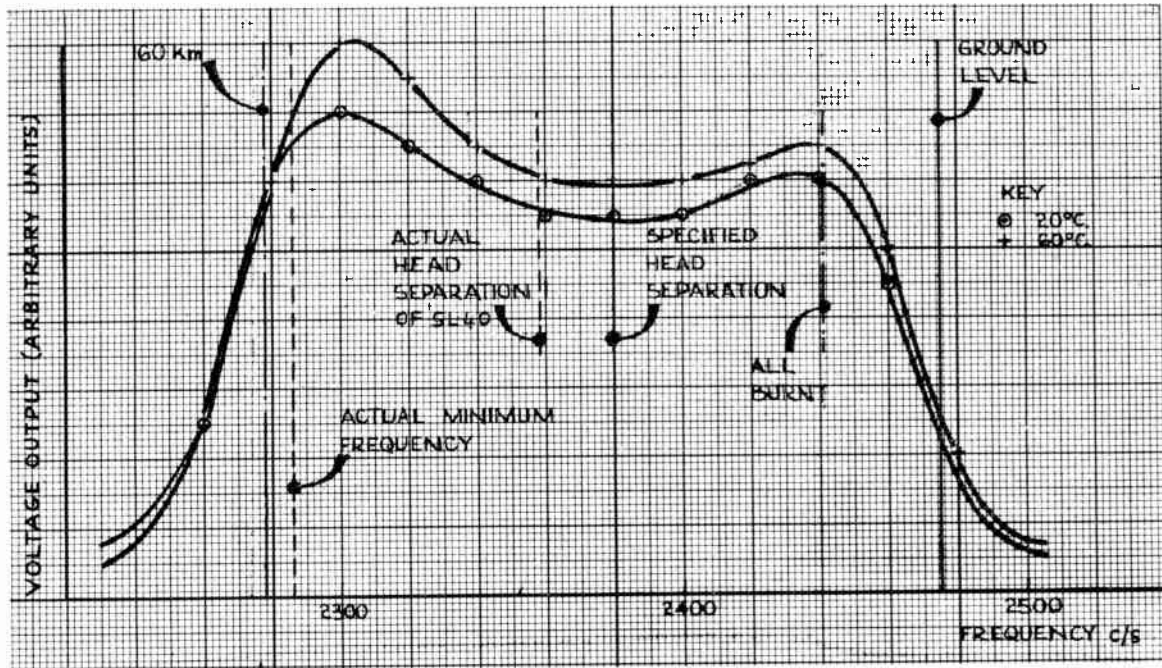

Fig. 3. Pneumatic probe assembly.

Fig. 4. Proton precession magnetometer circuit diagram.

L2—14 turns, 24 S.W.G.
L3—725 turns, 35 S.W.G.
   on pot core type LA 2103.
L4—725 turns, 35 S.W.G.
   on LA 2103 tapped at 125 turns.
RFC—12 turns $\frac{1}{4}$ in dia.
   20 S.W.G.
C1 is selected to tune L1.

(ii) After 0·6 seconds the relays de-energize and the sensing coil is connected to the tuned amplifier. The operation of RLA is delayed by a few milliseconds as a result of the capacitor connected across its coil.

(iii) The polarized protons in the sample now precess in phase, round the direction of the geomagnetic vector, and the rotating resultant of the proton magnetic vectors induces an e.m.f. (of the order of a few microvolts) into the sensing coil. This signal is amplified to a level suitable for feeding into the rocket telemetry system.

(iv) The signal finally decays exponentially as a result of the gradual loss of phase coherence in the precessing protons and, when the signal amplitude has fallen to a pre-determined level, the relays close and the cycle of operations is repeated.

In the original prototype design a low-microphony pentode was used in the first stage of the amplifier but, because of the very low signal level, some microphony was still encountered when the instrument was tested in a rocket. This difficulty is now eliminated by the use of transistors with an emitter follower input stage to obtain the high input impedance necessary to maintain the Q of the tuned circuits. The input circuit (VT1 and VT2) is a transistorized version of the well-known 'White' cathode follower. High-gain silicon transistors, selected for low noise, are employed in order to maintain a high input impedance over a wide temperature range. It was found that the noise factor of the circuit is critically dependent on the base

current of VT1 and accordingly the spread of transistor parameters is accommodated by selecting R1 to give each unit an optimum noise factor. The OA200 diode, V3, is incorporated to protect the transistors from the positive half cycles of the transient high voltage surges on switching off the polarizing current. When the emitter follower is loaded by the amplifier the input impedance is approximately 800 kΩ.

Fig. 5. The electronics package for use with a pneumatic probe.

Fig. 6. Frequency response of complete instrument.

The tuning of the amplifier is achieved by the three resonant circuits, each of which is adjusted to the centre frequency of the required pass-band. The bandwidth is determined mainly by the coupling constant in the pair of input resonant circuits L1, C1 and L3, C2 and is adjusted by varying the number of turns in L2. The loading on the third tuned circuit L4, C3 results in a slight detuning of its intrinsic resonant frequency and this detuning effect leads to a useful slight increase in the amplitude of the lower frequency hump of the band pass characteristic—the lower frequency corresponding to the upper part of the flight. Figure 6 shows the characteristic achieved for the instrument which was flown in the first instrument proving flight, *Skylark* SL40. The pass-band of the amplifier was adjusted to give the maximum signal between the heights where the *Raven* motor was expected to burn out ('all burnt') and the maximum expected height. At the same time it was necessary to arrange for sufficient signal amplitude at ground level to enable the instrument to be given a final test before launching.

In order to minimize the detuning effects of temperature changes in the two Ferroxcube pot cores, polystyrene tuning capacitors are used to tune the inductances; these have a negative temperature coefficient of -120 parts per million per degree Celsius which partly compensates for the coefficient of $+160$ parts/10^6/deg C for the LA2103 pot cores.

The diode, MR1, across the normally closed contacts of RLB, enables these contacts to be used to reset a series of Eccles-Jordan binary circuits if the limited telemetry bandwidth makes it necessary to determine the frequency of the precession signal in flight. Such a system would, however, result in the sacrifice of some accuracy in the telemetered data.

The relay switching is controlled by transistors VT7 to VT13 inclusive. This circuit consists basically of a multivibrator in which the 'on' time (which corresponds to the polarizing period) is fixed but the 'off' time (counting period) is variable and depends upon the amplitude of the precession signal. It is well known that the initial signal amplitude from a proton magnetometer is critically dependent on the orientation of the sensing coil relative to the geomagnetic vector; thus in an unstabilized rocket instrument the duration of each productive signal can vary from zero to several seconds. Since the data from this type of magnetometer are inherently discontinuous it is obviously desirable to obtain useful signals for as much of the available flight time as possible and hence, in the present design, the signal amplitude is sensed and the relays remain de-energized as long as a useful signal is present. The increased signal duration can be used either to obtain greater accuracy in the absolute determination of the magnetic field or to look for any change of precession frequency during the counting period, such as might occur if the rocket passes through a cloud of sporadic E during that time.

When the rocket is in an unfavourable attitude, and no signal is present, the 'off' period is reduced to a

minimum (about 250 ms) in order not to waste time, and a new polarizing cycle is initiated. The circuit used senses the total power output of the amplifier and hence cannot differentiate between useful signal and, say, noise due to interference. To guard against the contingency that excessive interference from the other rocket instrumentation might permanently lock the relays in the off position, in spite of the absence of a signal, the maximum counting period is set at about 2·5 seconds.

The variation of counting period is achieved as follows. A proportion of the output of VT6 is amplified by VT7 and, if it is of sufficient amplitude, it is rectified by VT8 and applies reverse bias to the base-emitter junction of VT9, switching it off; the multi-vibrator timing is now determined by the normal time-constants associated with VT10 and VT11. In the absence of a signal VT9 is conducting and the collector current discharges the 60 µF timing capacitor more rapidly, thus effectively reducing the time-constant. It is arranged that the voltage across the reservoir capacitor in the emitter circuit of VT8 and VT9 closely follows the envelope of the precession signal, thus achieving a continuous control over the timing periods.

A convenient method of controlling the signal level at which the relaxation oscillator trips into the 'on' state is by varying the resistance in the lead connecting the output of VT6 to the input of VT7. With the 12 kΩ resistor short-circuited the unit responds to signals down to the noise level of the amplifier at room temperature; with this resistor in circuit it triggers at a signal level about 3 dB higher. This allows for the increased noise and interference experienced in a *Skylark* rocket to be launched in the high temperature environment of Woomera.

The output of the multivibrator is buffered from the output stage, VT13, by means of the emitter follower VT12, the low output impedance providing adequate current to bottom the output stage with the 70 Ω collector load, presented by the two relays in series. In order to maintain the buffering effect of VT12 during the 'on' stage it is desirable to prevent it from bottoming and to this end the collector is taken to the unstabilized negative supply rail.

It is well known that the time during which a switching transistor is most liable to failure is during the period that it is changing from a 'bottomed' to a cut-off state and vice versa, since it is during this time that both appreciable currents and voltages are present concurrently. It is therefore essential to switch the transistors, in particular the output transistor VT13 driving the relays, as rapidly as possible; this implies that no appreciable capacitive load can be applied to any point where the voltage is required to change rapidly. In the present circuit the capacitive load is removed from the collector of VT11 during the time

this transistor is cut off and it is charged from the low output impedance point of VT12 via the 2·2 kΩ resistor, which serves to limit the base current through VT10. Thus, whilst the junction of MR5 and this resistor changes with a time-constant determined mainly by this 2·2 kΩ resistor and the 60 µF timing capacitor, the emitter of VT12 (and hence the base of VT13) is switched rapidly. When VT11 is 'bottomed' its collector presents a low impedance path to earth and the diode MR5 clamps the 60µF timing capacitor to this point thereby again permitting the emitter of VT12 to switch rapidly.

In order to ensure that VT13 is held off at high temperatures the emitter is biased slightly negatively by a voltage developed across the silicon diode MR6 in series with the 3·9 kΩ resistor.

The diode V19 damps down the voltage surge which would otherwise occur when the energizing current is removed from the relays.

2.3. *Mechanical Construction*

In order to facilitate servicing and to make the instrument more readily adaptable to be flown in different geographical locations, the electronics unit is divided into the following five pluggable sub-units.
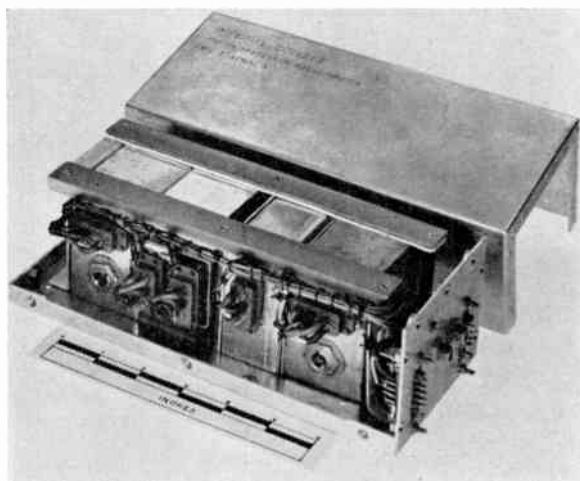

Fig. 7. Electronics package.

(i) Timer unit. (Transistors VT7 to VT13 inclusive together with their associated components.)

(ii) Emitter follower unit (VT1 and VT2).

(iii) Amplifier I (VT3 and VT4).

(iv) Amplifier II (VT5 and VT6 and including L4).

(v) Relay unit (both relays, L2, L3 and C1).

These plug-in stages are shown, assembled into a complete electronics unit, in Fig. 7.

Each sub-unit is encapsulated in a flexible polyester resin, to reduce contraction pressure and to provide a slight degree of cushioning thereby minimizing the effects of severe transient accelerations. A thin glaze of epoxy resin is finally applied to seal the units against moisture penetration. The 12-V dry battery, supplying power to the electronics unit, is also potted in epoxy resin (Fig. 5).

burnt out these plungers are used to eject the instrumented section of the rocket away from the magnetic field perturbations associated with the steel of the spent motor tube.

2.4. Monitoring

It is important, in any rocket equipment, to be able to diagnose the cause of any in-flight failure. In the
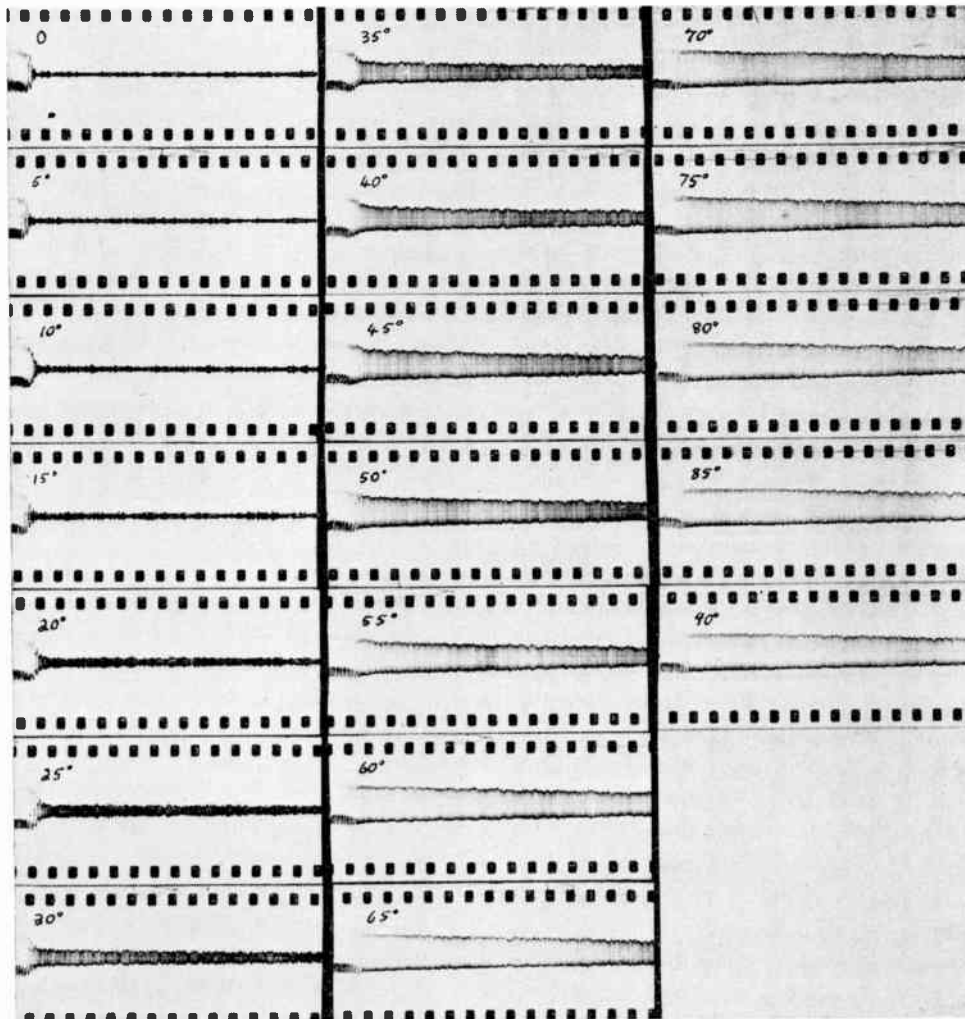
Fig. 8. Proton precession signals at various orientations of the sensing head.

The relay unit is enclosed in a mu-metal box to prevent interference signals from being induced into the pot core.

The power supplies are switched remotely by means of a 'Ledex' rotary stepping switch (Fig. 5).

In Fig. 5 can also be seen three pneumatically operated plungers, positioned round the circumference of the bay. Some time after the rocket motor has

present instrument the most likely cause of failure is to be associated with the operation of the two relays; accordingly the voltages of the dry battery and silver/zinc battery, used to provide the polarizing power, are each monitored continuously in flight. The steps in these voltages, which occur when the relays operate, thus provide a convenient monitor on the operation of the timer unit and the relays, and confirm that

polarizing current is being applied to the sensing coil. When an inflatable probe is flown, pressure transducers monitor the gas pressure in the reservoir bottles and in the pneumatic tubing and, as a final check on the deployment, the probe is photographed using a single shot camera, of a specially rugged construction to withstand impact with the ground.

2.5. *Laboratory Testing and Evaluation*

To test the instrument it is necessary to place the sensing head in a magnetic field environment corresponding to a precession frequency within the pass-band of the amplifier.

In order to synthesize the geomagnetic field corresponding to any rocket height above any geographical location, a coil system is used, constructed according to the design of Rubens.† The space occupied by the set of five coils is 6 ft cube and they produce a known magnetic field which is uniform to better than 0·1% within a cylinder 1·2 ft in diameter and 2·7 ft long. The sensing coil can be mounted in the centre of the coil system and can be rotated to any required value of θ, the angle between the coil axis and the magnetic vector. The axis of the coil system is arranged to be parallel to the earth's magnetic field vector, and the entire installation is screened and protected from the weather by means of 20 s.w.g. aluminium sheets. The field current through the coils can be controlled by means of a potentiometer with a 1000-μF capacitor across the terminals to prevent noise from being induced into the search coil under test as a result of changes in field current setting.

The signal amplitude, from a sensing coil performing the dual role of polarizing and pick-up coil, will be a maximum when θ is 90 deg and will follow a sine-square law to zero when θ = 0 deg. Figure 8 shows records of the signal amplitude at various values of θ from 0 deg to 90 deg. In these experiments the current through the field coils was adjusted to 100 mA, which corresponds roughly to a rocket altitude of 100 km above Woomera.

At this value of magnetic field the magnetometer can be seen to produce an identifiable proton precession signal down to values of θ of approximately 25 deg, a range representing over 90% of all possible orientations.

The effect on the magnetometer of the high temperature environment during the rocket flight will be to reduce the signal amplitude slightly,‡ to increase the noise in the system, to detune the three resonant circuits and to affect the polarizing and counting periods.

The way in which the signal/noise ratio is affected throughout the pass-band is illustrated in Fig. 6. It will be observed that, as a result of the design features discussed above, the change in shape of the pass-band characteristic, in heating from room temperature to 60° C, is quite small. The elevated temperature does, however, result in a slight increase in the gain and the noise level of the amplifier, the final result being a slight degradation of the signal/noise ratio. The timing of the relay switching is constant to better than 0·1% with variations of temperature from room temperature up to 65° C, and with supply voltage variations within the range 12–18 volts.

To ensure as far as possible that the equipment can survive, though not necessarily function, during the boost part of the rocket flight, each unit is subjected, whilst operating, to vibration tests covering the range 30–2000 c/s at maximum accelerations of 10 g (+20%−0%), the rate of frequency sweep being adjusted continuously, throughout the range, to permit the full build-up of any resonances present.

The checking of the sensing head includes an x-ray examination to search for any air or paraffin trapped in the potting and a vacuum test to ensure that there are no cracks in the potting, which might allow the paraffin sample to escape during flight. To make sure that the sensing head has not been contaminated with any magnetic material during manufacture it is placed close to a second, direct-reading instrument to detect any magnetic field which may be associated with it.

Since the e.m.f. induced into the sensing head is only of the order of a few microvolts and since the sensing head forms a very effective search coil, a very important pre-flight test is to operate the instrumented section of the rocket on the ground, with all instruments functioning, and to look for interference on the telemetered magnetometer signals. During this test the missile is powered by internal batteries since interference fields would be generated by the currents in the leads from external power supplies. Figure 2 shows this test in progress, on a fixed-probe *Skylark* rocket, at the Weapons Research Establishment, near Adelaide, South Australia.

3. Data Processing Equipment

During a rocket flight it is usual for the proton precession signal to be telemetered to ground, where it is recorded directly on magnetic tape together with a 50 kc/s standard frequency reference and timing signals. The 'raw' data can then be replayed as frequently as necessary.

A convenient method of measuring the frequency of the precession signal, to the required accuracy, is to mix it with another signal of a frequency which is accurately known and is close to that of the unknown.

---

† S. M. Rubens, "A cube surface coil for producing a uniform magnetic field", *Rev. Sci. Instrum.*, **16**, pp. 243–5, September 1945.
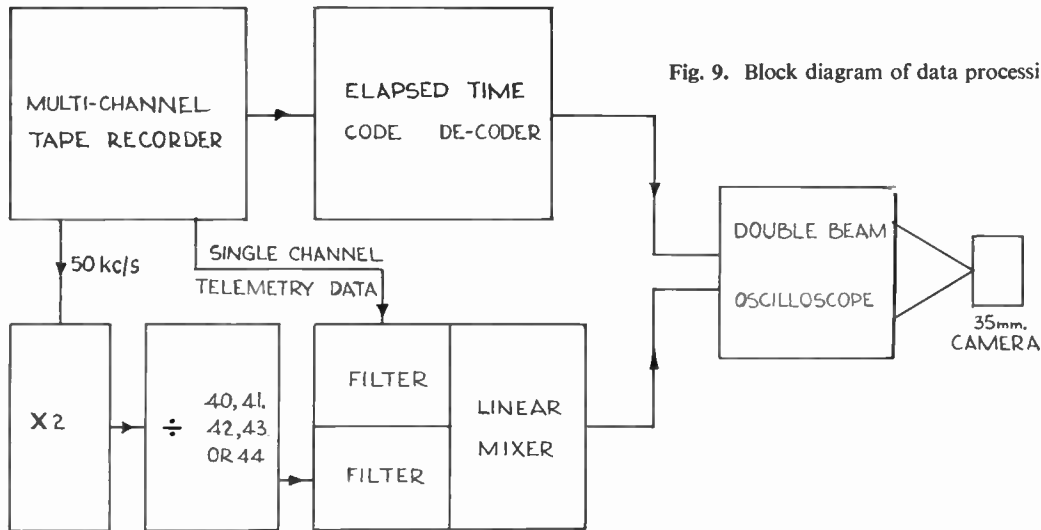
‡ K. Burrows, *loc. cit.*

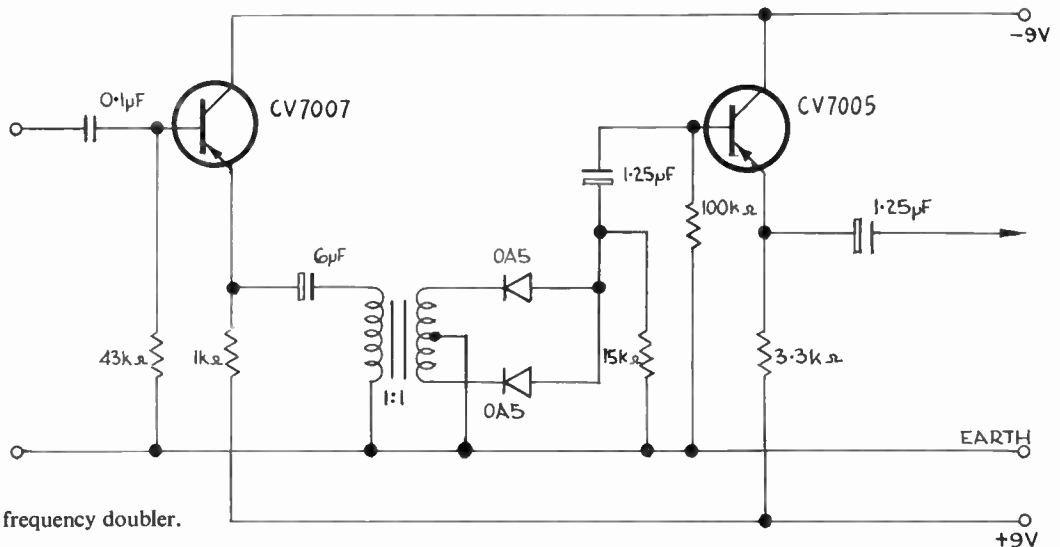Fig. 9. Block diagram of data processing equipment.

Fig. 10. Circuit of frequency doubler.

The difference between the accurately known and the required precession frequencies can then be determined by counting the resulting beats; this manual technique has the advantage over a completely automatic system in that, where the signal is of amplitude comparable with the amplifier noise, the regular beats can be seen and random noise rejected. Using this technique it is possible, in practice, to obtain accurate field determinations with the sensing head axis only 5 deg from the magnetic vector.

The method of obtaining and recording the beats is illustrated in Fig. 9. The 50 kc/s reference signal is first doubled, prior to dividing down, in order to increase the number of available reference frequencies close to the unknown precession frequency. The frequency doubler circuit is shown in Fig. 10. To

accommodate the range of precession frequencies encountered during a *Skylark* flight from Woomera, the 100 kc/s standard frequency is now divided by 40, 41, 42, 43 or 44 giving reference frequencies of 2500·00, 2439·02, 2380·95, 2325·58 and 2272·73 c/s respectively; the difference between any two adjacent frequencies does not, therefore, exceed 60·98 c/s. It is thus possible to arrange that, at all times during the rocket flight, the beat frequency lies conveniently within the range 5 c/s to 35 c/s approximately. The transistorized frequency divider, which was designed and manufactured by Venner Electronics Ltd., follows standard practice.

The circuit diagram of the filter/mixer unit is shown in Fig. 11; it is designed to fulfil the following important requirements in the data handling process:
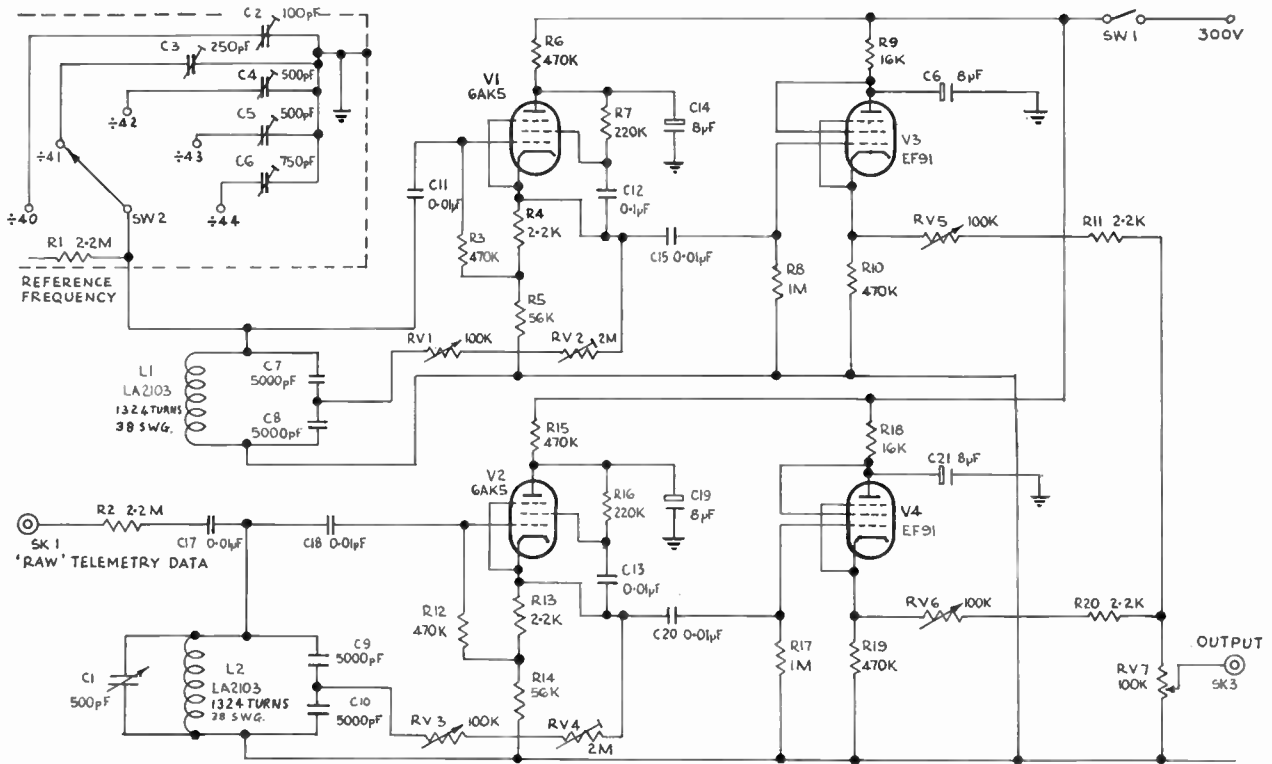
Fig. 11. Circuit diagram of filter circuits and mixer.

(1) Shaping the reference frequency waveform. The output of the divider unit is in the form of pulses whose mark/space ratio varies with the division factor. All higher harmonics are rejected by V1, with its associated circuitry, and the fundamental is fed to V3. The trimming capacitors C2 to C6 inclusive are physically situated in the divider unit and are switched in synchronism with changes in division factor.

(2) Filtering of the telemetered proton magnetometer signals. Since the bandwidth of the rocket instrument must necessarily accommodate the entire range of precession frequencies encountered during the rocket's flight, a considerable improvement in the quality of data can be achieved by reducing the bandwidth during playback. This filtering is performed by V2 with its associated circuitry. The changes in precession frequency are manually followed by varying C1 and the bandwidth can be controlled within the range 5 c/s to 30 c/s, by means of RV3.

In a typical *Skylark* flight the frequency excursion is about 200 c/s, hence the signal/noise ratio can be improved by an approximate factor of $(200/B)^{\frac{1}{2}}$, where B is the 3 dB bandwidth of the data channel. In practice there is a limit to the improvement attainable by this technique because of the variations in tape speed, during play-back, which lead to phase changes

in the output signal when the resonant circuit is not precisely tuned. It is found that errors due to this cause start to outweigh the improvement in accuracy by reducing the bandwidth at about $B = 10$ c/s.

(3) Formation of 'beats'. The two filtered signals are linearly mixed by the resistance network in the cathode circuits of V3 and V4.

Figure 12 shows a typical record of a 'raw' precession signal as it would appear at the input of the filter/ mixer unit and below it the same signal after filtering and mixing with a standard reference frequency. The precession signal shown in Fig. 12 was telemetered, from the first *Skylark* rocket to carry a proton magnetometer, when the missile was close to the apogee of its flight.

4. System Evaluation Flight

Skylark No. 40 (Fig. 2) was fired from Woomera (Lat. 30°56′ S Long. 136°31′ E; Geomagnetic Lat. −41·0°) on 27th September 1961 at 09.55 hours C.s.t. (00.25 hours G.m.t.); it reached a height of 152·5 km 200 seconds after launch, and impacted at a point 113 km down range. The measured values of precession frequency are shown, plotted against time from the start of the flight, in Fig. 13.
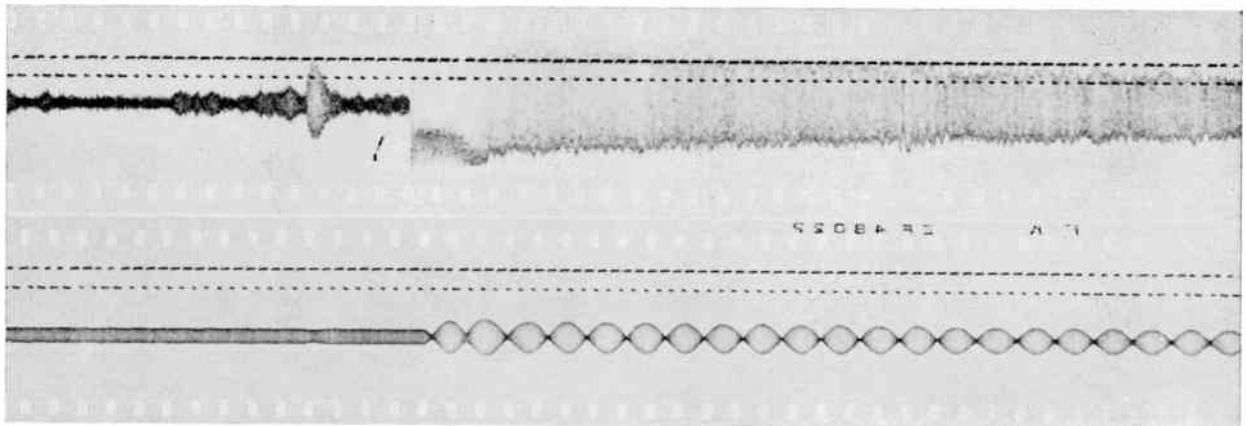
Fig. 12. (*above*) Typical telemetered precession signal; (*below*) same signal, after processing.
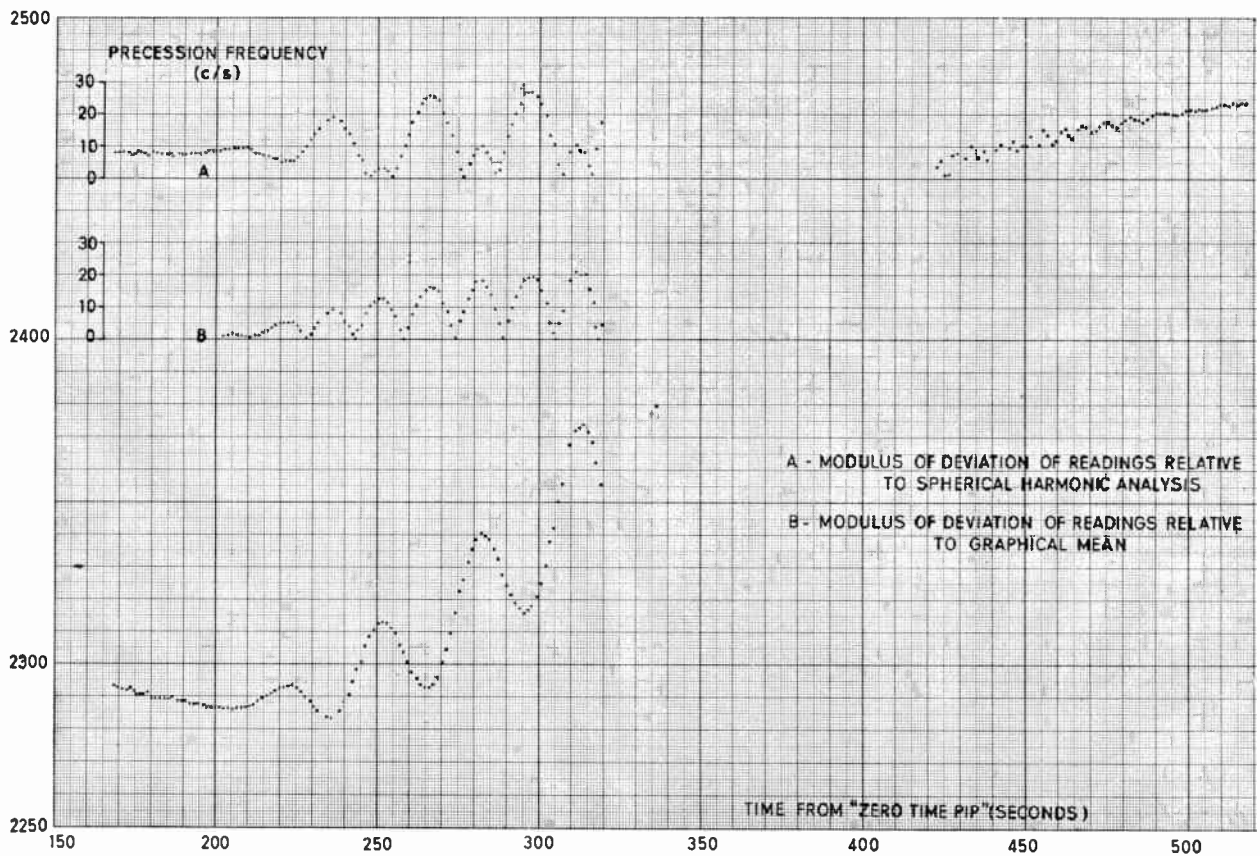
Fig. 13. Variation of precession frequency with time.

The full evaluation of these data involved a series of laboratory experiments on the effect of magnetic field gradients on a proton magnetometer and a ground magnetic survey of the rocket range, in addition to reference to the data from other rocket instrumentation. It will not therefore be discussed in detail.

The large periodic modulations of precession frequency, during the period 200 seconds to 320 seconds, are due to the close proximity of the spent *Raven* motor tube, resulting from an unsatisfactory head separation earlier in the flight, and the continuous increase in the amplitude of the modulations indicates that the instrumented head and the motor were moving closer to each other during this time. The break in the continuity of the readings is mainly due to noise induced by the severe mechanical vibrations which a rocket normally experiences on re-entering the earth's atmosphere. The long period changes in the gradient of the curve reflect the changes in the rocket's vertical velocity during the flight.

No magnetic discontinuity, which could be attributed to a current sheet in the ionosphere, can be resolved as a consequence of the large oscillations; however, an accurate absolute determination of the geomagnetic field close to the rocket's apogee was possible. The total scalar force at a point 150 km above Woomera was found to be $53\ 807 \pm 14$ gamma. This value can be compared with a value of 53 806 gamma deduced from a spherical harmonic analysis using coefficients calculated from the data of the *Vanguard III* satellite.†

† J. P. Heppner, private communication.

As a flight test of the rocket magnetometer the flight can be considered highly successful since the breaks in continuity of the data can be attributed to causes not directly associated with the instrument itself; indeed, although the flight electronics unit had been mechanically damaged by impact with the ground, it was found, on recovery, to be in a fully serviceable state.

5. Acknowledgments

INSTITUTION NOTICES

New Year's Honours

The Council has congratulated the following members of the Institution whose appointments to the Most Excellent Order of the British Empire appeared in Her Majesty's New Year's Honours List:

To be Knight Commander, Military Division: Instructor Rear-Admiral Charles Roy Darlington (Associate Member). Admiral Darlington was recently elected a member of the Institution's Council, and he has been a member of the Education Committee since June 1961. He is Director of the Naval Education Service, Ministry of Defence.

To be Officer, Military Division: Lieutenant-Colonel John Vevers, R.E.M.E. (Member). Colonel Vevers is an Assistant Director of Electrical and Mechanical Engineering at Headquarters, B.A.O.R.

To be Member, Civil Division, Frederick James Frank Properjohns (Associate Member). Mr. Properjohns is an Engineer II in the Electrical Inspection Directorate of the Ministry of Aviation.

Dissolution Honours

In the Dissolution Honours Her Majesty conferred a Peerage of the United Kingdom upon Sir Robert Renwick, Bt., K.B.E. (Member). Sir Robert was Controller of Communications at the Air Ministry, 1942–45, and he is now Chairman of Associated Television Ltd. He has taken the title of Baron Renwick of Coombe in the County of Surrey.

New I.E.R.E. Premium for Television Reception

At the Annual General Meeting of the Institution on 9th December the retiring President, Mr. J. Langham Thompson, announced the establishment of a new Institution Premium, the "P. Perring-Thoms Premium". The new award will be presented annually for the outstanding paper on television reception published in *The Radio and Electronic Engineer*.

The Premium has been endowed by Radio Rentals Ltd. to commemorate their founder, Mr. P. Perring-Thoms, who died in July of last year.

Papers on television reception published in the *Journal* during 1964 will be considered for the first award of the new Premium, which will be announced in the summer.

1964 List of Members

All Corporate Members, Companions, Associates and Graduates have been sent free of charge their copies of the 11th issue of the *List of Members* of the Institution. Registered students, whose names are *not* included in the list, may obtain copies from the Institution, price 5s. each.

Recognition of I.E.R.E. Qualifications

The Civil Service Commissioners have issued an amendment to the regulations relating to the appointment of Mechanical and Electrical Engineers in Government Departments. The following paragraph has now been added to the list of acceptable qualifications:

"Candidates must have achieved Corporate Membership of the Institution of Electronic and Radio Engineers having passed or obtained exemption from the examinations under the September 1962 syllabus and regulations or have passed, or obtained exemption from Sections A and B of the Institution examination under the same regulations and completed a 2-year apprenticeship, pupilage or equivalent training giving good basic engineering experience."

In addition, all candidates must demonstrate that both the examination subjects included in their qualifications and their practical experience are related to the normal work of the Government Department in which they seek appointment.

These regulations primarily cover engineering appointments in the Ministry of Aviation (including Civil Aviation Division), Ministry of Defence and the Government Communications Headquarters.

Symposium on Applications of Microelectronics

A Symposium on the Applications of Microelectronics will be held at Southampton University from 21st to 23rd September 1965. This is being arranged jointly by the I.E.E. Southern Electronics Section and the Institution's Southern Section in association with the Department of Electronics at the University.

It is intended that papers, which will be preprinted, will concentrate mainly on applications, although new circuit elements will also be of interest.

Titles of papers, with summaries not exceeding 300 words, should be submitted before 1st March to the Symposium Secretary, Department of Electronics, University of Southampton. Registration forms will be available from the same address from 1st April.

Correction

The following correction should be made to the report on "Instruction in Electronic Drawing for Students of Radio and Electronic Engineering at Professional Level", published in the September 1964 issue of *The Radio and Electronic Engineer*:

Page 199, Bibliography, Item 3. The date of this paper *should read* July 1953.

Enhancing the Angular Resolution of Incoherent Sources

By

A. C. SCHELL, Sc.D. †

Summary: The output of an antenna that scans an incoherent source distribution is 'smoothed', that is, it contains fewer rapid variations with angle than the true source distribution. This is because the antenna rejects or reduces high spatial frequency components of the source spectrum. Source spectrum components passed by the antenna can be restored to their correct value by data-processing but such techniques usually yield a non-physical approximation to the source distribution. In a new technique that enhances angular resolution, the best mean square match to the restored source data is determined, and the minimum amount of extrapolated data added to guarantee a physical approximation to the sources surveyed by the antenna.

1. Introduction

The output of an antenna at any instant of time can be expressed in terms of a weighted sum of the field strengths of all sources within the angular coverage of the antenna. Each source contribution is weighted according to the antenna field response in the direction of the source. If, after an observation period, the correlation between the fields received at each point in the aperture from any two points of the source distribution is negligibly small, the source distribution is incoherent. The apparent antenna response is thus linear in power; and if the sources lie in the far field of the antenna a superposition relation can be written for the case of a single angular variable as

$$P(u) = \int_{-1}^{1} T(u')A_r(u'-u)\,du' \qquad \ldots\ldots(1)$$

where $T(u)$ is the source distribution, $A_r(u)$ is the antenna receiving cross-section or gain pattern, $P(u)$ is the antenna's average output, and $u = \sin\theta$. Instances of this occur in radar mapping, radio astronomy, x-ray spectral analysis, and lenses illuminated by incoherent light.

2. Spatial Frequency Analysis

The effect of the antenna pattern on the observation of the source distribution, which is by some[1] called the 'aerial smoothing' of the source distribution, can be interpreted by analysing the properties of the Fourier transform of eqn. (1).[2-5] The variable of the transform of eqn. (1) is called spatial frequency and can be expressed either in units of length or in wave numbers by using the kernel exp $j(2\pi/\lambda)su$. For

† Air Force Cambridge Research Laboratories, L. G. Hanscom Field, Bedford, Massachusetts.

directive antennae with very little radiation at angles far from the pattern maximum, the finite limits of eqn. (1) can be replaced by $\pm\infty$. The transformed equation becomes, for a single angular variable,

$$p(s) = a(s) \cdot t(s)$$

where the antenna transfer function is

$$a(s) = \frac{\int g(x)g^*(x+s)\,dx}{\int gg^*\,dx}$$

and g, the aperture field distribution, is assumed to contain no components that oscillate in x more rapidly than once per freespace wavelength. Because $a(s)$ is the autocorrelation of the aperture field distribution, it tends to zero as $s \to 2L$, the length of the antenna. The source distribution is therefore weighted by the transfer function; and for all values for which $a(s)$ is zero, the antenna output contains no information about the source.

In the absence of noise, dividing $p(s)$ by $a(s)$ will give the source spectrum at all frequencies for which $a(s)$ is not zero. This portion of the true source distribution is known as the principal solution. If uncorrelated measurement error or noise of zero mean and variance $\langle n(s)\,n^*(s)\rangle$ is present, multiplying $p(s)$ by

$$\tau_R = \frac{a^*(s)}{aa^* + \langle nn^*\rangle}$$

will yield the minimum mean square error restoration of the antenna output.[6] The restored output, although containing a more accurate spectral distribution than the antenna output, does not provide a physically acceptable answer in the angular domain for a great many cases. Indeed, the cases for which restoration is most needed are usually those for which the principal

solution yields a source distribution that has substantial negative values over an extended angular range. Since the actual source distribution cannot have regions of negative power, the principal solution is clearly not a solution for these cases. The difficulty rests in part with the sharp spectral cut-off at $s = 2L$, representing the limit of the spatial frequencies passed by the antenna. The principal solution does not represent all that is known about the source distribution; whereas the restored output has the correct spectral distribution from $s = 0$ to $s = 2L$, the Fourier transform of the spectral distribution must be positive, and thus some additional spectral content is usually necessary to assure a physical solution.

The finite limits of integration of eqn. (1) have repeatedly been cited[7, 8] as justification for analytic continuation of $a(s)$ and $p(s)$ into the region $s > 2L$. Very little is gained from the analytic nature of $a(s)$. however, because the propagation of error from the measured values to the extrapolated values is so great.[5, 9]

3. A Technique of Incoherent Source Data Enhancement

The output spectrum $p(s)$ is a distorted and limited representation of the source distribution $t(s)$. Further, measurement error and noise may be present at the output. The input to the restoration process may therefore be considered as $p(s)+n(s)$ where $n(s)$ is an additive error of zero mean. If the restoration process is to give the correct result on the average, the spatial frequency characteristic of the restoration filter should be $\tau_R(s) = a^{-1}(s)$ and yield a restored output

$$p_R(s) = \tau_R(p+n) = t(s) + \frac{n(s)}{a(s)} \qquad |s| < 2L$$

which shows the magnification of errors by the restoration process in regions where $a(s)$ is small. For $s > 2L$, $p_R(s) = 0$. The restored output, if transformed back to the angular domain, seldom provides a representation of the sources that is everywhere positive, and that is therefore a possible solution.

The problem of enhancing the source data may be stated as that of finding a physically acceptable match for the restored output, consistent with the error distribution. To minimize the difference between this physical answer, $\tau(s)$, and the restored output, it is necessary to allow $\tau(s)$ to extend beyond $2L$. A conservative assumption for this addition of spectra that were not received by the antenna is to add the minimum amount possible to construct a physical solution. For purposes of analysis, a minimum mean-square error match is sought. A weighting function $H(s)$ is introduced to reduce the effect of the regions of large errors in $p_R(s)$. To find its form, minimize the average of the fit of the source distribution

and a weighted restored output

$$\varepsilon_1^2 = \int_0^{2L} \langle |t(s) - H(s)p_R(s)|^2 \rangle \, ds$$

This error, ε_1^2, is minimized by

$$H(s) = \frac{aa^* \langle tt^* \rangle}{aa^* \langle tt^* \rangle + \langle nn^* \rangle}$$

for which

$$\varepsilon_1^2 = \int_0^{2L} \frac{\langle nn^* \rangle \langle tt^* \rangle}{\langle nn^* \rangle + aa^* \langle tt^* \rangle} \, ds$$

The equation determining the enhanced output is

$$\varepsilon_2^2 = \int_0^{2L} H^2(s)|p_R(s) - \tau(s)|^2 \, ds + \int_{2L}^{2W} |\tau|^2 \, ds = \min$$

$$\ldots\ldots(2)$$

The distinction between the restoration process and the weighting function is apparent from this equation. All antenna output data, whether noisy or not, are restored by the reciprocal of the antenna transfer function since this is the only way the correct source spectrum can be obtained. The restoration process magnifies the error in some regions, however, and the weighting function reduces contributions from the unreliable regions to the total error. The function τ must be an autocorrelation if its transform is to be everywhere positive. The value $s = 2W$ is chosen as the limit of the data enhancement; at that value and for all greater s, $\tau = 0$.

Related studies of antenna functions[10] show that under certain conditions, the minimum of

$$\varepsilon_2^2 = \int_{-2W}^{2W} H^2(s)|\tau_D(s) - \tau(s)|^2 \, ds$$

is defined by the solution to the integral equation

$$f(x) = \text{constant} \times \int_{-W-x}^{W-x} H^2(s)[\tau_D(s) - \tau(s)] \times$$
$$\times f(x+s) \, ds \quad \ldots\ldots(3)$$

where f is an analytic function existing over the interval $2W$, and τ is the autocorrelation of f. The nature of eqn. (3) can be better understood by a reduction of the functions to sets of sample values. Because the antenna power pattern and the observed data exist over a finite angular range, their Fourier transforms can be defined by a set of evenly spaced samples. The antenna is described as a linear array of M isotropic elements with feeding coefficients G_k. The antenna transfer function is

$$A_l = \sum_{k=1}^{M-l} G_k G_{k+l}^* \qquad l = 0, 1, 2, \ldots, M-1$$

The element separation is $\lambda/2$. The spatial frequency spectrum of the antenna output is represented by a set of samples P_{Ak}. The interval between samples is set by the angular range of the data. For a source distribution within the range $-\pi/2 < \theta < \pi/2$ the

sample interval is $\lambda/2$. Equation (3) becomes

$$F_n = \text{constant} \times \sum_{-N-n}^{N-n} H_k^2(\tau_{Dk} - \tau_k) F_{k+n} \quad \ldots\ldots(4)$$

where

$$\tau_{Dk} = \frac{1}{A_k} P_{Ak} \qquad\qquad k = 0, 1, \ldots, M-1$$

$$\tau_{Dk} = 0 \qquad\qquad k = M, M+1, \ldots, N$$

$$H_k = \frac{|A_k|^2 \langle t_k t_k^* \rangle}{\langle t_k t_k^* \rangle |A_k|^2 + \langle n_k n_k^* \rangle} \qquad k = 0, 1, 2, \ldots, M-1$$

$$H_k = 1 \qquad\qquad k = M, M+1, \ldots, N$$

In a typical problem M values of P_{Ak} are given, and the array coefficients G_k are known. Some knowledge of the statistics of the source and the measurement error must be assumed to determine the form of H.

The choice of the ratio N/M depends on the amount and distribution of noise in the data, and upon the source spectrum and the desirability of resolution enhancement for a given system use. In many cases, the resultant τ is relatively insensitive to small changes in the value of N. A simplified but convenient method of choosing N/M is to assume a flat spectrum of t and n, and determine the ratio of N/M that provides the mean minimum mean square error for a few simple and regular shapes of τ. For example, if the restored spectrum were flat, and the resultant τ were symmetrical about $\tau = 1/2$, the added spectral power would equal the difference from the restored spectrum when $N = 2M$. For noisy data the limit of enhancement would be less than $N = 2M$.

4. Examples of Data Restoration

Solutions to the minimum mean square error match by an extended transfer function to the restored data have been found by iterating the defining relation, eqn. (4), on a large digital computer. Illustrations of the technique follow. In all examples, the antenna array consists of 10 uniformly illuminated isotropic elements with interelement spacings of $\lambda/2$.

Figure 1(a) shows the antenna output for a single point source at $\theta = 0$ and no noise; the restored output obtained by dividing the antenna output spectrum by the antenna transfer function; and the physically realizable source distribution that is the best mean square match to the restored output and adds a minimum amount of data in the spectral range from the antenna cut-off to twice the antenna cut-off.

Figure 1(b) shows the antenna output, the restored output, and the enhanced output, for a point source located at $\theta = -30°$. This illustrates the invariance
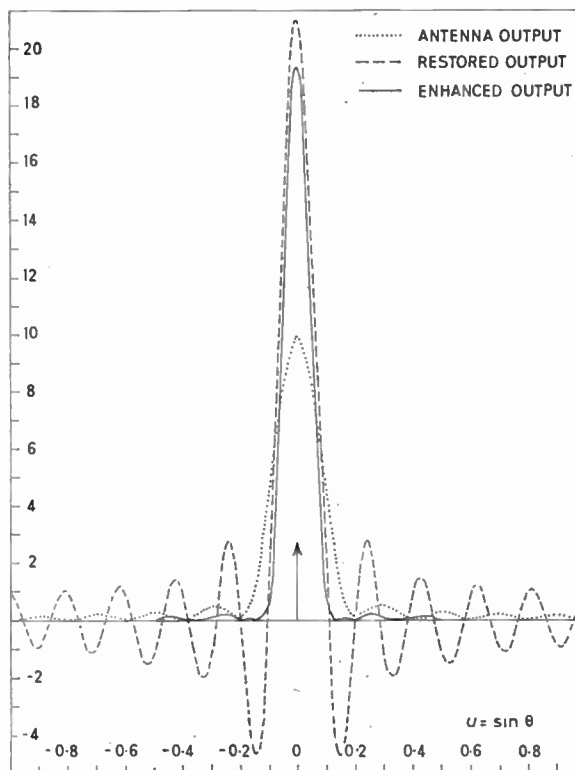
(a) $\theta = 0$.
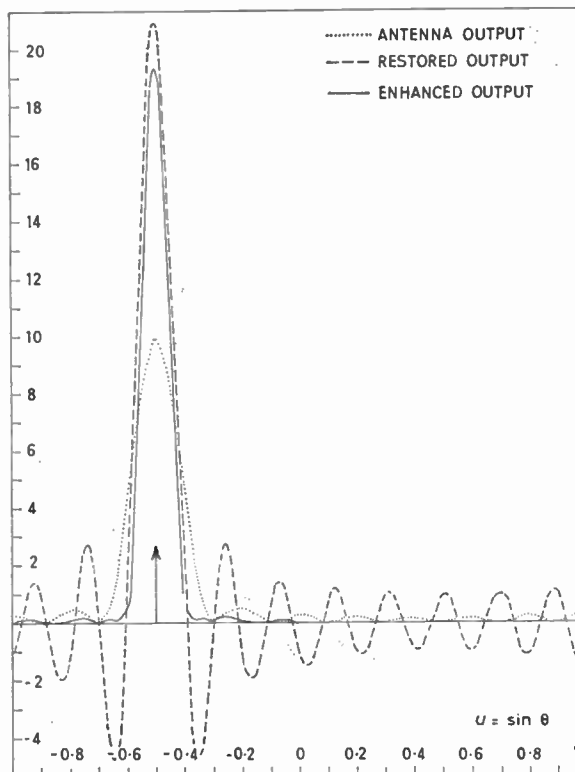
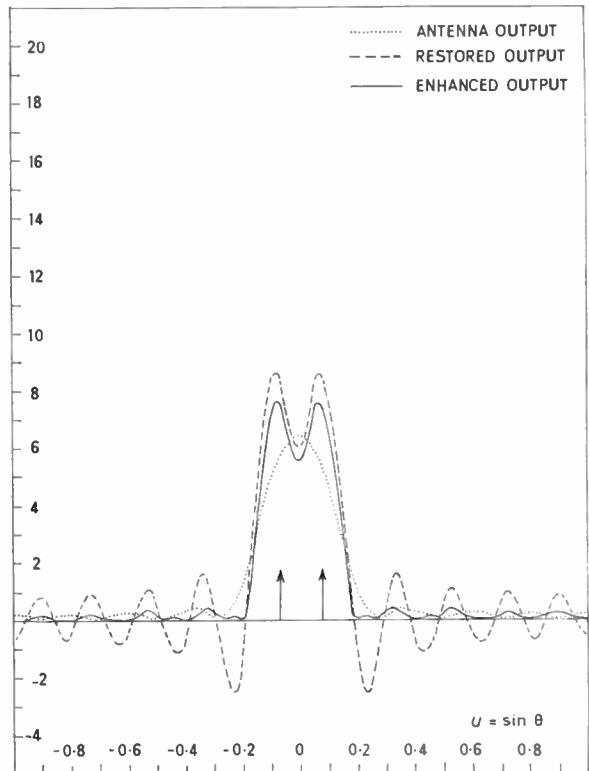(b) $\theta = -30°$.

Fig. 1. The antenna output, the restored output, and the enhanced output for the observation of a single point source by a 10-element uniform array with $\lambda/2$ interelement spacing.
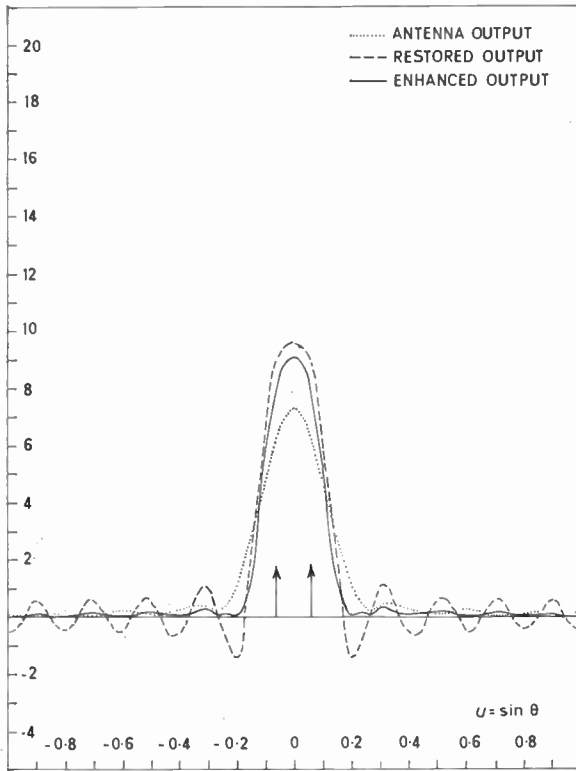
(a) Sources located at $\theta = \pm\ 3\cdot5°$.

(b) Sources located at $\theta = \pm\ 4\cdot1°$. The antenna output does not resolve the sources. The restoration procedure and the enhancement technique clearly show the two sources, although the restored output has large negative lobes.
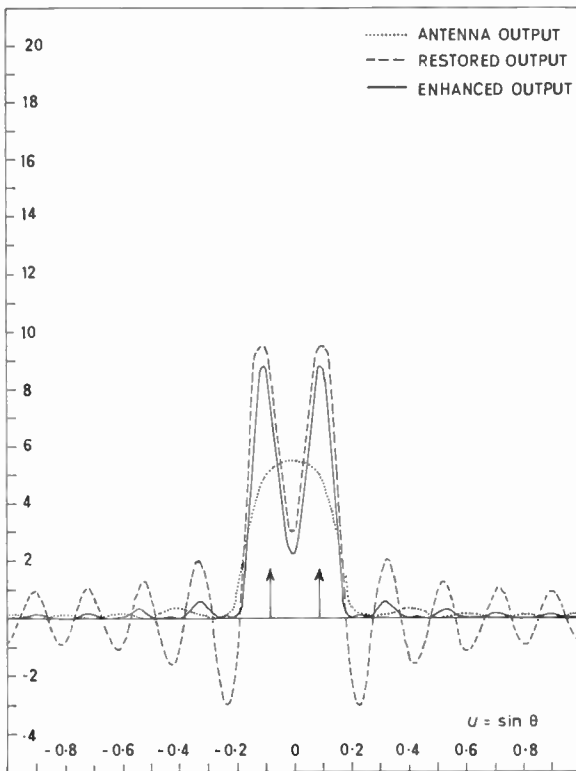
(c) Sources located at $\theta = \pm\ 4\cdot8°$.

of the technique with source location even though the enhanced data function is matching to spectral data with a rapidly changing phase.

Figures 2(a), (b) and (c) illustrate the resolution limit for the enhancement technique. The extended data cover twice the spectral range of the observed data. The examples show that data enhancement substantially increases the resolution of the unprocessed antenna output.

Figures 3 and 4 show the effect of data enhancement on the resolution of two sources of unequal power. In Fig. 3, two point sources with a 4 : 1 power ratio are observed by the 10-element array. The restoration of the spectral composition of the sources masks the smaller source, as is shown by the dashed curve. The data enhancement technique clearly shows the two sources. The power ratio of the two sources in Fig. 4 is 9 : 1. Again the data enhancement technique accurately resolves the sources.

The output improvement shown in these examples has been confirmed for other source shapes and also in the presence of additive error.

Fig. 2. The outputs of the antenna, the restoration process, and the enhancement process for two equal-power point sources.
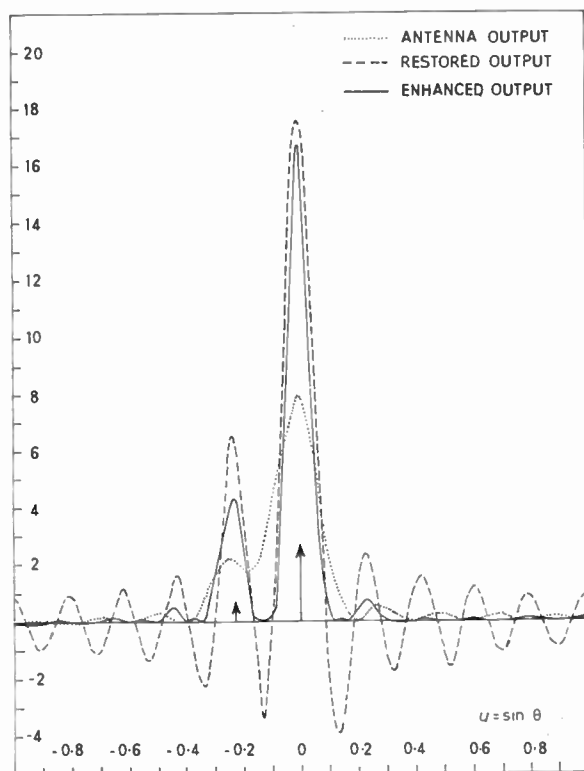
Fig. 3. The outputs for the observation of two unequal point sources by the 10-element array. The power ratio of the two sources is 4 : 1, with the stronger source at $\theta = 0$ and the weaker at $\theta = -12\cdot8°$.
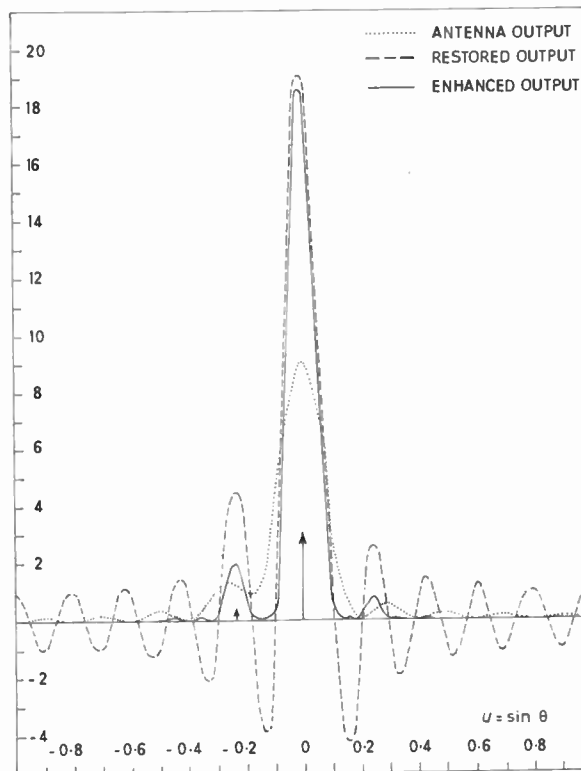

Fig. 4. The outputs for the observation of two point sources with a power ratio of 9 : 1. The weaker source is masked in the restoration process; however, the correct ratio of powers is present in the enhanced output.

5. Conclusions

A technique of enhancing the output data of an antenna used for surveying incoherent source distributions consists in finding the best match, in the mean square sense, for the restored spatial frequency spectrum of the antenna output. The spatial frequency range of the enhanced data is greater than that supplied by the antenna; some frequency content is therefore added to the received spectrum. All added spectral data are treated as errors, and so the minimum necessary to yield a physically acceptable solution is added. Basic to the enhancement technique is the determination of the autocorrelation function covering the extended range that best fits the restored data. This provides an approximation to the source distribution that is everywhere positive and is therefore a possible solution to the problem of determining the sources surveyed by the antenna.

6. Acknowledgment

I wish to thank Miss Joan E. Morison for her assistance in the computation of the examples.

7. References

1. R. N. Bracewell and J. A. Roberts, "Aerial smoothing in radio astronomy", *Aust. J. Phys.*, **7**, pp. 615–40, December 1954.

2. P. B. Fellgett and E. H. Linfoot, "On the assessment of optical images", *Phil. Trans.*, **247**, No. 931, pp. 369–407, 1954.

3. J. Arsac, "Application of mathematical theories of approximation to aerial smoothing in radio astronomy", *Aust. J. Phys.*, **10**, pp. 16–28, 1957.

4. E. J. Burr, "Sharpening of observational data in two dimensions", *Aust. J. Phys.*, **8**, pp. 30–53, 1955.

5. R. M. Chisholm, "Transfer functions and the resolving power of radio telescopes", in "Electromagnetic Theory and Antennas", edited by E. C. Jordan, pp. 1281–4, (Macmillan, New York, 1963).

6. R. N. Bracewell, "Restoration in the presence of errors", *Proc. Inst. Radio Engrs*, **46**, pp. 106–11, January 1958.

7. Y. T. Lo, "On the theoretical limitations of a radio telescope in determining the sky temperature distribution", *J. Appl. Phys.*, **32**, pp. 2052–3, 1961.

8. A. A. Ksienski, "Spatial frequency characteristics of finite aperture antennas", in "Electromagnetic Theory and Antennas", edited by E. C. Jordan, pp. 1249–65, (Macmillan, New York, 1963).

9. R. H. MacPhie, "On Increasing the Effective Aperture of Antennas by Data Processing," Technical Report 58, Electrical Engineering Research Laboratory, University of Illinois, July 1962.

10. A. C. Schell, "The Selection and Evaluation of Antennas for the Survey of Incoherent Source Distributions", in "Electromagnetic Theory and Antennas", edited by E. C. Jordan, pp. 1233–48, (Macmillan, New York, 1963).

DISCUSSION

Under the chairmanship of Mr. R. N. Lord

Professor M. Ryle: I think there may be difficulties in applying these methods in radio astronomy, where the source is superimposed on a non-zero background, containing gradients and curvature. It will also be surrounded by weaker sources and by noise which, if properly filtered, will have the same angular structure as the aerial pattern. Under these circumstances the procedure for minimizing the negative deflections seems likely to be inaccurate and may not even lead towards the correct solution.

Dr. A. C. Schell (*in reply*): The applicability of this or any method of data enhancement depends to a great extent on the user's criteria. One should note that for source distributions with spatial frequency spectra extending past the antenna cut-off, neither the antenna output nor the principal solution is a 'correct' solution. The method described here is capable of providing a better fit to the data than is provided by the uncorrected antenna output. It is relatively unaffected by broad background radiation since the low spatial frequencies are not appreciably changed by the method. Noise, especially radiometer system error, is suppressed by the technique if it does not conform to a possible source distribution. In the final analysis, however, it is the user's assessment of the relative merits and deficiencies of processing or extending the output in a given situation that determines correctness, particularly when the true distribution cannot be determined.

Dr. G. O. Young: Is it not possible that reconstructing the target spatial spectrum from samples lying outside the physical aperture may lead to an erroneous image?

Dr. Schell (*in reply*): It is important to note that the described technique is not one of extrapolation of the measured values to the region outside the aperture. It is one of finding a physically acceptable distribution that best fits the corrected data and adds the minimum amount of unmeasured spectrum. The restored spatial frequency spectrum, or principal solution, does not represent all that is known about a distribution containing narrow sources. Higher frequency components must be added to the principal solution if an everywhere-positive distribution is to be obtained. This method permits determination of a solution that adds a minimum amount of unobserved spectrum by a procedure that can be consistently applied to each situation. Although it is undoubtedly possible to arrange spectral components so that the method does not work, many simulated distributions involving multiple

sources and noise have been used for testing this method, and it has performed satisfactorily.

Dr. G. H. Keitel: Dr. Hans Wilhelmsson of the Research Laboratory of Electronics, Chalmers University of Technology, Gothenberg, Sweden, has examined the de-smoothing process for the particular case of observations of the hydrogen line spectrum at 1420 Mc/s.† In this case, he is concerned with kernel in the integral eqn. (1) of the form

$$A_r (u' - u) = \frac{1}{\sigma \sqrt{2\pi}} \exp \left[-\frac{(u' - u)^2}{2\sigma^2} \right]$$

where A_r represents the frequency response of the receiver, $P(u)$ the observed spectrum, and $T(u')$ the source spectrum.

In his papers, he first considers obtaining the source spectrum by approximating the observed spectrum by functions for which the solution of (1) with the Gaussian kernel is both known and always positive. The results for several hydrogen line profiles is quite good compared with the Eddington second-order approximation,‡

$$T(u) = P(u) - \frac{\sigma^2}{2} \frac{\mathrm{d}^2 P(u)}{\mathrm{d}u^2}.$$

Wilhelmsson then considers the relationship between the Fourier transforms of the observed and source spectra, which for the Gaussian kernel results in heavier weighting for the larger λ, where

$$P(u) = \int_0^\infty [a(\lambda) \cos (\lambda u) + b(\lambda) \sin (\lambda u)] \, \mathrm{d}\lambda.$$

Rather than introduce a sharp cut-off in the Fourier transform of the observed spectrum, he applies a smooth cut-off above a certain λ by multiplying the Fourier transform of the observed spectrum by an additional factor. For two different choices of cut-off multiplier, this results in source spectra which do not go negative.

Dr. Schell (*in reply*): The technique by Dr. Wilhelmsson is a very interesting one and appears especially useful for line spectral observation when the observed curve can be approximated by simple functions.

† H. Wilhelmsson, "Accounting for smoothing effects in 21 cm observations", *Arkiv för Astronomi*, **3**, pp. 187–99, 1963.
ibid., "The problem of de-smoothing of 21 cm observations", *Sitzungberichte der Heidelberger Akademie der Wissenschaften*, pp. 115–23, 1962–63.

‡ A. S. Eddington, "Correction of statistics for accidental error", *Monthly Notices of the Royal Astronomical Society*, **100**, p. 354–61, 1913.

Transistor Parameters in the Avalanche Mode

By

M. N. S. SWAMY, B.Sc.(Hons.), D.I.I.Sc., M.Sc., Ph.D. †

Summary: While the literature is quite complete on transistor parameters below the avalanche region and a considerable amount of work has been directed to the region where complete breakdown occurs, the intermediate region has received very little study. This paper deals with the behaviour of the transistor in the border region of avalanche and particularly treats transistors of very high cut-off frequency. This is done in terms of the general four-terminal network parameters. The effects of avalanche on the α cut-off frequency and the maximum frequency of oscillation are discussed by using the admittance parameters and the short circuit current gain, which were measured experimentally. Further, it is shown that operation under avalanche conditions can extend the maximum useful operating frequency.

1. Introduction

In early applications of junction transistors, the collector voltage was limited to values far below the junction breakdown voltage. The reason for this was associated with the imperfect properties of early transistors in which the surface leakage currents across the collector junction far exceeded theoretical values. Many circuit designs are not tolerant of such leakage currents and it was necessary to restrict them by operating at low voltages.

For the past few years an increase of the operating ranges and applications for junction transistors has become permissible. Extensive production improvements have reduced the leakage currents and improved the stability, thus allowing the use of higher collector voltages up to the theoretical limits and making it possible to study and make use of the avalanche breakdown phenomenon.[1-3] It has been found that in the pre-breakdown region, a carrier multiplication takes place. This multiplication can lead to values of the current amplication greater than unity. Thus, in such transistors, α is less than, equal to, or greater than unity, depending on the collector voltage. New applications of junction transistors have thus become possible. They can replace point contact transistors in the region where $\alpha > 1$. They have also been used in switching circuits.

While the literature is quite complete on transistor properties below the avalanche region and a certain amount of work has been directed to the region where complete breakdown occurs,[4-7] the intermediate region has received little study. This paper deals with this intermediate region, and particularly treats

† University of Saskatchewan, Regina, Canada.

transistors of very high cut-off frequency.[8] It is hoped that a little further insight is developed into their properties.

2. Equivalent Circuit

A general equivalent circuit for a transistor in the common-base configuration is shown in Fig. 1. The various elements contained in the circuit may be identified with the physical phenomenon occurring in the transistor. r_B' is the extrinsic base resistance (ohmic spreading resistance of the base). Y_1 can be identified with the forward biased emitter-base diode and Y_3 with the reverse biased collector-base diode. Y_2 represents the feedback effect of the collector on the emitter. Y_m is associated with the carrier transport from the emitter to the collector, as controlled by the emitter-base potential and is a measure of the gain of the transistor.

The equivalent circuit of Fig. 1 is quite general, and given appropriate values for Y_1, Y_2, Y_3 and Y_m can be made to fit almost any transistor over a wide range of frequencies.
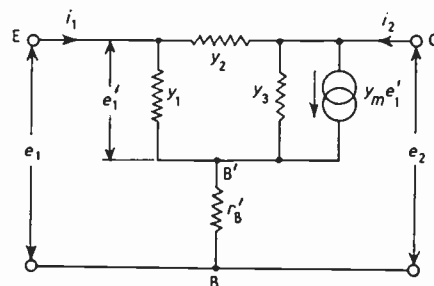

Fig. 1. A general equivalent circuit for a transistor in the common base configuration.
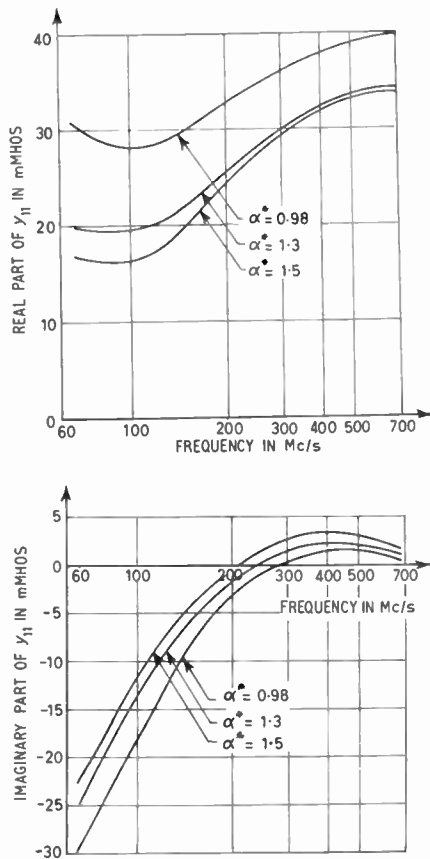
Fig. 2. Variations of the real and imaginary parts of y_{11} with frequency.

The first is an alloy junction drift transistor and has a nominal cut-off frequency of 100 Mc/s. The second is a diffused base transistor and has a nominal cut-off frequency of 600 Mc/s.

3. Measurements of the Parameters

The admittance parameters and the short circuit current gain were measured for transistor type 2N384 in the common base configuration. The emitter current I_e was adjusted to the usual operating value of 1·5 mA and the collector voltage varied. The base current I_b was measured for three different values of α^* equal to I_c/I_e, corresponding to the normal and avalanche modes. The different parameters are plotted in Figs. 2–6.

3.1. Input Admittance

The real and imaginary parts of the input admittance y_{22} are plotted against frequency for different values of α^* and are shown in Fig. 2. It is seen that the conductance part of the input admittance decreases with increasing α^*, whereas the susceptance part increases.

Hence, the admittance parameters are fundamental. Measurements of the admittance parameters for transistors in the common base configuration have been made and the corresponding parameters for the common emitter and the common collector configurations may be obtained by using the indefinite admittance matrices.[9, 10] Also, the other parameters of the transistor, such as the z, h, etc., may be obtained from the admittance parameters.

The admittance parameters have been measured using a G.R. Transfer Function and Immittance Bridge Type 1607–A.[11] The emitter bias was adjusted to the usual operating bias and the collector voltage varied so that the transistor could operate in the avalanche mode. The emitter direct current I_e and the base current I_b were measured. I_c, the collector current was computed by $I_c = I_e - I_b$. The admittance parameters and α, the short circuit current amplification factor, were measured for different values of $\alpha^* = I_c/I_e$.

The measurements were made on two different transistors, namely type 2N384 and type 2N1142.

Fig. 3. Variations of the real and imaginary parts of y_{22} with frequency. (The dotted line indicates the real part and the solid line the imaginary part.)

3.2. Output Admittance

The conductance and susceptance parts of the output admittance y_{22} are plotted in Fig. 3. It is seen that both these quantities increase with increasing α^*. The conductance has a maximum at about 300 Mc/s, whereas the susceptance steadily increases
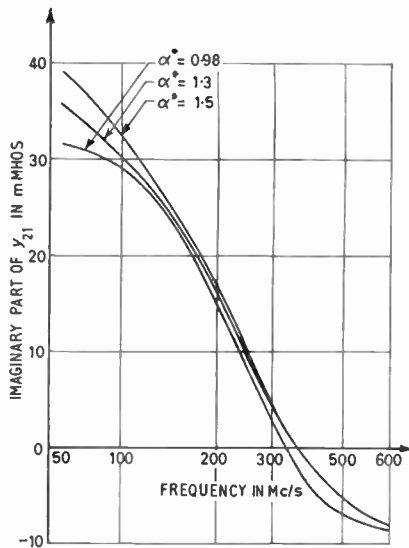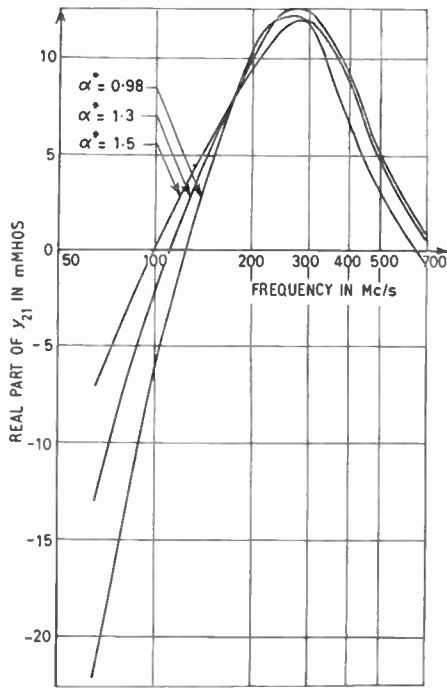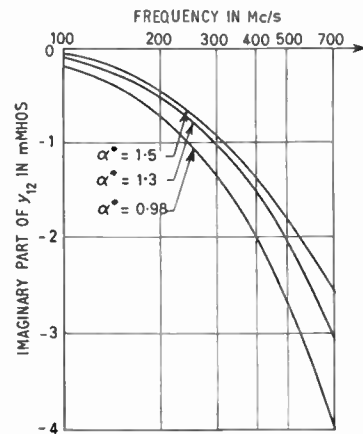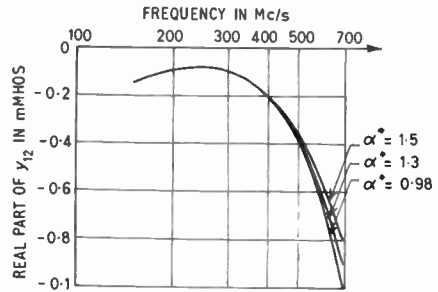

Fig. 5. Variations of the real and imaginary parts of y_{12} with frequency.

with frequency. By drawing a polar plot of the output admittance it can be seen that both the amplitude and the phase angle of the output admittance decrease with increasing α^*.

3.3. Forward Transadmittance

The plots of the conductance and susceptance parts of the forward transadmittance y_{21} against frequency are shown in Fig. 4. The conductance increases to a maximum round about the cut-off frequency and starts decreasing again. The susceptance decreases steadily up to about 500 Mc/s and is almost constant after that. It is capacitive up to about 400 Mc/s and inductive for higher frequencies. By drawing a polar graph of y_{21} it can be seen that the amplitude of y_{21} steadily decreases as the frequency is increased. It is also seen that the amplitude is not very much changed with the increase of α^* for frequencies greater than 400 Mc/s.

3.4. Reverse Transadmittance

Figure 5 shows the variations of the real and imaginary parts of the reverse transadmittance y_{12} with frequency. The imaginary part steadily decreases

Fig. 4. Variations of the real and imaginary parts of y_{21} with frequency.
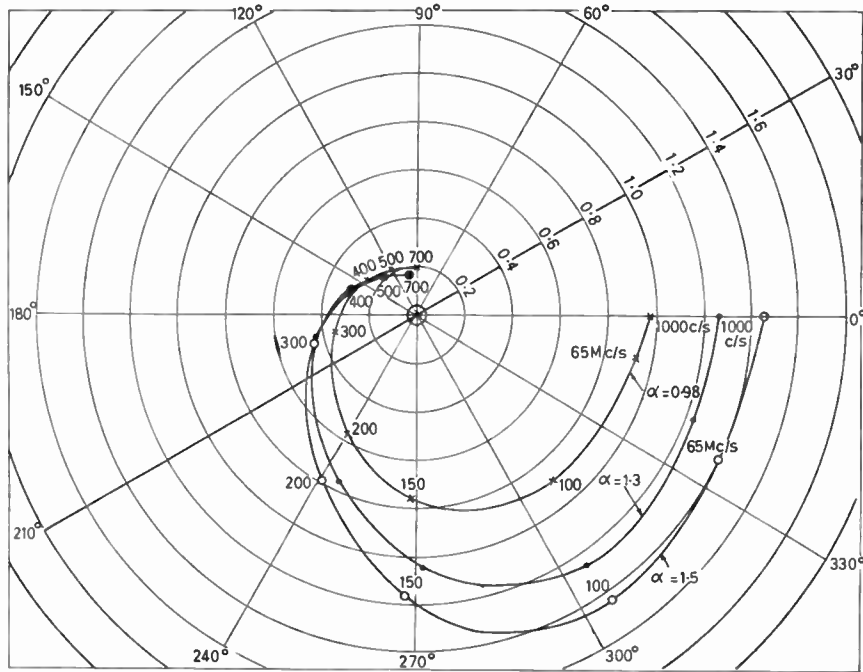
Fig. 6. Polar plot of the variation of α with frequency.

with increasing frequency. The conductance part increases with increasing α^* for frequencies above about 500 Mc/s. The susceptance part is capacitive and becomes less capacitive as α^* is increased.

3.5. Short-circuit Current Amplification Factor

The short-circuit current gain α is plotted against frequency for different values of α^* in Fig. 6. Also the amplitude of α is plotted against frequency in Fig. 7.

It can be seen that α increases with increasing α^*. Hence, by operating the transistor in the avalanche mode, an increased α becomes available. It can also be seen that for frequencies greater than 500 Mc/s, α^* has not much effect on the amplitude of α.

The values of α at a low frequency of 1000 c/s and α^* are plotted for different values of collector voltage V_c in Fig. 8. It can be seen that there is a sudden increase in α and α^* in the avalanche region. α is nearer to α^* at voltages less than the avalanche voltage than at voltages greater than the avalanche voltage. This may be due to increased surface leakage currents in the avalanche region.
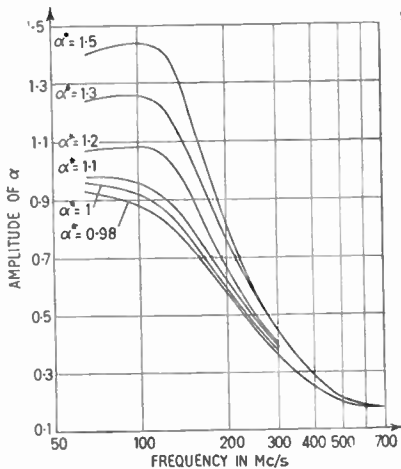
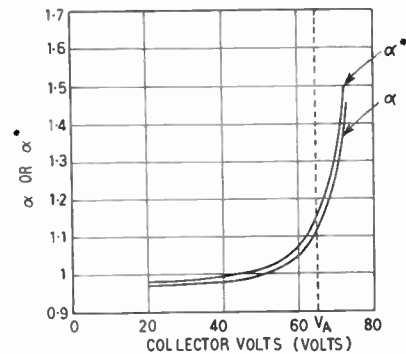Fig. 7. Variation of the amplitude of α with frequency.

Fig. 8. Variation of α at 1000 c/s and α^* with frequency.

3.6. α Cut-off Frequency

The α cut-off frequency f_c for a transistor is defined as that frequency at which α decreases to 0·707 of its low frequency value.

From Figs. 7 and 8, it is seen that when α^* is 0·98, the cut-off frequency is about 160 Mc/s. Also when α^* is 1·3 or 1·5, f_c is approximately 170 Mc/s. Thus, the cut-off frequency is not very much changed when the transistor is operated in the avalanche mode. Since the cut-off frequency is inversely proportional to the base width, it may be said that the base width remains constant when the transistor is operated in the avalanche mode.

However, from the point of view of circuit applications, one is more interested in the magnitude of the ratio of the collector to emitter current. It can be seen from Fig. 7 that this ratio increases when the transistor is operated in the avalanche region.

If f_c' is defined as that frequency at which α decreases to 0·707 of its low-frequency normal mode value, it can be seen that f_c' is approximately equal to 160 Mc/s, 215 Mc/s and 220 Mc/s for α^* equal to 0·98, 1·3 and 1·5 respectively. In other words, the frequency at which α is equal to 0·707 of its low-frequency normal mode value is increased when the transistor is operated in the avalanche mode.

Fig. 10. Variation of the function U with frequency.

$$U = \frac{|y_{21}-y_{12}|^2}{4(g_{11}g_{22}-g_{12}g_{21})}$$

is greater than unity. If the function U is less than unity, it cannot be made to oscillate under any circumstances.

The maximum frequency of oscillation f_0, (that is, the frequency up to which the transistor may be made to oscillate with proper feedback and terminations) is an important parameter in determining the useful high frequency range of operation. It is now calculated under normal bias conditions and then the effect of avalanche on this frequency is studied.

The function U is plotted as a function of frequency in Fig. 10. It can be seen that the maximum frequency of oscillation has increased from 345 Mc/s to 440 Mc/s when α^* is increased from 0·98 to 1·3. That is, an increase of the maximum frequency of oscillation results, when the transistor is operated in the avalanche region.
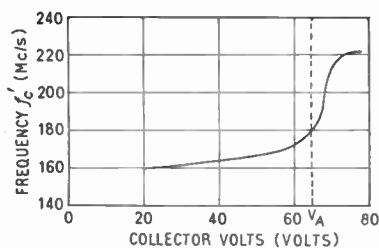

Fig. 9. Variation of f_c' as a function of collector voltage.

The frequency f_c' is now plotted in Fig. 9 as a function of the collector voltage with the help of Figs. 7 and 8. It is seen from Fig. 9 that, at collector voltages less than the avalanche voltage, the frequency f_c' rises slowly as the collector voltage is increased. But it rises suddenly after the avalanche voltage is reached. This clearly shows that the increase in f_c' is due to avalanche.

When α^* is increased from 1·3 to 1·5, there is not a great increase of f_0, the rise being only 10 Mc/s. This may be because α itself is not very much increased for frequencies greater than 400 Mc/s when α^* is increased from 1·3 to 1·5.

3.7. Maximum Frequency of Oscillation

It has been shown by Mason[12] that any four terminal network can be made to oscillate, with appropriate external feedback and terminations, only at frequencies for which the function,
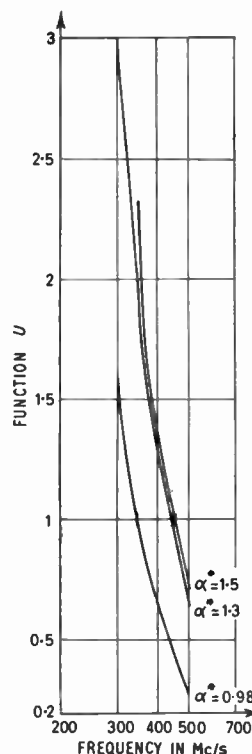
Measurements of the parameters were repeated with type 2N1142 and similar results were obtained.

4. Conclusions

(1) When the transistor is operated in the avalanche mode, the conductance part of the input admittance decreases, whereas the susceptance part increases.

(2) Both the amplitude and phase angle of the output admittance decrease when the transistor is operated in the avalanche mode.

(3) The forward transadmittance in the avalanche mode is greater than that for normal operation up to a certain frequency (near about the cut-off frequency). Above this frequency, the forward transadmittance for normal operation is slightly greater than that for the avalanche mode.

(4) The conductance part of the reverse transadmittance in the avalanche mode is greater than that for the normal operation. The susceptance part is less capacitive in the avalanche mode than that for the normal mode.

(5) The short circuit current amplification factor is greater than that for the normal operation. It rises suddenly from its normal value when the transistor is operating in the avalanche mode. However, after a certain frequency, which is well beyond the normal cut-off frequency, avalanche does not seem to increase α very much from its normal mode value.

(6) The α cut-off frequency does not change appreciably when the transistor is operated in the avalanche mode. Since the cut-off frequency is inversely proportioned to the base width, it may be said that the base width remains constant, when the transistor is operated in the avalanche mode. However f'_c the frequency at which α is equal to $0 \cdot 707$ of its low frequency normal mode value, is increased when the transistor is operated in the avalanche mode. This increase is by about 35% for type 2N384 and 20% for type 2N1142.

(7) The maximum frequency of oscillation is increased when the transistor is operated in the avalanche mode. This increase is by about 30% for type 2N384 and 18% for type 2N1142.

Even though the conclusions are based on experimental results, and the paper does not include either a discussion of the usability of this region, or the relationship between the parameters measured and the physical effects causing them, the author believes that, as not much work has been done in this field, a report of this nature may help in throwing some light as to the usefulness of this region, and also help in deducing an equivalent circuit for a transistor in the avalanche mode.

5. Acknowledgments

6. References

1. K. G. McKay and K. B. McAffee, "Electron multiplication in silicon and germanium", *Phys. Rev.*, **91**, p. 1079, 1st September 1953.

2. K. G. McKay, "Avalanche breakdown in silicon", *Phys. Rev.*, **94**, p. 877, 15th May 1954.

3. S. L. Miller, "Avalanche breakdown in germanium", *Phys. Rev.*, **99**, p. 1234, 15th August 1955.

4. S. L. Miller and J. J. Ebers, "Alloyed junction avalanche transistors", *Bell Syst. Tech. J.*, **34**, p. 883, September 1955.

5. J. R. A. Beale, W. L. Stephenson and E. Wolfendale, "A study of high-speed avalanche transistors", *Proc. Instn Elect. Engrs*, **104B**, p. 394, 1957.

6. J. E. Lindsay, "A decade-ring counter using avalanche operated junction transistors", *I.R.E. Trans. on Circuit Theory*, **CT-4**, p. 262, September 1957.

7. W. G. Magnuson, "Variable width pulse generation using avalanche transistors", *I.E.E.E. Trans. on Instrumentation and Measurement*, **IM-12**, p. 56, September 1963.

8. M. N. S. Swamy, "Measurements of transistor parameters in the avalanche mode", University of Saskatchewan, Canada, August 1960.

9. J. Shekel, "Matrix representation of transistor circuits", *Proc. Inst. Radio Engrs*, **40**, p. 1493, November 1952.

10. M. N. Srikanta Swamy and K. K. Nair, "Analysis of active networks by admittance matrices", *J. Inst. Telecom. Engrs (India)*, **5**, p. 186, 1959.

11. "Transfer Function and Immittance Bridge (Type 1607A)." (Instruction Manual), General Radio Company, West Concord, Mass.

12. S. J. Mason, "Power gain in feedback amplifiers", *I.R.E. Trans. on Circuit Theory*, **CT-1**, p. 20, 1954.

The Recording and Analysis of Seismic Body Waves using Linear Cross Arrays

By

F. E. WHITEWAY, B.Sc.

(Associate Member) †

Summary: Seismic signals from a single event usually contain a number of components (phases) which have travelled by different propagation paths, or with a different mode of propagation. These may be superimposed and obscure signal components of interest. Seismic background noise may also be of sufficient amplitude to obscure the signal onset, which is often of relatively small amplitude, or even obscure the whole signal.

An array of seismometers, spaced over a distance comparable to the signal wavelength, can be used as a filter to separate and help identify signal components on the basis of azimuth and apparent velocity at the Earth's surface. A signal/noise ratio improvement is also obtained for the first arrival, improving the accuracy of locating the hypocentres using triangulation methods from several stations.

Linear cross arrays have been operated during recent years by the United Kingdom Atomic Energy Authority and many events analysed, an example of which is shown. The theoretical performances of symmetrical cross and L-shaped arrays are given in the form of directivity patterns, and their method of use described. Correlation methods are shown to be necessary for obtaining a good azimuth or velocity response, and their advantages and limitations considered.

List of Symbols

σ_s^2 — variance of signal component

σ_n^2 — variance of noise

σ_{sr}^2 — variance of signal at rth seismometer

σ_{nr}^2 — variance of noise at rth seismometer

n — total number of seismometers in array

m — number of seismometers in line A

Δf — frequency bandwidth of noise

T_1 — integration time

θ — azimuth of signal component (Fig. 2)

θ_1 — azimuth to which array is tuned

V — apparent velocity of signal component

V_1, V_2 — apparent velocities to which array is tuned

f — frequency of signal component

$\lambda = V/f$ = apparent wavelength of signal component

$\lambda_1 = V_1/f$ (by definition)

D — length of each line array (Fig. 2)

D_A, D_B distance of centre point of lines A, B to point of intersection of lines

Δ_A, Δ_B phase difference between adjacent seismometers in lines A, B after insertion of delays (if any)

E_A, E_B normalized output amplitudes of summed line arrays A, B

E_n normalized output amplitude of complete array

d spacing between adjacent seismometers (Fig. 2)

1. Introduction

Earthquake seismology‡ has in the past been dependent upon recordings made at a large number of observatories situated throughout the world. The instrumentation at these observatories differed considerably in characteristics such as gain and frequency response. Recent interest in the problem of underground nuclear detection has led to the provision

† Atomic Weapons Research Establishment, Aldermaston, Berkshire.

‡ K. E. Bullen, "An Introduction to the Theory of Seismology". (Cambridge University Press, 1963.)

C. F. Richter, "Elementary Seismology". (W. H. Freeman, San Francisco, 1958.)
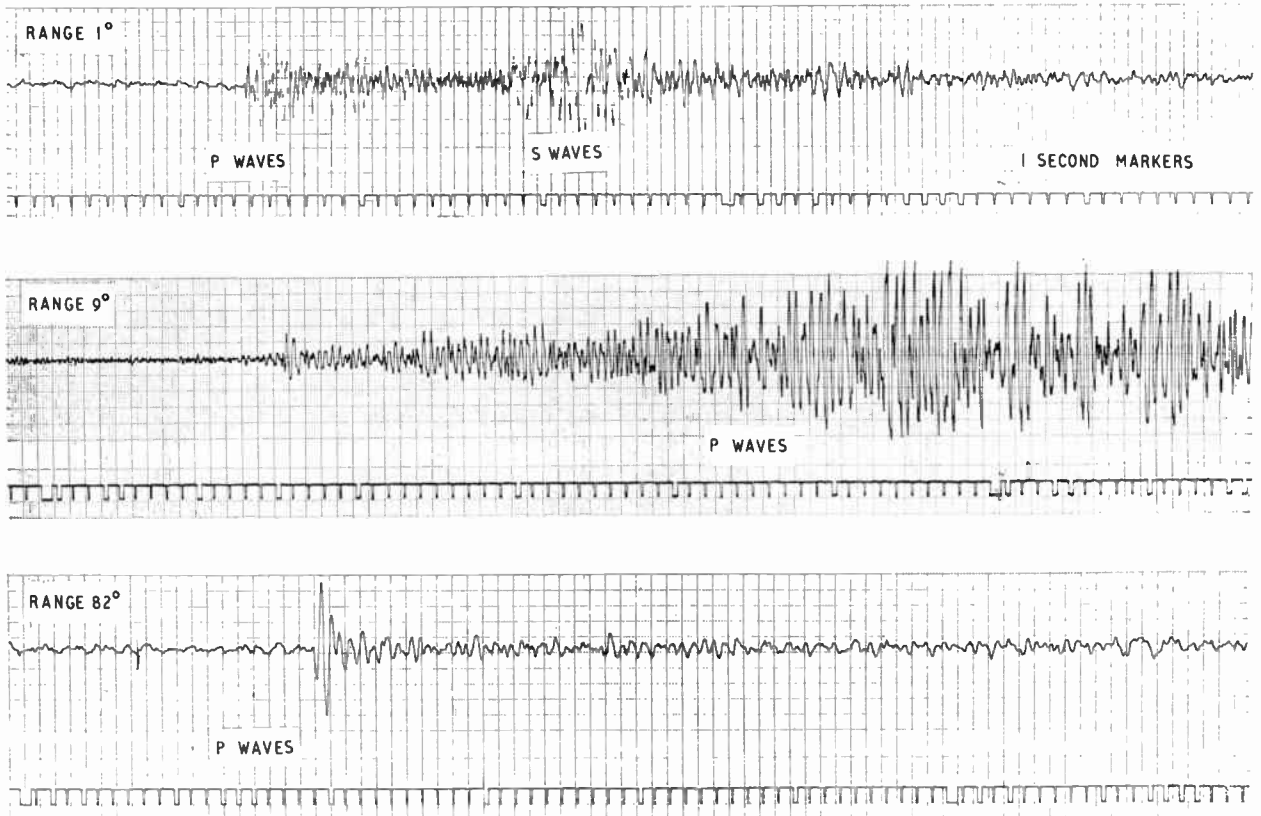
Fig. 1. Seismic signals from explosions at different ranges.

of modern, standard equipment for many of the observatories, which now contain very sensitive short-period instruments, recording seismic body waves in the range $\frac{1}{3}$–10 c/s, and long period instruments recording surface waves having periods of 10–100 seconds. In addition, a number of seismometer arrays have been installed. Experimental work in the United Kingdom has so far concentrated on the use of linear cross arrays, spaced over a distance comparable to the longest wavelengths of the signal. Each seismometer is recorded on a separate track of magnetic tape. On playback, delays are inserted which phase the array for a range of azimuth and/or velocity. The phased outputs are processed by summation and correlation methods, resulting in discrimination against seismic noise and unwanted signal components. In this way, the onset of signal components may often be determined when obscured in a single seismometer output by previous arrivals or noise. It is also possible to determine the azimuth and velocity of many of the signal components of interest, thus aiding their identification.

The above improvements obtained by the use of arrays have a number of applications. For example, the improvement in signal/noise ratio enables the onset time of weak signals to be determined more accurately. This increases the accuracy of the determination of epicentre location and depth of focus using triangulation methods from a number of similar stations; it is probable that a relatively small number of well-sited array stations would be better than the existing world-wide network of observatories. The improvement in identification of later signal arrivals is of particular importance in the determination of crustal structure, where seismograms are often very complex, containing a large number of superimposed signal components.

2. Signal and Noise Characteristics

Earthquakes generate two types of short period seismic body waves, namely primary (P) waves, characterized by compressions and rarefactions in the direction of propagation, and secondary (S) or shear waves, which have transverse motion and a lower velocity than P waves. These waves radiate in all directions from the source, incurring reflections, refractions and mode conversions at boundaries between rock of different elastic properties. As a

result, the signal arriving at the recording station may contain many superimposed signal components (referred to in seismology as 'phases') which have travelled by different paths and/or mode of propagation. Figure 1 shows the first minute of signals recorded from explosions at Great Circle ranges of approximately 1 deg, 9 deg and 82 deg. These signals were recorded on short-period vertical component seismometers. The main P and S wave bursts of energy are clearly distinguishable for the near event, the shear energy being produced by mode conversion near the source. The second record (from the 'Gnome' nuclear explosion) shows only part of the P wave arrivals. The signal had a duration of more than 10 minutes, and many signal components, including multiple reflections within the crust, have been identified by processing the array data. It will be noticed that the dominant frequency is much lower than in the first record, due partly to absorption of the higher frequencies in the propagation path and partly to source characteristics. The third record consists of a very simple burst of P wave energy, followed by a low amplitude coda. This record is characteristic of the simple impulsive source function, and the simplicity of the propagation path, which lies mainly in the relatively homogeneous mantle.

Table 1

Apparent ground velocity of signal components P, S, PP, PPP and PcP as a function of range

Range degrees	Apparent ground velocity km/s				
	P	S	PP	PPP	PcP
2	7·8	4·4	7·8	7·8	—
10	8·1	4·5	7·8	7·8	117
30	12·5	7·0	8·5	8·1	43·5
60	16·2	8·7	12·5	10·5	27·8
90	23·8	12·3	13·8	12·5	25·2

The signal components arrive at the recording site at the P or S wave propagation velocity V_P or V_S in the medium immediately underneath the station at an incident angle α to the vertical. The waves appear to propagate along a horizontal plane at the Earth's surface at a velocity of $V_P/\sin \alpha$ or $V_S/\sin \alpha$. This apparent velocity is also equal to the rate of change of distance along the Earth's surface with travel time, and for events at ranges of greater than 1 deg is virtually independent of near surface rock velocities if the surface layering is horizontal. The actual values of α, V_P and V_S are therefore relatively unimportant for a horizontal array, and the apparent ground velocities can be calculated directly from

travel time curves. Table 1 gives values for a number of seismic signal components as a function of range, and was derived from the Jeffreys-Bullen travel-time tables. The symbols PP and PPP denote P wave signal components which have incurred one and two reflections respectively at the Earth's surface without mode conversion. PcP denotes P waves which have been reflected from the Earth's core without mode conversion.

Table 2

Seismic noise spectra at Eskdalemuir and Yellowknife

Centre frequency c/s	Particle velocity ($\frac{1}{2}$ c/s bandwidth) 10^{-7} cm/s r.m.s.	
	Eskdalemuir	Yellowknife
0·25	89	22
0·75	5·0	0·72
1·25	1·25	0·14
1·75	0·48	0·060
2·25	0·38	0·051
2·75	0·34	0·040
3·25	0·33	0·050
3·75	0·35	0·045
4·25	0·40	0·083
4·75	0·28	0·055
5·25	0·25	0·108
5·75	0·26	0·107
6·25	0·28	0·053

Noise is caused by a variety of sources of both instrument and seismic origin. The main peak in the seismic noise spectrum occurs at a period of about 6 seconds, and is due to the effect of storms at sea. Energy is coupled to the ocean bottom, and is propagated over large distances in the form of seismic surface waves, known as ocean microseisms. It is partly because of this high peak that it is the usual practice to use separate instruments to record the short period and long period waves, with sharp filtering to reject the microseismic band. Other forms of seismic noise are caused by the action of waves on the coast, wind on the ground and obstacles such as trees, traffic, machinery and other sources of vibration. Table 2 gives details of the total seismic noise spectra measured on records taken at the array stations at Eskdalemuir and Yellowknife. These spectra were obtained by measuring the mean square values of the noise passed by filters of $\frac{1}{2}$ c/s bandwidth (-3 dB points), and comparing them with calibration sinewaves in the centres of the pass-bands. It will be noticed that the amplitudes are much lower at Yellowknife, due mainly to the distance from the

coast. Nevertheless, the noise amplitude at Eskdalemuir is much lower than in most other parts of the British Isles. The characteristics of the total seismic noise vary from site to site and contain both random and coherent components. These characteristics can only be determined by analysing recordings taken at the individual sites.

Referring to Table 2, it is seen that the total particle velocity due to seismic noise can be as low as 10^{-7} cm/s r.m.s. in the band $\frac{1}{2}$–2 c/s. The corresponding output from a Willmore Mk. II seismometer with a 3300-ohm coil and 5·6-kilohm external damping resistor is $0·35\,\mu$V r.m.s. It is, therefore, necessary for the following pre-amplifier to have a noise level of less than $0·2\,\mu$V r.m.s. referred to the input in order to avoid increasing the total noise significantly. Noise may be an important factor elsewhere in the recording system, particularly if magnetic tape recording is used. The sensitivity can be chosen such that the average noise level is low compared to seismic noise. However, magnetic tape drop-outs may cause spikes of large amplitude which distort the signal, and particular care is necessary in transcribing data.

3. Array Performance

Figure 2 shows the array configurations which are considered below, namely a symmetrical cross array and an L-shaped array. Each comprises two lines of ten seismometers spaced at equal distances d. The total length D of each line is equal to $9d$ for the configurations considered. The distances D_A, D_B between the centre points of lines A, B and the crossover points of the two lines are equal to zero for a symmetrical cross array, and to $5d$ for the L-shaped configuration. The array performance for coherent signal or noise components is considered first, followed by the performance for random noise.

3.1. Coherent Signal or Noise Components

It was shown in Section 2 that seismic signal and noise components cover a wide range of apparent velocity and wavelength as well as the full azimuth range. If the velocity is unknown, a single line array cannot be phased to receive signals from a unique azimuth. The array must extend into at least two dimensions if azimuth and velocity information are required.

Referring to Fig. 2, phase shifts are incurred between adjacent seismometers when a coherent signal component is propagated across the array. For the signal component shown, the phase shifts are $2\pi(d/\lambda)\cos\theta$ in line A and $2\pi(d/\lambda)\sin\theta$ in line B, where λ is the apparent wavelength at the earth's surface. These phase shifts can be cancelled for the complete frequency range by inserting delays so that a required

signal is in phase at all outputs. For a signal component of apparent velocity V_1, azimuth θ_1, the delays required are equal to $(d/V_1)\cos\theta_1$ and $(d/V_1)\sin\theta_1$ in lines A and B respectively. When a signal is received from another azimuth θ and/or with another apparent velocity V, nett phase shifts occur between the seismometer outputs which cause a reduction in amplitude on summation. The nett phase shift between adjacent seismometers in line A is given by

$$\Delta_A = 2\pi\left(\frac{fd}{V}\right)\cos\theta - 2\pi\left(\frac{fd}{V_1}\right)\cos\theta_1 \quad ......(1)$$

Equation (1) may be rewritten

$$\Delta_A = 2\pi\frac{d}{D}\left(\frac{D}{\lambda}\cos\theta - \frac{D}{\lambda_1}\cos\theta_1\right) \quad ......(2)$$

Similarly for line B

$$\Delta_B = 2\pi\frac{d}{D}\left(\frac{D}{\lambda}\sin\theta - \frac{D}{\lambda_1}\sin\theta_1\right) \quad ......(3)$$
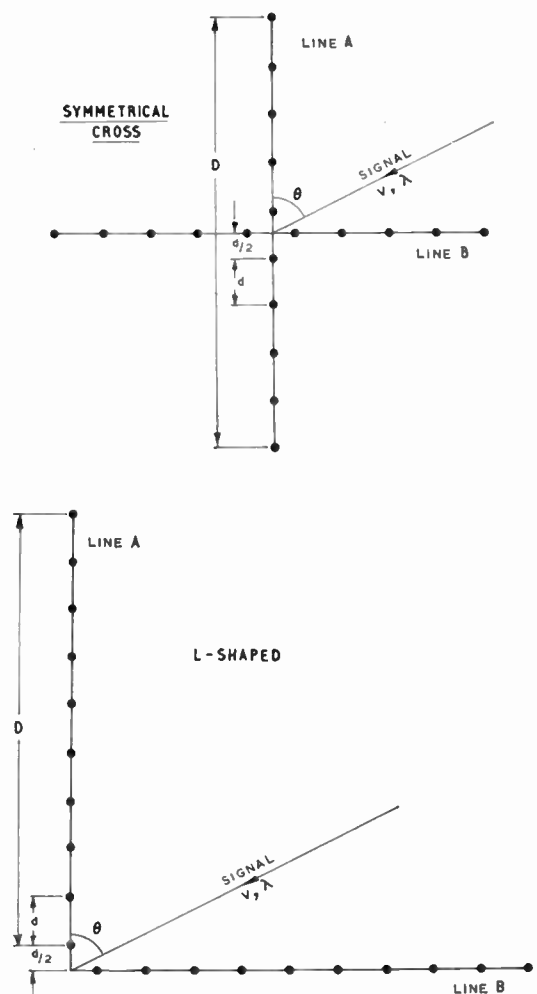

Fig. 2. Array configurations.
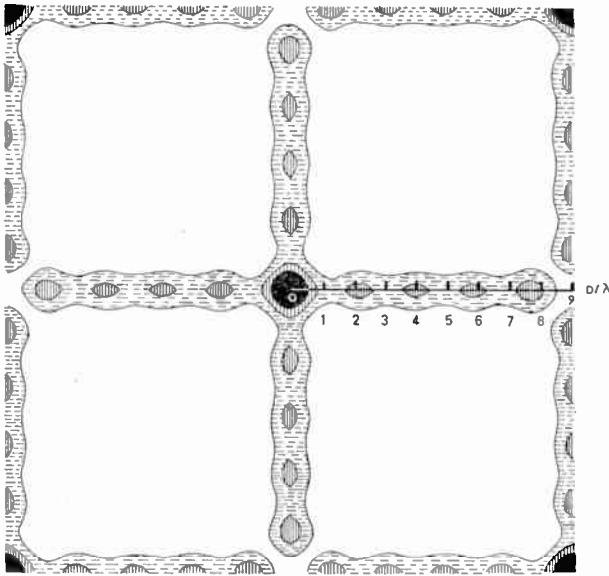
+ ½ to + 1

+ ¼ to + ½

+ ¹⁄₁₆ to + ¼

Fig. 3. Sum squared response of symmetrical cross array. $m = (n-m) = 10$.

It must be stressed that, in eqns. (2) and (3), λ and λ_1 are apparent wavelengths at the Earth's surface and correspond to the same frequency. Normally the signals of interest cover at least an octave in frequency, and hence a corresponding range of at least $2 : 1$ in the values of λ and λ_1. The effect of this is discussed later in this Section.

The normalized responses of lines A and B are then given by

$$E_A = \frac{\sin(m\Delta_A/2)}{m\sin(\Delta_A/2)} \qquad \ldots\ldots(4)$$

$$E_B = \frac{\sin[(n-m)\Delta_B/2]}{(n-m)\sin(\Delta_B/2)} \qquad \ldots\ldots(5)$$

where $m = (n-m) = 10$ for the arrays considered.

The total, normalized sum-squared response for a symmetrical cross array is thus given by

$$E_n^2 = \left[\frac{\sin(m\Delta_A/2)}{m\sin(\Delta_A/2)} + \frac{\sin[(n-m)\Delta_B/2]}{(n-m)\sin(\Delta_B/2)}\right]^2 \bigg/ 4 \ldots(6)$$

It is convenient to show the responses in polar form $(D/\lambda, \theta)$ for zero inserted delays, i.e. for $D/\lambda_1 = 0$. The diagrams are then normalized in terms of the array dimensions and are independent of the phasing conditions. Figure 3 gives the sum squared response of eqn. (6) in this form for the 20-element symmetrical cross array shown in Fig. 2. The response is in the form of contours, which correspond to fixed values of attenuation relative to the in-phase condition at the origin. Normally, far more contours would be required than those shown, and colours used to avoid confusion.

The response for an unphased array, (zero delays), may be obtained for a given azimuth as a function of D/λ simply by constructing a line from the origin at the appropriate value of azimuth and noting the values of D/λ corresponding to the points of intersection with the contours. Figure 4 shows the continuous responses derived from eqn. (6) for $\theta = 0$ and $\theta = \pi/4$. These may be compared with the contoured diagram, and it is clear that more contours are needed. From Figs. 3 and 4 it can be seen that the attenuation is low for directions normal to either of the line arrays.

The use of the polar diagrams when delays are inserted can be seen from inspection of eqns. (2) and (3). The terms inside the brackets, e.g. $(D/\lambda)\cos\theta$, represent the projections of the signal vectors $(D/\lambda, \theta)$, $(D/\lambda_1, \theta_1)$ on the axes of the array ($\theta = 0$ and $\pi/2$). The nett phase shift in each line corresponds to the difference vector. Thus, when the array is phased to $(D/\lambda_1, \theta_1)$, the response for any signal $(D/\lambda, \theta)$ may be obtained directly after moving the origin to the
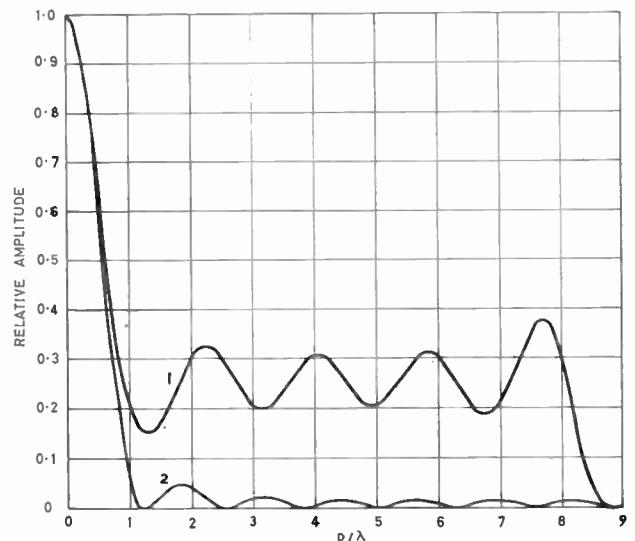

Fig. 4. Sum squared response of symmetrical cross array. $m = (n-m) = 10$. Curve 1: $\theta = 0$; curve 2: $\theta = \pi/4$.
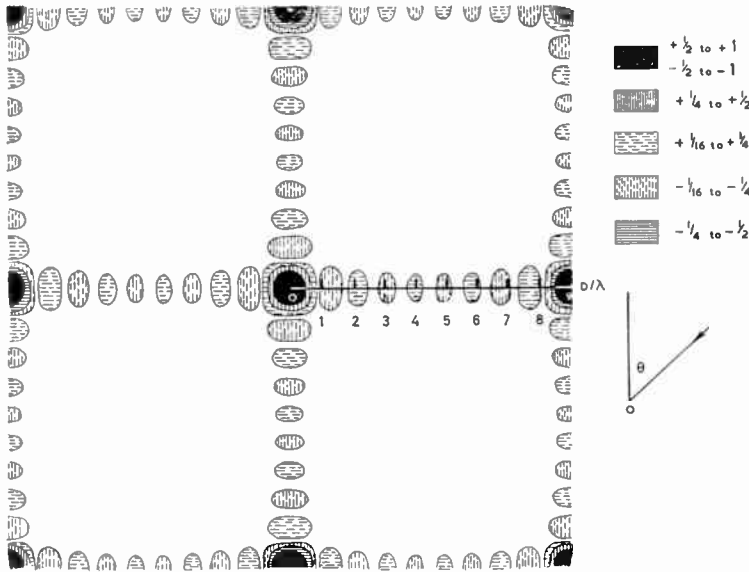
point $(D/\lambda_1, \theta_1+\pi)$. This is illustrated by Fig. 5. Point B represents the new origin for a given value of λ_1, corresponding to apparent velocity V_1 and frequency f_1. The distance AB is thus equal to D/λ_1, i.e. $f_1 D/V_1$. The locus of the signal vector $(D/\lambda, \theta)$, i.e. $(f_1 D/V, \theta)$, is a circle for a constant value of V_1/V and variable θ. When $V_1/V = 1$, the circle passes through A at $\theta = \theta_1$, representing the in-phase condition. Alternatively, if the value of θ is maintained constant at θ_1, whilst the value of V_1/V is varied, the locus of the signal vector $(f_1 D/V, \theta)$ is a line from B passing through A. The distance from B along this line is proportional to V_1/V, point A corresponding to $V_1/V = 1$.

Fig. 5. Locus of signal vector (V, f, θ) for tuned array.

If the values of V_1 or f_1 are changed, the value of λ_1 will be different (λ_2, say). The displaced origin will move from point B to point C (Fig. 5), where $AC = D/\lambda_2 = f_2 D/V_2$. If $V_2 = V_1$ then $\dfrac{AC}{AB} = \dfrac{f_2}{f_1}$; the locus of the signal vector for fixed values of (V, θ) will move from point D to point E, where the projection of ED passes through the origin A. The loci of the signal vector for frequencies intermediate between the limits f_1 and f_2 lie on the line DE at a distance from A proportional to frequency. The output of the array can thus be determined as a function of frequency if the spectrum of the signal is the same at all seismometers and is known. Determination of the total signal power involves an integration along

DE, which smoothes the response and renders narrow, isolated peaks of low attenuation less important.

Whilst θ and V are defined as the azimuth and velocity of the signal component, and θ_1 and V_1 as the values to which the array is phased, the definitions can be interchanged when desired. The interchange of θ and θ_1 simultaneously with λ and λ_1 in eqns. (2) and (3), results in phase shifts of the same amplitude but opposite polarity. The array response is identical, however.

3.2. Application of Correlation Methods for Coherent Signals

The sum-squared response for a cross array is unsatisfactory, since it has low attenuation for unwanted signals which are in phase in either line, even when they are rejected by the other. The responses can be considerably improved by cross correlating the summed outputs of the two lines. This involves multiplying the summed outputs and averaging the product over a period of time T_1. Alternatively, the averaging may be accomplished using an exponential integrator of time-constant T_1, which gives greatest weight to the most recent information. The mean correlator output is proportional to the product of the individual responses of the two summed line arrays, and the cosine of the phase difference between the centre points. The normalized correlator output is given by:

$$2\varphi_{AB} = \frac{\sin(m\Delta_A/2)}{m\sin(\Delta_A/2)} \frac{\sin[(n-m)\Delta_B/2]}{(n-m)\sin(\Delta_B/2)} \times$$
$$\times \cos[(D_A\Delta_A - D_B\Delta_B)/d)] \quad ...(7)$$

The responses given by equation (7) for the symmetrical cross and L-shaped arrays are shown in polar form by Figs. 6(a) and (b). They are considerably better than the sum-squared responses, although the contours of least attenuation still occur in directions normal to the array axes. The normalized correlator response for the symmetrical cross array remains the same if one of the arms is deleted, resulting in a T-shaped array. This configuration has not been adopted by the author since the summed outputs of the individual lines are also used, and the response of the reduced line is inferior.

The contoured correlator responses are used in the manner described in Section 3.2. Comparing Figs. 6(a) and (b), it is seen that the response is sharper for the L-shaped array, i.e. the area within the high-level contours is smaller. The response of this array is asymmetrical, with the width of the centre peak considerably reduced in directions $3\pi/4$ and $7\pi/4$. This results in a much sharper velocity response in these directions, whilst the sharpest azimuth response occurs in directions $\pi/4$ and $5\pi/4$.

■	$+\frac{1}{2}$ to $+1$
	$-\frac{1}{2}$ to -1
	$+\frac{1}{4}$ to $+\frac{1}{2}$
	$+\frac{1}{16}$ to $+\frac{1}{4}$
	$-\frac{1}{16}$ to $-\frac{1}{4}$
	$-\frac{1}{4}$ to $-\frac{1}{2}$

Fig. 6(a).
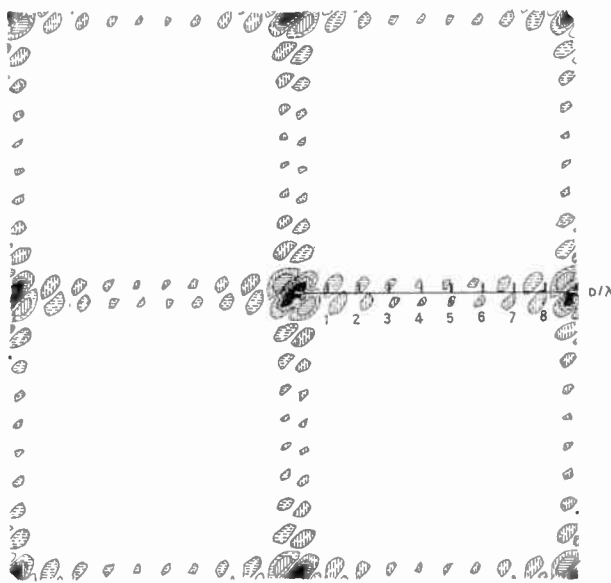Correlation response of symmetrical cross array.
$m = (n-m) = 10$.

Fig. 6(b). Correlation response of L-shaped array.
$m = (n-m) = 10$.

3.3. *Azimuth and Velocity Responses*

The method previously described for obtaining the mean correlator output as a function of velocity or azimuth using the contoured response only gives a number of points corresponding to the contour values. The continuous curves can be determined for a given set of conditions directly from eqns. (2), (3) and (7), where $\lambda_1/\lambda = V_1/V$. Figure 7 gives an example of an azimuth response for the L-shaped array previously considered. The value chosen for θ_1 (i.e. zero) gives

approximately average beamwidths. From this curve it is seen that for $d/\lambda = 0 \cdot 1$, i.e. for wavelengths equal to the effective length of the lines, the beamwidth at the half maximum output level is 36 deg. This corresponds to 72 deg for a symmetrical cross array. For shorter wavelengths the beamwidths are correspondingly smaller.

Figure 8 gives an example of a velocity response for the L-shaped array for $\theta_1 = 0$. The values of V_1/V for the half maximum output level are 0·70 and 1·30 for $d/\lambda = 0 \cdot 1$. The corresponding values for a symmetrical cross array are 0·38 and 1·62. For sharp velocity filtering with high attenuation of signals from the same azimuth it is clear that the dimensions of the array should be at least equal to several signal wavelengths. Excessive dimensions are likely to result in a loss of signal amplitude due to lack of signal coherence.

3.4. *Azimuth and Velocity Determination*

The United States Coast and Geodetic Survey publishes bulletins giving details of a large number of earthquakes recorded by the world-wide net. These details include computed epicentres; hence, in a research programme where events are analysed some time after being recorded, the azimuth of the signal is usually known. The signals are then processed by inserting delays which correspond to the known azimuth, and a suitable range of velocity. The apparent velocity of an isolated signal component may be determined by noting the value corresponding to the maximum correlator output at a given time. When the signal is affected by an earlier arrival of different velocity and/or azimuth, the change in correlator output (referred to as 'the differential
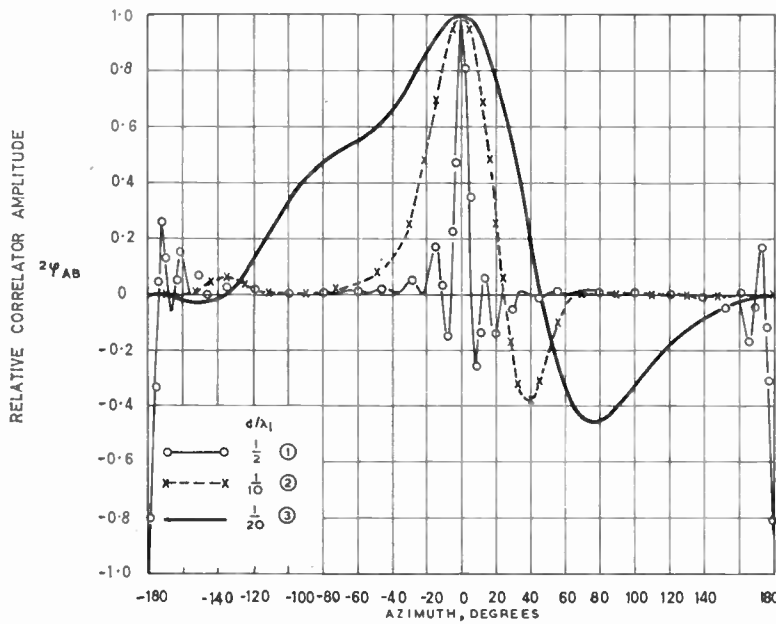
Fig. 7. Correlator azimuth response for L-shaped array.
$\theta_1 = 0; m = (n-m) = 10;$
$V = V_1; D_A = D_B = 5d.$
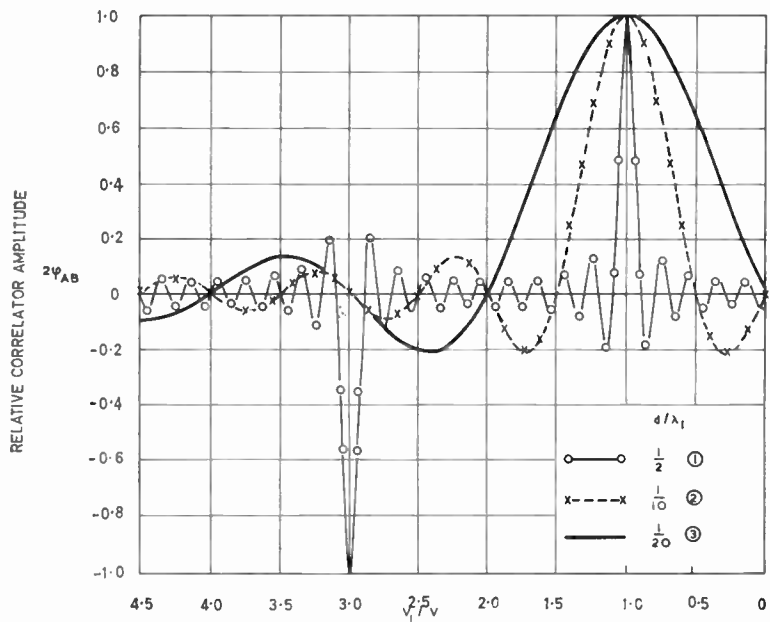
Fig. 8. Correlator velocity response for L-shaped array.
$\theta_1 = 0.$

correlator output') should be measured as a function of velocity. This uses the correlator output immediately before the arrival of the signal component of interest as a base-line.

When the azimuth of the signal is unknown, the signals are processed by inserting delays corresponding to variable azimuth for several fixed values of velocity in the range of interest. If the actual velocity is appreciably different from that to which the array is phased, the correlation peak may be substantially reduced, or even displaced if the response is asymmetrical (as for the L-shaped array). In general, the larger the dimensions of the array, the sharper will be the array response, and the larger the number of values of velocity required when carrying out the azimuth search.

3.5. Errors in Azimuth and Velocity Determination

Errors in azimuth and velocity determination may arise from geophysical causes. Reflections from vertical discontinuities may cause deviations from the true azimuth, whilst non-uniform layering within the crust will affect the apparent ground velocity. A simple example of the latter case occurs when the

Mohorovicic discontinuity at the base of the crust is inclined. Allowance for errors of this kind can be made by crustal calibration methods.

Errors may also be introduced by incorrectly assessing the position of the peak correlator output. The accuracy to which this can .be ascertained depends upon the beamwidth, which in turn depends upon the ratio of the wavelength to the dimensions of the array. It also depends upon the azimuth or velocity increments used in computing the correlation function; interpolation errors will occur if these increments are too large. Another factor, which occurs in a digital analysis system, is the effect of quantization noise produced on the correlation function by inserting delays which can only be an integral product of the sampling time interval. For this reason, it is desirable to use a sampling rate of at least 10 samples per cycle of the dominant frequency. Another important source of error is the effect of interfering coherent signals. Even when the differential correlator output is used for azimuth and velocity determinations, the curve may be affected by cross-product terms. This is because the signals are often of short duration, and short averaging times must be used. For this reason, undue reliance must not be placed upon the values of velocity and azimuth determined for weak arrivals in the presence of strong interfering coherent signals or noise, except where these are considerably attenuated in the summed outputs of both lines in the velocity range of interest.

3.6. *Random Noise*

The problem of discriminating against random noise is mainly restricted to the detection of the signal onset in the presence of locally-generated seismic noise (for example, caused by wind). However, part of the noise generated by a signal in the vicinity of the recording station may also be random in character, and of sufficient amplitude to confuse subsequent wavetrains.

If the seismometer outputs each consist of a coherent, in-phase signal of variance σ_s^2, and random noise of variance σ_n^2, then the power signal/noise ratio is improved by a factor equal to the number of seismometers when the outputs are summed. If the variances of the signal and noise outputs of the seismometers differ, then the output should be weighted in proportion to $\sigma_{sr}/\sigma_{nr}^2$. The resultant power signal/noise ratio is then a maximum, and is equal to the sum of the individual power signal/noise ratios.

The advantages of using correlation methods are limited by the relatively short duration of the signals, which may only contain a few cycles. Furthermore, even when signals are of long duration, the increase in signal/noise ratio by the use of long correlator averaging times does not improve the accuracy of

determining the signal onset, which is one of the main requirements.

In using correlation methods for detecting the presence of a signal in random noise in the output of a cross array, the following methods may be adopted:

(*a*) Compute and sum the cross-correlation integrals of all possible pairs of seismometers as a function of recorded time, applying appropriate time shifts to phase the wanted signal.

(*b*) Compute the mean-square value of the summed output of the whole array as a function of recorded time with appropriate phase shifts.

(*c*) Cross-correlate the summed outputs of the two lines of seismometers continuously as a function of recorded time and with correct phasing. (As in Section 3.2.)

Method (*b*) differs from method (*a*) in that the computed output contains the sum of the mean powers of all seismometer outputs in addition to the sum of the correlation integrals of all possible pairs. Thus if bursts of noise occur, e.g. due to gusts of wind or tape faults, the output will contain a positive pulse which may be mistaken for a signal.

The correlator output signal/noise ratio may be defined as the ratio of the mean correlator output to the standard deviation after the arrival of the signal. If the array comprises n seismometers with in-phase signals of equal variance σ_s^2, and random noise of equal variance σ_n^2 with a flat frequency spectrum over a band Δf, and zero elsewhere, then for a correlator averaging time T_1:

Method (*a*)
correlator s/n ratio :

$$= (2\Delta f T_1)^{\frac{1}{4}} \frac{\sigma_s^2}{\sigma_n^2} \frac{(n(n-1)/2)^{\frac{1}{4}}}{(1+2(n-1)\sigma_s^2/\sigma_n^2)^{\frac{1}{4}}} \quad \dots (8)$$

Method (*c*), for two lines of $n/2$ seismometers
correlator s/n ratio :

$$= (2\Delta f T_1)^{\frac{1}{4}} \frac{\sigma_s^2}{\sigma_n^2} \frac{n}{2(1+n\sigma_s^2/\sigma_n^2)^{\frac{1}{4}}} \quad \dots\dots (9)$$

For high values of σ_s^2/σ_n^2, the correlator output signal/noise ratio is the same in each case, namely:

$$\text{correlator s/n ratio} \simeq \left(\frac{n\Delta f T_1}{2}\right)^{\frac{1}{4}} \frac{\sigma_s}{\sigma_n} \quad \dots\dots (10)$$

For very low values of σ_s^2/σ_n^2, such that $2(n-1)\sigma_s^2/\sigma_n^2 \ll 1$, the signal/noise ratio is a factor of $\sqrt{2}$ higher for method (*a*). However, experiments with a range of input signal/noise ratios showed a negligible difference in the probability of correctly detecting the signal onset for the three methods (*a*), (*b*) and (*c*).
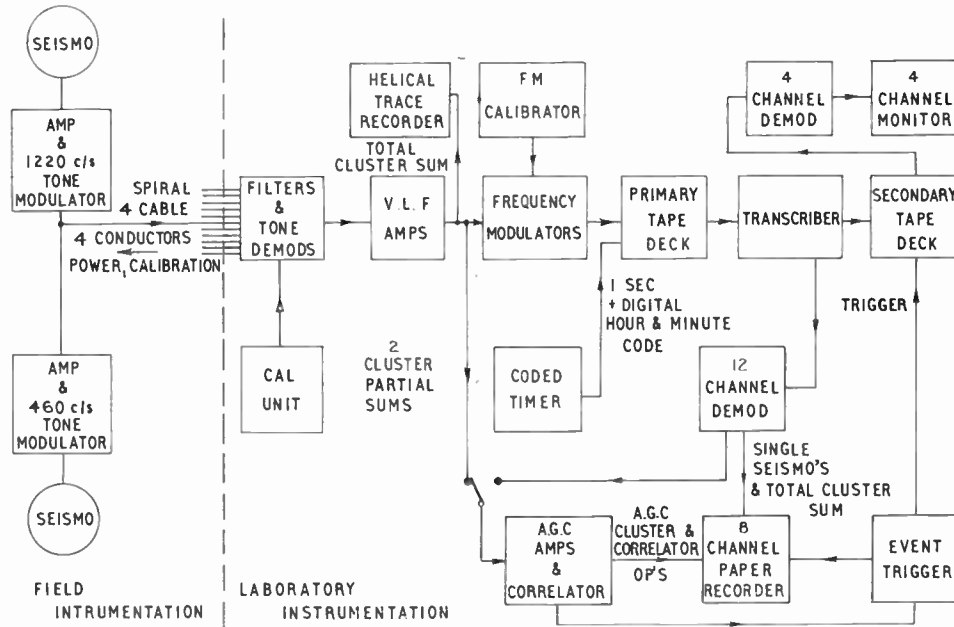
Fig. 9. 'Yellowknife' recording system.

4. Instrumentation

4.1. Experimental Arrays

The first experimental cross array was established on Salisbury Plain in February 1961, and recordings made of depth charges detonated at distances of 100–200 km. The energy recorded from these explosions travelled mainly in the Earth's crust. The array comprised two lines of six seismometers spaced at 350-metre intervals. The apparent signal wavelengths concerned were in the range 1–2 km. The results from these experiments showed the practical feasibility of using an array to facilitate the separation and identification of the various seismic signal components.

A second array was installed at Pole Mountain, Wyoming, U.S.A., in December 1961, comprising two lines of seven seismometers spaced at intervals of 1·5 km. The array was operated for nearly two years, and a considerable number of explosion and earthquake records obtained. Many of these were processed using the techniques described. A third array was established at Eskdalemuir, Dumfriesshire, and has been in operation since June 1962. The array and recording system has been described by Truscott.[†] A fourth array with larger dimensions was installed at Yellowknife, in Northwest Territories, Canada, in conjunction with the Canadian Department of Mines and Technical Surveys. This array now comprises two

lines of ten seismometers, with 2·5 km spacing, and is designed primarily for the recording and analysis of teleseismic events (ranges > 25°).

Detailed papers on the array recording and analysis systems were presented at the I.E.R.E. Symposium on "Modern Techniques for Recording and Processing Seismic Signals" held on 13th May 1964.[‡] It is, therefore, proposed to give only a brief description of the recording and analysis systems in this paper.

4.2. Yellowknife Recording System

The block diagram of the Yellowknife recording system is given in Fig. 9. Willmore Mk. II Seismometers are used, recording the vertical component of earth motion. The seismometers are at present adjusted to have a natural period of 1 second, and have a substantially flat velocity response for frequencies above 1 c/s. The seismometers are installed in pits on level concrete platforms well grouted to the bedrock. The output signals are conveyed to senders installed in the pits, where they are amplified and used to amplitude-modulate audio carriers. The modulated tones are transmitted along semi-armoured cable to the recording station. Economy in cable costs is effected by using different carrier frequencies for

---

† J. R. Truscott, "The Eskdalemuir seismological station", *Geophysical Journal of the Royal Astronomical Society*, 9, No. 1, pp. 59–68, October 1964.

‡ D. Platt and W. Mowat, "Earthquake recording systems". J. R. Truscott, "Approaches to seismological array processing". W. Hutchins, "A real-time seismic data processor and its associated event selector".

adjacent pits, and feeding two signals down one pair in the cable. Further economy is not possible owing to the problem of supplying the pit instrumentation with power, which is conveyed over the same cable. A second pair in each cable is used for seismometer and system calibration. The signals are demodulated in the recording station, amplified and recorded continuously on separate tracks of 1-in magnetic tape using frequency modulation. The carrier frequency in this case is 270 c/s, and the recording speed 0·3 in per second. In addition to the seismometers in the cross array, a close spaced cluster of 24 seismometers is being installed. This cluster is 1·8 km in diameter, with seismometers spaced as uniformly as practicable over the area. The seismometer outputs will feed pre-amplifiers in the pits, and will be summed in two groups of twelve in the centre of the cluster. The summed signals will be recorded on the primary tape deck, and also supplied to an on-line correlator. This correlator will not provide phase shifts, and will give maximum output for coherent signals which have a large wavelength relative to the dimensions of the cluster. It will be used for detecting such signals in the presence of noise, and supplying trip pulses to a second tape deck and a relatively high speed paper recorder. These will record the output signals from replay heads mounted on the primary tape deck. A delay of about 18 seconds is incurred between the record and replay heads of the primary tape deck, enabling the signal onsets to be recorded on the triggered recorders. In this way edited tape and high quality paper records will be obtained for nearly all events of interest, thereby reducing transcription and playback requirements at the central analysis facility. The correlator uses automatic gain control to allow for long term variations in the ambient noise, and will be adjusted so that the number of spurious trips due to noise is about 10 per day. A similar on-line correlator is operating successfully at Eskdalemuir.

Time is recorded from a coded timer which produces one second, ten second and one minute markers. Absolute time in minutes, hours and days is recorded each minute by means of a digital code. The edited tape and paper records will therefore only need to be a minimum of 1 minute in duration for absolute time to be recorded. The drift is in the region of 10 milliseconds per day, i.e. one part in 10^7, and facilities are incorporated to correct this against transmitted time standards.

4.3. *Analysis Instrumentation*

An analogue system has been used up to the present time for processing all the array data. In this system the f.m. signals are transcribed repeatedly from a storage loop tape deck on to a delay loop tape deck.

This uses a loop of 1½-in wide magnetic tape, with replay heads staggered at regular intervals. The incremental delay incurred is varied by adjusting the servo-controlled tape speed after each pass of the record. The incremental delays required for the two lines are seldom in a simple ratio, and quantization errors are introduced in selecting the nearest head positions for the seismometer signals. On replay from the delay deck, the signals are demodulated and passed through a bank of adjustable band-pass filters to a PACE analogue computer type 231R. This is used to equalize the signal amplitudes, to sum the seismometers into two groups, and to compute the cross-correlation integral as a continuous function of recorded time for each value of azimuth and velocity. In order to obtain the correlator output as a function of velocity or azimuth at a fixed time, it is necessary to make measurements on a series of processed records.

A new system is under development which will process the data for 20 search conditions in real time. It will provide correlator outputs which are a function of recorded time for each search condition, and also a histogram display which will show the correlator output as a function of search conditions. Phased sum outputs will also be available for each search condition. The system contains an analogue input section, with facilities to apply frequency filtering and to equalize the signal amplitudes of the individual channels. The outputs are then sampled sequentially at a mean rate of 20 samples/second per channel. The samples are converted into ten-bit words and read into a 4096-word core store. This store holds the data for a total of about 9 seconds, during which time it is regressed through the store. Delays corresponding to 20 search conditions are inserted by selecting appropriate cores in the matrix in accordance with a program stored in a separate core store. The words are sequentially read out of the data store in order of channel number and search condition. Summation and multiplication is carried out digitally, the output converted back to analogue form and separated into channels corresponding to the search conditions. Phased sum outputs are then available for display. The correlator outputs are individually smoothed and are also available for display. They are also sampled sequentially to give a histogram output, from which a rapid assessment of azimuth or velocity can be made.

5. Experimental Results

Many events have been analysed using the techniques described. The detailed presentation and discussion of these results is more appropriate to a geophysical journal. Figure 10 shows a simple example of the use of velocity determination. The
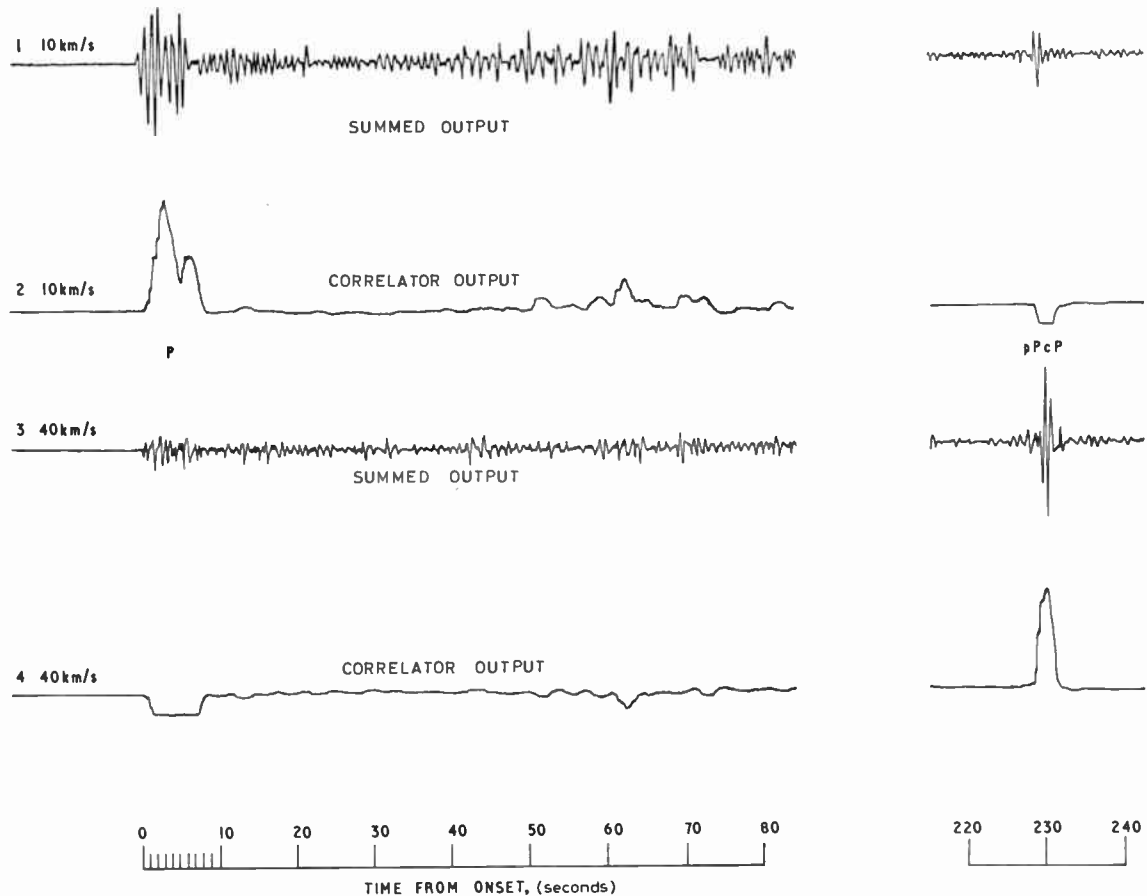
Fig. 10. Fox Island earthquake.

earthquake was recorded on an array at Yellowknife comprising two lines of 4 seismometers spaced at intervals of 5 km, one seismometer being common. The signals were processed for a range of velocity for the correct azimuth, which was known beforehand. The total phased sum and correlator outputs are shown for the signal onset, and for a burst of energy which occurred later in the record. It can be seen from these records that the second arrival has a much higher velocity. Figure 11 shows the correlator outputs as a function of velocity at a fixed time shortly after the signal onset, and at another fixed time during the second arrival. The curves have been normalized in amplitude and also to the velocity V_1 at which the correlator peaked, namely 10·8 km/s for the signal onset and 43 km/s for the second arrival. Comparing these curves with the curves of Fig. 8, it is seen that curve 1 should be more symmetrical. The response is much sharper than for the second arrival, owing to a difference in wavelength. The signal onset is the direct P wavetrain, which is expected to have an apparent ground velocity of about 12·5 km/s at this range. The second arrival is deduced to be pPcP, i.e. a P wavetrain which has been reflected first at the Earth's surface and then at the core without mode conversion. This deduction closely fits the travel time for the depth given (202 km), whilst the calculated ground velocity (43 km/s) is in agreement with the value obtained. The absence of PcP, the direct reflection from the core, is attributed to the radiation pattern of the source.

6. Conclusions

Linear cross arrays have been operated successfully during the past three years, accumulating data from large numbers of seismic events. Analysis of selected events has shown that velocity and azimuth filtering techniques can usefully be employed to give enhancement of required signal components relative to noise and interfering signals. In addition, the velocity and azimuth information obtained aids their identification. The use of correlation methods is essential if a good azimuth or velocity response is required, although they do not result in a substantial improvement against
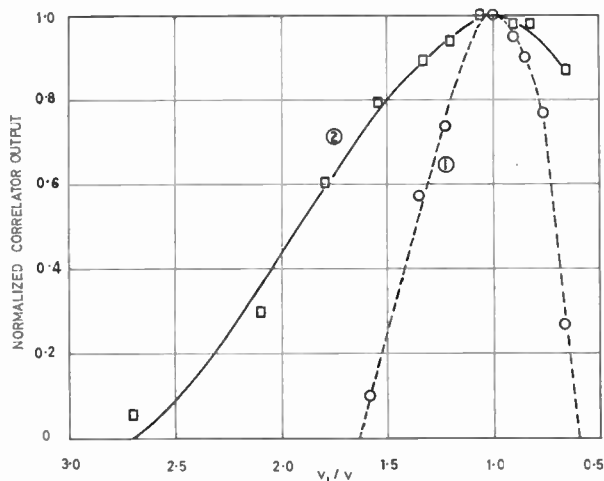
Fig. 11. Experimental correlator velocity response, Fox Island event. Curve 1: P wave arrival, $V_1 = 10\cdot8$ km/s; curve 2: pPcP arrival, $V_1 = 43$ km/s.

random noise compared to the summed output because of the short duration of the signal. An L-shaped array has a sharper response in general than a symmetrical cross array which has lines of the same length. Its response is asymmetrical, however, and may introduce errors in azimuth determination if this is carried out at an incorrect velocity. An accuracy

of a few degrees in azimuth, or a few percent in velocity, is feasible when the signal wavelengths are comparable to the length of the lines. Much greater accuracies are theoretically possible by increasing the dimensions of the array, but this will depend very much upon the homogeneity of the earth's crust under the recording site and the distance to the epicentre.

There appears to be little likelihood of being able to design a single array which gives a sufficiently accurate estimate of the location of the epicentre at teleseismic distances. For example, an accuracy in azimuth determination of about $\pm0\cdot1$ deg, corresponding to ±10 km, would be required at a great circle distance of 90 deg. Furthermore, a determination of range would require the measurement of the onset time of at least two suitable seismic signal components (e.g. P and S), to an accuracy of about $0\cdot1$ second, with a corresponding accurate knowledge of travel time data for the path concerned.

7. Acknowledgments

DISCUSSION

Under the chairmanship of Dr. R. Benjamin

Dr. B. S. McCartney: The contour responses for the symmetrical cross and L-shaped arrays show peaks along the two axes, whilst the contours for concentric ring arrays tie in similar concentric rings. Is there any deep significance in this relationship?

Mr. F. E. Whiteway (*in reply*): When a coherent signal component is received from a direction at right angles to an unphased line array, the seismometer outputs are in phase and no attenuation occurs in the summed output. The correlator response, is, therefore, determined by the product of the response of the in-line array and the cosine of the phase angle between the centre points of the two lines. At directions other than those normal to one or other of the lines, the signals are out of phase in both lines, and the contour levels are much lower. The sum-squared response of a solid pattern rectangular array would be of similar form.

The concentric ring configuration shown on a slide at the symposium consists of a ring of 6 seismometers inside a second ring of 12 seismometers. The array has circular symmetry, consisting of six identical sectors. The response

of the summed array for any given direction is, therefore, identical to that for azimuths displaced by multiples of 60 deg. This results in the circular shaped response shown at the symposium, the contours being repeated every 60 deg.

Dr. K. Milne: Could Mr. Whiteway give a little more detail of the possibilities of determining angle of arrival, etc., by correlating seismic records with records of past events?

Mr. Whiteway (*in reply*): The cross-correlation coefficient for seismic records from any two events is usually very low, since the signal waveforms are affected by source characteristics, depth and propagation path. The only cases where previous records are likely to be of assistance is in detecting explosions from the same location.

Dr. D. Herbison-Evans: Mr. Whiteway considers the response of an array projected on to the horizontal plane. As an electromagnetic aerial designer, I think in terms of an array's three-dimensional polar diagram, and hope I may be forgiven for talking this way.

Which form of noise predominates: coherent or incoherent; is it of P or S type? If coherent noise is important, is there any variation in its magnitude with angle of arrival for the two wave types? I gather that, so far, processing has been such as to synthesize 'uniformly illuminated' arrays. Has any thought been given to 'tapering'? This may be used to take advantage of any anisotropy of the received coherent noise distribution.

A wideband signal is to be detected. Is the medium dispersive to S or P waves over the frequency band of interest? If there is a variation of velocity such as to reduce the dependence of wavelength on frequency, this would simplify directional synthesis.

An alternative approach, using the computer, would be to filter the output of each element into a number of narrower bands by Fourier analysis, synthesize the array for each band separately, and then reconstruct the signal by adding the array Fourier components together. It would be possible in principle to extend this type of analysis and synthesis to reproduce the response of a supergain array, which could give any desired signal/noise ratio up to a limit set by the degree of signal incoherence. An optimum trade-off would be determined in practice by data accuracy, increased search time due to the narrow beamwidth, and increased processing time due to multiple frequency channels. This procedure may be of use when the various types of signal from an event overlap.

Is the medium isotropic around the detectors for the two types of wave? No mention is made of vertical arrays. They have the advantages of horizontal compactness and the possibility of synthesizing an angular response with a horizontal nodal plane. Have these been considered?

Mr. Whiteway (*in reply*): The angle of incidence of a seismic signal to the vertical is dependent upon the type of wave propagation (body or surface wave), and also on the medium immediately underneath the station. Therefore, it is more convenient in the case of a two-dimensional array to express the responses in terms of apparent surface velocities and wavelengths, which are unaffected by near surface velocities for horizontal layering.

The noise characteristics vary from site to site. Coherent noise is certainly important, and at Eskdalemuir it is mainly in the form of surface waves. At very quiet sites it is possible that coherent body wave noise from the mantle may predominate, but this has yet to be proved.

Some theoretical work has been carried out on tapering using a Dolph-Chebyshev optimum distribution, but this has not been used in the experimental results. Weighting would certainly be of value in reducing the amplitude of coherent noise when this predominates over random noise.

No dispersion has been observed in the case of seismic body waves. Consequently, there would appear to be no advantage in the Fourier analysis method suggested.

The medium in the immediate vicinity of any one detector can be considered to be substantially isotropic at a good site, although some variation may occur horizontally across the whole array, and considerable variation with depth (the dimensions of the arrays are comparable to the thickness of the crust). Faults, velocity gradients and discontinuities occur within the crust, resulting in a reduction of signal coherence across the array and the production of signal generated noise.

Experiments with single seismometers and also vertical arrays in boreholes are being carried out in the U.S.A. A useful signal/noise improvement can often be obtained, even in the case of single seismometers, due to the reduction of the amplitude of surface wave noise with depth. The problems are mainly technological, depths in the order of 10 000 ft being usually required for worthwhile improvements at frequencies of about 1 c/s. At least three boreholes would be needed if azimuthal information is required, and such an array would be costly.

HIGH-POWER V.L.F. RADIO STATION FOR N.A.T.O.

To augment the communications facilities of the North Atlantic Treaty Organisation, the British Post Office has been responsible for building a high-power very-low-frequency (v.l.f.) radio-telegraph station at Anthorn on the coast of Cumberland. The use of high power and a very low frequency is to ensure that the transmission will be as immune as possible from the effects of ionospheric disturbances.

The site, which is a disused airfield between the villages of Anthorn and Cardurnock on the Solway Firth, is particularly suitable for a v.l.f. station; it has an area of some 700 acres at the extremity of a peninsula in a region of fairly flat land of low resistivity, the subsoil is capable of supporting heavy mast loadings without undue difficulty, and an adequate public power supply is available.

Aerial System

The transmitter is located at the centre of the site and the aerial, which consists of 6 rhombic-shaped sections arranged in a radial formation and suspended from 13 masts 618–748 ft high, covers practically the whole site. Seen from the ground, it appears as a six-pointed star formed by six diamond-shaped panels radiating from the top of a 748 ft high centre mast. The points of the star are supported by six masts 618 ft high forming an outer ring with a radius of 2148 ft. The mid-points of the panels are secured by an inner ring of six masts, each 678 ft high and 1277 ft from the centre. Each corner of each panel is attached to a halyard through a tension insulator string. Thus the aerial system is completely insulated from the steel masts and their stays which are all connected to the station earthing system.

This arrangement of the aerial enables each section to be lowered to the ground for maintenance without fouling mast stays or any other obstruction. Each panel can be raised or lowered by 4 halyard winches, remotely operated from a control room on the roof of the transmitter building. The aerial has been built of steel-cored aluminium conductors about 1 inch in diameter to enable it to withstand the working voltage (120 kV) without perceptible corona under adverse weather conditions, and also be strong enough to support a heavy coating of ice. Should the ice loading on the conductors increase beyond a prescribed value, halyard tension-limiting gear will cause the winches to lower the aerial automatically so as to prevent the halyard tension rising above a safe maximum value.

The insulators at the four corners of each of the six aerial panels are attached to halyards which pass through sheaves at the mast heads and down to ground-mounted automatic winches. Each winch is fitted with upper- and lower-limit switches which allow the halyard to pay out when the tension reading reaches the predetermined load of 31 tons, equivalent to 62 tons at the mast head. The loading is registered on a dial on the appropriate winch and relayed to the 24 slave dials in the central control tower.

The aerial is insulated by strings of compression-type insulators so that failure of any unit insulator will not result in collapse of the aerial.

The galvanized steel masts are of conventional design, triangular in section, stayed in three directions at intervals of about 150 ft and pivoted at the base. The posts are of solid round section to minimize wind loading and will, in the worst case, transmit a maximum thrust approaching 1000 tons to the mast foundation.

The station earth is virtually a copper mat covering the whole of the site. It is made up of 8 s.w.g. soft copper wires laid horizontally at 9 to 12 in below ground. These radiate in lines from the centre mast with 2 degrees of arc between each line. This gives a total of 180 'rays' with alternate 'ray' lengths of 2000 ft and 3000 ft. All joints have been welded to obviate bi-metallic corrosion.
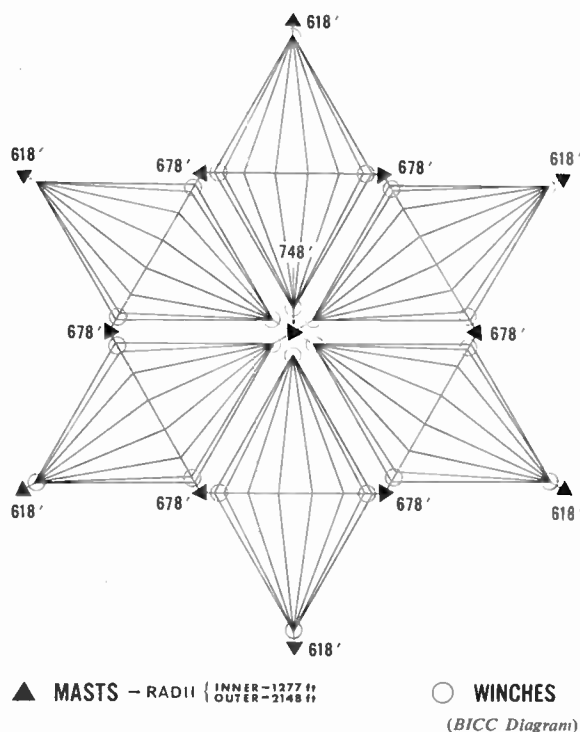
Layout of the aerial system at the N.A.T.O. V.L.F. station at Anthorn.

Transmitter and Building

The transmitter building, being at the centre of the aerial system, has been extensively screened against electrical losses and this screening is connected via a mesh of wires to the radial earth-wire system. All metal work in the building is bonded to the earth system.

The aerial is tunable over the frequency range 16–20 kc/s by variometers in series with a fixed helical inductor. One second variometer is automatically controlled to compensate for variations in aerial capacitance due to weather effects and so ensures that the aerial circuit is always tuned. These inductors are accommodated in a copper-lined room in the transmitter building and the
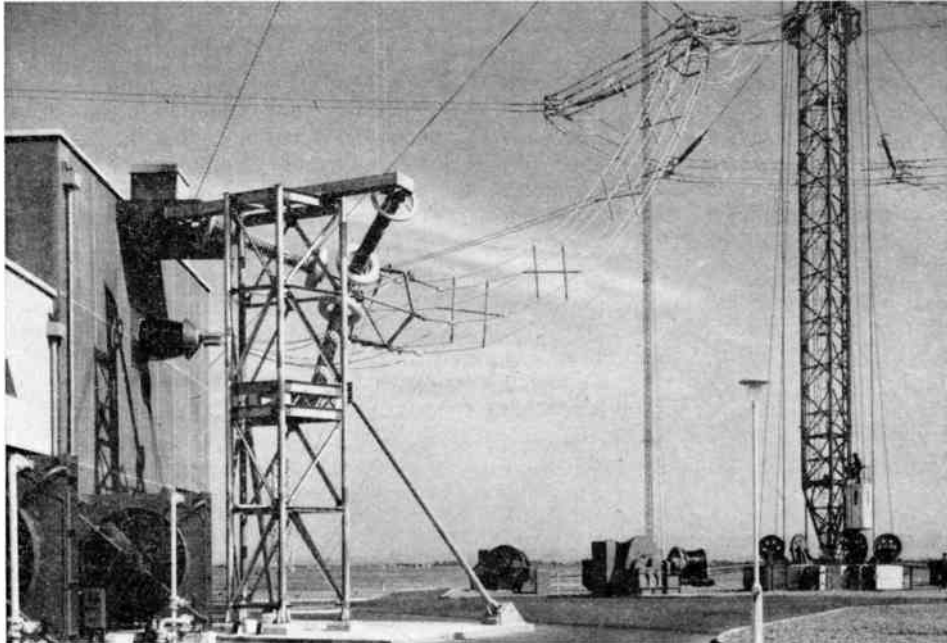
(*BICC Photograph*)

Conductor feeder from transmitter building to distributor ring
at the Anthorn V.L.F. Station.

lead-out to the aerial is taken via a large bushing in the wall of the inductor room.

The radio-frequency valves are air-cooled and the mercury vapour high-voltage rectifier valves are provided with overload protection equipment which will operate to remove power from the transmitter in about 5 microseconds. To avoid interruption due to failure of valves or other equipment, the transmitter is built of duplicate sections which can be worked individually or in parallel.

The tank-circuit for the output stage of each half of the transmitter comprises a fixed inductor of toroidal form connected in parallel with variable oil-filled capacitors. The use of the toroidal form for the inductor minimizes the external field and, therefore, the space required for this item. Coupling to the aerial-circuit is effected via matching networks which enable the aerial to be energized by either or both halves of the transmitter.

The frequency synthesis and drive equipment delivers 250 mW to the transmitter. The entire equipment is duplicated to provide main and standby facilities and fault detector circuits are incorporated to effect automatic changeover when necessary.

Output frequency of the 550 kW transmitter is controlled with an accuracy of at least 1 in 10^{10} per day (1 in 10^9 per month); the output frequency can be set in steps of 0·1 kc/s over the range from 16 to 20 kc/s.

Variable frequency oscillators are provided for use in conjunction with the frequency synthesizers to allow any frequency over the operating range to be set with an accuracy of one quarter of a cycle per second. The frequency synthesizer can be set from the control console to any of four preset frequencies in the operating range. These preset frequencies can be changed within a few seconds.

Any carrier frequency in the range 16–20 kc/s may be obtained from a frequency-synthesizer controlled by a highly stable crystal oscillator. Telegraph signals modulate this carrier in a drive unit, the output from which is applied to the low-power amplifying stages of the transmitter. The whole transmitter and aerial system is capable of operation at signalling speeds up to 50 bauds with frequency-shift (F1) or amplitude (A1) modulation, when F1 is selected, f.s.k. oscillator and driver units are employed which provide a deviation of up to 50 c/s per second.

Monitoring and control facilities are provided at a central control console enabling the transmitter to be started, stopped and tuned, operating conditions to be selected and the operation of the transmitter verified. Visible and audio alarms, showing a fault or abnormality in operation, are also included.

The power supply will normally be taken from the mains but two 600 kW generators are provided for standby purposes and these can be started remotely from the console. Each generator is connected so as to supply independently one half of the transmitter and miscellaneous loads.

DISCUSSION on

"Multiplicative Receiving Arrays"†

At the Symposium on "Signal Processing in Radar and Sonar Directional Systems" in Birmingham from 6th–9th July 1964

Under the Chairmanship of Dr. M. I. Skolnik

Dr. G. O. Young: What are the authors' opinions of the use of coherent (synchronous) demodulation rather than square law demodulation for both linear and product arrays?

Dr. A. Ksienski (*in reply*): It is quite clear that wherever possible coherent demodulation is to be preferred to other types of demodulation. In radio astronomy, for example, where the signal waveform is not known *a priori*, this is not possible. Even when the object field is illuminated by a known transmitted signal it may sometimes be difficult to obtain a reasonably good correlation between the transmitted and received signals due to target scintillation, Doppler, and medium effects. However, if a reasonably 'clean' return signal is received coherent demodulation is to be preferred. It should be pointed out that in the presence of multiple targets the resulting pattern will be rather complicated. From a study of such returns it is clear, however, that a significant resolution improvement is available although it is difficult in some cases correctly to identify the exact target situation. As to the question of which of the two (or more) targets does one lock on in phase, one may slowly sweep the local oscillator phase (or have a bank of parallel outputs each demodulating the incoming signal with a different lock-on phase). The returns from the individual targets will then peak when their correct phase is reached.

Dr. D. E. N. Davies (*in reply*): I doubt whether synchronous demodulation has any significant practical application to directional arrays except for certain special applications related to experimental measurements. This is owing to the fact that for more than one target the synchronous local oscillator cannot be simultaneously phase locked to the phases of several different sources or target returns. If on the other hand, the phase of the oscillator sweeps through all possible phases rapidly the resultant output is not truly demodulated at all and still requires envelope detection.

Professor D. G. Tucker: In both the papers by Mr. Blommendaal and by Dr. Ksienski much use is made of multiplicative arrangements, using one large and one small antenna. Now the signal/noise performance of such an

arrangement is limited to that of the smaller antenna. Does this mean that the practical radar applications are much more concerned with improved resolution than with signal/noise ratio? The sacrifice seems large.

Dr. Ksienski (*in reply*): There are some radar applications where signal/noise ratio is relatively high and one can afford to sacrifice some of it in order to obtain more detail. If, however, the signal/noise ratio is reduced too far one may lose rather than gain detail because the noise will begin to drown the signal.

In many radar applications even splitting the array into two equal parts is not permissible if the signal/noise ratio is marginal with the full array length.

Mr. R. Blommendaal (*in reply*): The signal/noise is indeed determined by the smaller antenna. In our application, which is a short range harbour radar, resolving power is all we are after. The drawback of the system can sometimes be compensated by extending the smaller antenna in the other plane.

Mr. A. G. Halliday: Would any of the authors care to comment on the problem of resolving more than two targets with a multiplicative system? More specifically, how well does such a system perform the resolution of a marked target in the presence of distributed clutter or reverberation?

Mr. Blommendaal (*in reply*): The response of a multiplicative system on a complex target distribution is very difficult to calculate, and depends on the character of the targets. From our first experiments we have the impression that improved resolution can be obtained in the presence of sea-clutter. We have to make sure, however, that this is not caused by the different vertical pattern of the multiplicative system.

Mr. E. Shaw (*in reply*): The performance of product arrays to distributed clutter is determined from their signal/noise performance since the signals received on each element due to isotropic returns from clutter or reverberation is uncorrelated between elements. It may, therefore, be grouped with array noise or other presummation noise. Calculated in terms of r.m.s. signal/noise ratios these arrays have a worse performance than an additive array followed by square or linear law detection. However, it would be useful if more calculations were available on the effect of these processes upon probabilities of detection. Some initial studies that we have made suggest that there is very little loss of probability of detection even at low signal/noise ratios and low false alarm rates.

Dr. Ksienski (*in reply*): I assume that Mr. Halliday is interested in a comparison between the performance of multiplicative and square law detected arrays. The problem

of multiple target interaction is quite complicated for both multiplicative systems as well as a square law detecting one which is a particular case of a multiplicative system. However, just as the single target response in a linear array may be used to deduce the response to a multiplicity of targets so can the two-target response be used for the prediction of the response of the multiplicative system to any number of targets. Thus superposition may be applied although here the responses to each pair of targets are added (these include both the self-terms of each target and the cross-terms between each two targets). In the case where the returns of the various targets are temporally uncorrelated due to scintillation or Doppler, the cross terms vanish under averaging and one may add the response to each separate target. Hence the statement that for incoherent returns the multiplicative system is linear in power, or that linear superposition may be applied to the power of the returns.

In the case of clutter a multiplicative system may be inferior to a square law detecting one due to the lower directivity of each of the antennas of the multiplicative array as compared to the square law detecting one which uses the full aperture. However, this will depend on the correlation between the clutter returns and that of the marked target. In the case of ground based radar the returns will in general be more highly correlated than in an airborne radar where averaging over several pulses may substantially suppress the interfering cross terms.

Dr. C. S. Clay: Do you feel that the result of looking at multiple source problems with point sources and fixed phases may be misleading relative to irregular sources. The usual display (i.e., p.p.i.) may present only envelope information and the actual result or display is the combination of many reflections. Should, or could the signals be averaged over a distribution function of phase to simulate the sequence of returns.

Dr. Ksienski (*in reply*): As mentioned in the answer to the question by Mr. Halliday, the two-target response is representative of the response to more complicated returns. As for the question of fixed phase or a variable phase averaged over several returns, both correspond to realistic situations. In the case of the return of a single pulse of rather small duration the relative phases may be considered fixed since very few targets scintillate at megacycle rates. If, however, a train of pulses is averaged, the relative phase between returns may be expected to change and perhaps fluctuate around some means phase difference ϕ. Thus in the figures shown throughout my paper one parameter is a fixed phase representing the mean phase difference and the other parameter, the correlation coefficient ρ, is representative of the fluctuation and integration time permitted. Averaging over a phase distribution has in fact been used with the distribution function assumed uniform over a specified interval. This interval was varied from zero for perfect coherence ($\rho = 1$) to an interval of 2π which corresponds to complete incoherence ($\rho = 0$). Other distribution may, of course, be assumed, although the results will probably be similar.

Mr. Shaw (*in reply*): The analysis involving point sources is probably quite relevant to stationary targets but

rather restricting in terms of its general significance; we have given some consideration to the possibility of removing the effects of extended targets by using an interferometer receiver which has a small response to a target extending over several interferometer lobes. This technique appears to fail for radar applications owing to the multiple reflections of large targets giving non-uniform reflections over the surface.

However, the complex reflections can in some instances assist resolution, since for such targets small changes of aspect can produce large rates of change of phase of the reflection and thus reduce the coherence between the reflections from two such targets.

Mr. L. C. Walters: I should like to know what progress has been made in determining optimum post-detection bandwidths for multiplicative systems. Unlike linear detection systems, multipliers lead to doubled bandwidths but noise distributions are presumably different from those obtained using square law detectors. It would seem that the optimum post-multiplier bandwidth is a function of signal/noise ratio but what function? Also how does signal/noise performance of a multiplicative system compare with that of square law or linear systems when each is optimized?

Dr. Davies (*in reply*): Only ideal synchronous demodulation does not increase the bandwidth of a signal. Both square law detection and multiplication double the bandwidth; however, the shapes of the demodulated spectra and noise distributions are different. I do not know of any work that has studied the optimum post-multiplier bandwidth for such application, but I would expect the optimum bandwidth to be not very different from that associated with square law detection. Published work on optimum bandwidths for radio astronomy correlators is not very relevant to radar applications.

Dr. Ksienski (*in reply*): A substantial amount of work was done by various researchers on multiplicative, or correlation arrays with respect to their signal/noise characteristics as compared to, for example, square law detecting arrays.[†] Hence, the discussion will be rather brief.

Regarding signal bandwidth, there is little difference between square law detection and multiplication since both parts of the multiplicative array carry the same signal (any time delay between them will be removed when the antenna is scanned towards the source). As to the noise it depends to some extent whether it is external (e.g. background) or internal (e.g. amplifier) noise. External noise arriving from the same direction as the source will be affected the same as the signal, otherwise its contribution will depend on its

† J. J. Faran and R. Hills, "The application of correlation techniques to acoustic receiving Systems", Acoustics Research Lab., Harvard Univ., Tech. Memo No. 28 (November 1952).

M. J. Jacobson and R. J. Talham, "Comparison analysis of four directional receiver correlators", *J. Acoust. Soc. Amer.*, **33**, pp. 518–26, April 1961.

V. G. Welsby, "The signal/noise gain of ideal receiving arrays", *Proc. Instn Elect. Engrs*, **109**, pp. 108–16, 1962 (I.E.E. Monograph No. 470E, September 1961).

correlation along the array. If it is highly correlated there will be little difference between the response of the square law detected array and the multiplicative one; if on the other hand the noise entering one arm of the multiplicative array is uncorrelated with the other, the multiplicative array will be relatively free of noise/noise terms in the output while the square law detecting one will have them. This same situation is true for receiver, or amplifier, noise if the outputs of the two arms are separately amplified before multiplication. With respect to bandwidth the noise/noise terms will cause a doubling of the noise bandwidth in the square law detecting array while the signal/noise terms will have the original noise bandwidth widened only by the signal bandwidth.

The optimum filtering to be used depends, of course, upon the relative power levels and spectral shapes of the various signal and noise terms in the output. If the receiver noise terms are significant, the multiplicative array usually has smaller output noise power and a smaller output noise bandwidth than the corresponding square law array. It is certainly true that the optimum post-multiplier or post-detector filter bandwidth is a function of the signal/noise ratio. Indeed, not only the filter bandwidth but also the attenuation characteristic for all frequencies is a function of the signal/noise ratio, and the types and sources of noise. The optimum filtering depends upon what optimization criterion is used. For example, if it is desired to maximize the average signal/noise ratio, a very narrow filter centered on the peak of the signal spectrum is often optimum. On the other hand, if the shape of the signal is of importance, then a wider filter is used, very often one whose width is determined by the cross-over of the signal spectrum and the noise spectrum, that is, that frequency at which the two spectral densities are the same.

In most cases the output signal/noise ratio of square law detecting linear array is higher than that of a multiplicative array, but it is due to the reduced aperture size of each of the two parts of the overall array which are multiplied. The true linear or coherently detecting system is, of course, the optimum demodulation system, and wherever applicable is superior to the non-linear ones.

Mr. P. M. Woodward: Could the authors help me to understand the 'magic' of multiplicative arrays by interpreting them in terms of a conventional antenna, such as a paraboloid which performs a linear integration over its aperture? Consider, for example, a sky containing a number of sources all radiating on the same frequency. These sources will give rise to a distribution of field over the receiving aperture, determined completely in terms of amplitude and phase. This distribution, over the finite aperture, can be equally well described by its Fourier series components, with no loss of information. These components can be measured directly by pointing an ordinary (uniformly illuminated) antenna successively in the 'sample directions' which correspond to the Fourier terms. With a coherent detector, or more strictly a pair of detectors in quadrature, we have now obtained a sequence of complex voltages without loss of information. To what further processing does the multiplicative array correspond? Is some interpretation along these lines possible?

Dr. Davies (*in reply*): The technique described by Mr. Woodward gives the Fourier components of the field in each sample direction, but the problem arises of how to demodulate the output since there will be several sources within one beamwidth in each direction, and each will have a different phase. The form of demodulation of an array is a parameter that can be varied in order to optimize some suitable criterion, such as a least squares error fit to the far field signal strength. It is important to consider the effect of the demodulation upon the directional pattern; for example, a least squares error interpolation of the far field sources may be obtained from pointing an array with a $(\sin x)/x$ response in the appropriate directions, but the response of a linear array with 'linear law diode' rectification is $|(\sin x)/x|$ which will not give the same results.

Dr. Ksienski (*in reply*): Multiplicative arrays do not carry more information than additive arrays but they are more effective in extracting from the incoming signal angle of arrival information. Another well-known example of improved information extraction is the (monopulse) difference pattern which combined with the *a priori* information that a single target is present locates the target with substantially higher accuracy than can be obtained by observing a p.p.i. display. In fact the direct display of the output of an additive array and its examination by an observer is far from being an optimum way for extracting the information available in the phase and amplitude distribution over the receiving aperture.

The multiplicative process is not necessarily optimum either, but it utilizes more effectively the phase across the aperture (which carries angle of arrival information). Compare, for example, the output resulting from the addition of two (isotropic) elements in an array to that of the output of a product of these two elements. The product output will result in an expression whose amplitude will vary twice as fast with the observation angle as the sum will. In the general case of multiplicative arrays the output will thus be more sensitive to angular information than the additive array but will, of course, have other problems as discussed in the papers presented.

Mr. M. J. Withers: In a practical radar case, where a linear array output is multiplied by output of omni-aerial, the transmitter directivity pattern will affect the performance of the system. In fact the two-way system directivity should be considered for comparison purposes. Also the directivity transmission pattern helps to reduce the 'capture effect' of strong target returns within close proximity of a weak target.

Mr. Blommendaal (*in reply*): In considering the two-way pattern of a radar system, it should be noted that the receiving pattern, which as a rule has the smaller beamwidth in a multiplicative system, has a dominant role. The nulls will determine the nulls in the two-way pattern. If, for instance, a uniform array with a $(\sin x)/x$ pattern is used for transmitting, and a $(\sin 2x)/2x$ multiplicative receiving system is used for receiving, then the two-way response, $(\sin x)/x \,.\, (\sin 2x)/2x$, corresponds to a linear array system with beamwidth $\Delta x_{3dB} = 0{\cdot}67$. This is closer to the receiving beamwidth ($\Delta x_r = 0{\cdot}69$) than to

the transmitting beamwidth ($\Delta x_t = 1 \cdot 39$). These beamwidths are compared with that of a two-way pattern of $(\sin x/x)^2$ taken as $\Delta x_t = 1$.

Dr. D. C. Cooper: In answering an earlier question, Dr. Ksienski mentioned some work on resolution in multiplicative systems when noise was assumed present. Could he offer more information about the methods used in this work? Were Monte Carlo techniques used?

Dr. Ksienski (*in reply*): The signal/noise ratio at the output of multiplicative arrays were compared to that of a square law detected linear array. The input was assumed to consist of two signals corresponding to the returns of two targets and each one of the signals was assumed to be independently corrupted by noise. The resolution was then compared of the two systems as a function of input signal/noise ratios and target separation. Monte Carlo techniques were not employed. The computation was performed analytically and the results plotted for comparison.

Dr. B. S. McCartney: Would the authors please comment on the following. Since in many sonar and radar applications the target density is independent of range there is a great likelihood of two targets being within a pulse length in range and a beamwidth in angle at long ranges, where the signal/noise ratio is also likely to be poorer. The signal/noise ratio is therefore of greater significance and the improved resolution of a multiplicative system may not be significant if the signal/noise ratio is deteriorated below threshold.

Dr. Davies (*in reply*): I quite agree with this point but I would also add that there are several practical radar situations in which it would be very attractive to obtain improved resolution at the expense of some signal/noise ratio. Two such examples are probably airfield surface movement radars and harbour radars as mentioned by Mr. Blommendaal.

Mr. Shaw and I are at present concerned with some analysis of the effect of noise on multiplicative signal processing which is not described in the paper. In assessing the loss of range performance due to this processing, the effect of the change in r.m.s. signal/noise ratio after multiplication is not a good criterion. The correct comparison involves comparing the different input signal/noise ratios to the multiplier and detector which maintain the same output probability of detection. The initial results of these studies seem to indicate that the multiplicative system is less than 1 dB worse off for low false alarm rates.

We have also made some experimental measurements of the effect of resolution in the presence of noise and although the results are not yet fully analysed it appears that the multiplicative system gives superior resolution even at low signal/noise ratios.

Dr. G. O. Young: There is a signal/noise ratio above which the product array is better and below which the linear array is better. A self-adaptive array could be used which adjusts to the signal/noise ratio so that whichever is better can always be used.

STANDARD FREQUENCY TRANSMISSIONS

(Communication from the National Physical Laboratory)

Deviations, in parts in 10^{10}, from nominal frequency for December 1964

December 1964	GBR 16kc/s 24-hour mean centred on 0300 U.T.	MSF 60 kc/s 1430–1530 U.T.	Droitwich 200 kc/s 1000–1100 U.T.	December 1964	GBR 16 kc/s 24-hour mean centred on 0300 U.T.	MSF 60 kc/s 1430–1530 U.T.	Droitwich 200 kc/s 1000–1100 U.T.
1	− 151·1	− 152·5	+ 5	17	− 151·1	− 151·3	− 5
2	− 150·6	− 150·2	—	18	− 150·2	− 149·9	− 5
3	− 150·9	− 150·9	+ 6	19	− 151·3	− 150·7	− 4
4	− 150·3	− 151·0	+ 8	20	− 150·9	− 149·9	− 3
5	− 149·8	− 150·0	+ 9	21	− 151·0	− 151·0	− 3
6	− 150·6	− 151·0	+ 8	22	− 150·3	− 150·5	− 3
7	− 150·9	− 150·3	− 8	23	− 149·8	− 149·7	− 4
8	− 150·7	− 149·6	− 8	24	− 150·1	− 151·7	—
9	− 150·9	− 151·6	− 8	25	− 150·9	− 150 0	—
10	− 151·4	− 150·8	− 9	26	− 150·4	− 148·6	+ 1
11	− 151·5	− 150·9	− 8	27	− 149·5	− 149·2	—
12	− 150·5	− 149·6	− 7	28	− 149·8	− 151·0	+ 2
13	− 149·6	− 148·5	− 6	29	− 150·8	− 150·1	+ 1
14	− 149·6	− 149·8	− 6	30	− 150·1	—	+ 3
15	− 149·5	− 150·1	− 6	31	− 150·3	− 150·0	+ 1
16	− 149·8	− 149·2	− 5				

Nominal frequency corresponds to a value of 9 192 631 770 c/s for the caesium F,m (4,0)–F,m (3,0) transition at zero field.

Notes: The phase of the GBR and MFS time signals will be retarded by 100 milliseconds at 00 00 U.T. on 1st January 1965.

The frequency offset for 1965 will be − 150 × 10⁻¹⁰

Multiplicative Processing Antenna Systems for Radar Applications

By

A. KSIENSKI, Ph.D. †

Summary: Several non-linear antenna systems are investigated in detail and their responses compared. The response of these antennas is computed for two targets with the following parameter variations: (1) target angular separation varying from zero to one null-to-null beamwidth; (2) target correlation varying between zero and unity; (3) target relative phase varying between zero and 360 deg. The resulting data are presented in the form of resolution curves and pointing errors, where the pointing error is given by the angular deviation of the peaks of the antenna response from the actual target locations. The results indicate that non-linear processing improves resolution, defined as the ability to separate two closely-spaced targets, for all levels of correlation between the target returns. The amount of improvement beyond that of a linear array varies somewhat with the particular array configuration and, in general, depends on the sacrifice in gain, or signal/noise ratio.

The theoretical studies were accompanied by an experimental program which both confirmed the theoretical results and demonstrated the practical feasibility of non-linear processing antennas for radar applications.

1. Introduction

The advantage of non-linear (multiplicative) antenna systems in improving resolution has been demonstrated both theoretically and experimentally in radio astronomy[1-3] and acoustic applications.[4-7] The fact that the energy received from stars is both temporally and spatially random is largely responsible for both the successful use of these schemes as well as the relative ease with which the system may be analysed. In the case of acoustical applications, such as sonar, for example, the returns from various targets are relatively uncorrelated and often justify the assumption of uncorrelated targets as in radio astronomy. The extent to which this assumption is correct depends, of course, on many circumstances among which are the target characteristics (moving or stationary) the medium and its turbulence and the wavelength. Thus, it is possible to find situations where acoustic returns may be highly correlated. In the case of radar certain situations such as fast-moving airborne targets (aircraft, rockets, satellites) justify the assumption of relative lack of correlation between returns; on the other hand, many applications such as mapping or surveillance involve strongly

† Hughes Aircraft Company, Research and Development Division, Culver City, California.

correlated returns, in fact almost perfectly correlated ones. It is thus necessary to investigate the response of the non-linear antenna to partially correlated multiple target returns with the correlation coefficient varying between zero (complete lack of correlation) and unity (perfect correlation). As correlation between returns becomes significant, the effect of relative target phase plays a very important role. This, of course, is true for both linear and non-linear antennas. The material which appears in the literature to date regarding the response of non-linear arrays is restricted to the specific cases of a single target,[4, 7, 8] extended incoherent sources,[2, 3] multiple targets which are relatively uncorrelated,[5] and multiple coherent targets whose returns add in phase at the phase centre of the antenna.[9] It is thus necessary to extend the investigation to multiple coherent targets with arbitrary phase relationship, and partially coherent targets. Since in the case of non-linear antennas it is not possible to deduce the response of one type of antenna configuration from the response of another one, one must select for analysis antenna systems which are as close as possible to the actual systems expected to be used operationally.

Four antenna systems were investigated in detail and their responses compared. All four were of the single correlation type, i.e. where the signal undergoes

only a single non-linearity, since the amount of image distortion of multiple correlation arrays restricts their potential usefulness to relatively few applications. The particular choice of arrays was made in accordance with their expected improvement in resolving capabilities at the expense of reduced gain. The first array considered consists of a linear array whose output is multiplied by a single element whose location coincides with the end of the linear array. The performance of this array, which has the smallest gain for its aperture size, is compared to that of a linear array whose output is square law detected and which has the largest gain for its aperture size.† The next array examined is that consisting of a product of a linear array and an overlapping interferometer. The fourth array considered involves the product of two adjacent linear arrays of equal size. The various arrays considered trade increasing amounts of gain for corresponding (expected) improvements in resolution. The response of the above antennas was computed for two targets with the following parameter variations: (1) target angular separation varying from zero to one null-to-null beamwidth ($\theta \simeq 2\lambda/L$ where L is the aperture size, λ is the wavelength and θ the angular separation); (2) target correlation varying between zero and unity; (3) target relative phase varying between zero and 360 deg. The resulting data (computed and reduced by an IBM 7090 computer) are presented in the form of resolution curves and pointing errors, where the pointing error is given by the angular deviation of the peaks of the antenna response from the actual target location.

2. Comparison between a Product Array and a Square-law-detected Linear Array

The first antenna chosen for investigation consisted of a linear array whose output was multiplied by that of an omnidirectional element whose location was coincident with the end element of the linear array (see Fig. 1). The choice of this array configuration was based on the following considerations.

Of the various possible configurations for single product antennas, this is the only scheme which shows no distortion for coherent multiple and extended target distributions. This property is strictly true only for targets whose returns add in phase at the phase centre of the antenna, but it was expected that due to this characteristic the antenna would suffer less distortion on the average than other schemes for targets with arbitrary phase relationships.

The expression representing the output of the presently considered non-linear scheme is given by

$$I(x') = \int_{-1}^{1} \int_{-1}^{1} O(x)O(y) \frac{\sin A(x-x')}{A(x-x')} \times$$
$$\times \cos\left[-A(x-x')+\phi(x)-\phi(y)\right] dx\, dy \quad (1)$$

where $x' = \sin\theta'$ is the scan angle of the antenna, x and y are each representing $\sin\theta$ where θ is the observation angle, $O(x)$ and $O(y)$ are the amplitudes of the target distributions while $\phi(x)$ and $\phi(y)$ are their phases, and A is $2\pi d/\lambda$ where $2d$ is the length of the linear array. In the above monochromatic radiation is assumed. If it is assumed that $\phi(x) = \phi(y) = 0$

$$I(x') = \int_{-1}^{1} O(x) \frac{\sin 2A(x-x')}{2A(x-x')} dx \int_{-1}^{1} O(y)\, dy \quad ...(2)$$

and the output represents an image identical to the one that would have been obtained by a linear array of twice the physical size of the actual antenna. The response for other phase angles and object distribution has to be obtained for specified target conditions. The ability of the system to resolve two closely spaced targets with fixed but arbitrary phase and amplitude relationships is presently of interest. Assuming one target of unity strength and zero phase at the origin ($\sin\theta = 0$) and another target of strength C and phase ϕ at $\sin\theta = a$ we have‡

$$\int_{-1}^{1} \int_{-1}^{1} \left[\delta(x)+C\delta(x-a)\right]\left[\delta(y)+C\delta(y-a)\right] \times$$

$$\times \frac{\sin A(x-x')}{A(x-x')}\left[\cos -A(x-x')+\phi(x)-\phi(y)\right] dx\, dy$$

$$= \frac{\sin Ax'}{Ax'}\cos Ax' + C^2 \frac{\sin A(a-x')}{A(a-x')}\cos A(a-x') +$$

$$+ C \frac{\sin Ax'}{Ax'}\cos(+Ax'-\phi) +$$

$$+ C \frac{\sin A(a-x')}{A(a-x')}\cos\left[-A(a-x')+\phi\right] \quad ...(3)$$

where $\delta(x)$ is the Dirac delta function.

The first two terms of the right side of eqn. (3) represent the 'self terms' or the undistorted terms with beams corresponding to double the size of the linear array. The last two terms consist of the cross products which produce the distortion effects.

Examining the cross terms we see that they consist of two parts, one part given by

---

† The square law detected linear array may also be used as a comparison standard since many conventional radars employ this type of detection.

‡ This assumption does not limit the generality of the conclusions regarding the response of two targets since the absolute phase and amplitude of one of the two targets may be arbitrarily assumed.
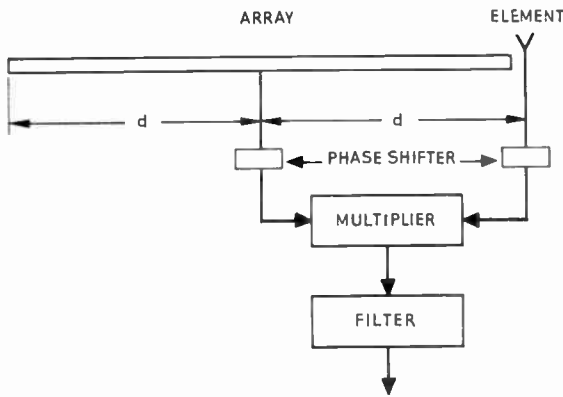
Fig. 1. Product array consisting of a linear array whose output is multiplied by that of an end element.

$$\alpha(x') = C\left[\frac{\sin Ax'}{Ax'}\cos Ax' + \right.$$
$$\left. + \frac{\sin A(a-x')}{A(a-x')}\cos A(a-x')\right]\cos\phi \quad ...(4)$$

which amplifies or attenuates the 'self terms' and

$$\beta(x') = C\left[\frac{\sin^2 Ax'}{Ax'} + \frac{\sin^2 A(a-x')}{A(a-x')}\right]\sin\phi \quad ......(5)$$

which causes distortion, that is shifts the peaks of the resultant pattern (i.e. boresight errors) and also affects resolution. It can be seen that the terms in the square

bracket of eqn. (5) vanish respectively at $x' = 0$ and $x' = a$ and build up towards the centre of the interval between the target locations. At this spot a dip is expected to occur in the antenna response indicating the presence of two targets. Now if ϕ is between zero and -180 deg, $\beta(x')$ will accentuate that dip, while for ϕ between zero and $+180$ deg the dip will be filled out. One can therefore expect an improvement in resolution for negative ϕ and a deterioration for positive ϕ. This can be seen in Fig. 2, where for $\phi = -45$ deg the resolution is improved, while for $\phi = +45$ deg the resolution deteriorates. It is clear therefore that the resolution in the case of closely spaced targets is dependent on their relative phase. This, however, is true not only for non-linear arrays but linear ones as well. Thus for two equal targets which are in phase with respect to the phase centre of the linear array the two targets will appear as one target for all separations below 2/3rds beamwidth. On the other hand, for two equal targets which are 180 deg out of phase the linear array will resolve them independently of their separation, although the indicated target locations will be in error and the amplitude of the peaks will approach zero as the targets approach each other (see Fig. 3).
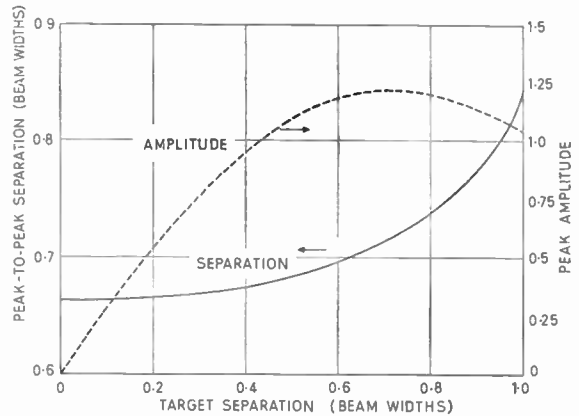

Fig. 3. Response characteristics of a linear array in the presence of two equal strength out of phase targets.

Fig. 2. Response of the non-linear antenna to two coherent equal strength targets separated 3 deg. (approx. 0·3 beamwidths) for various relative phases.

Relative phase: $+45$ deg. - - - -
0 ————
-45 deg. — · —

In these discussions two targets are considered to be resolved when the pattern gives a clear indication of the presence of two beams rather than one. The magnitude of the dip separating the beams is not very important since once a dip occurs a small increase in target separation will rapidly amplify the dip.

Figures 4 and 5 present the resolution curves for the product array depicted in Fig. 1 and a square-law-detected linear array respectively. The equation representing the averaged response of the product array to two targets of equal amplitude is given by
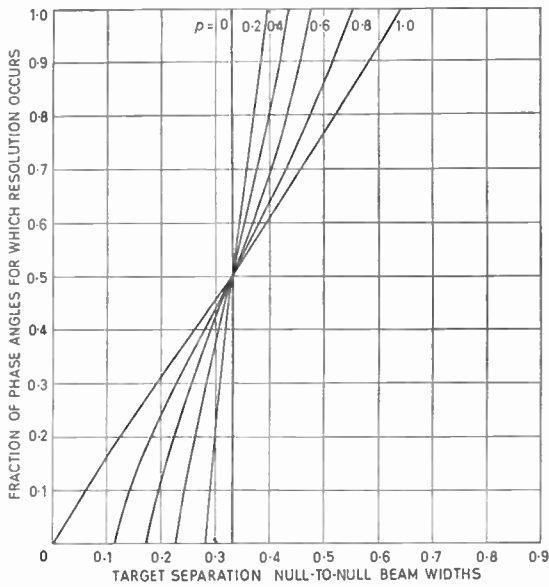
55

Fig. 4. Resolution of an antenna consisting of a product of a continuous aperture and a single end element; two equal amplitude targets. ρ is the correlation coefficient between the target returns.

$$I_1(x') = \frac{\sin Ax'}{Ax'}\cos Ax' + \frac{\sin A(a-x')}{A(a-x')}\cos A(a-x') +$$

$$+ \rho\left[\frac{\sin Ax'}{Ax'}\cos(+Ax'-\phi)\right] +$$

$$+ \rho\left\{\frac{\sin A(a-x')}{A(a-x')}\cos\left[-A(a-x')+\phi\right]\right\} \quad (6)$$

The response of the square law detected linear array is given by

$$I_2(x') = \left(\frac{\sin Ax'}{Ax'}\right)^2 + \left[\frac{\sin A(a-x')}{A(a-x')}\right]^2 +$$

$$+ 2\rho\frac{\sin Ax'}{Ax'}\frac{\sin A(a-x')}{A(a-x')}\cos\phi \quad (7)$$

where ρ denotes the correlation between the two targets and the other symbols are the same as eqn. (3).† In general target returns are neither perfectly correlated nor completely uncorrelated; also they are partially coherent, that is, they are neither monochromatic nor incoherent as in radio astronomy.

---

† In the statistical sense ρ is the normalized covariance between the cosine and sine components of the two target returns, $A_{1,2}\cos(t+\phi_{1,2})$. In the temporal sense, if the transmitted signal is, for example, amplitude modulated, ρ represents the time averaged product of the modulation envelope functions of the two returns. Note that in eqns. (6) and (7) ϕ is the mean phase difference between the returns. See Appendix for a more detailed discussion and derivation of the above equations.

Consequently, the relative phase angle cannot be ignored and has to be considered in conjunction with ρ.

This accounts for the rather complex response characteristics of the correlation antenna or for that matter the square-law-detected linear array. It is thus apparent that, although Figs. 4 and 5 represent the reduction of a very large number of data, they present nevertheless a relatively clear picture of the resolution characteristics of the systems considered under a large variety of conditions. Comparing Figs. 4 and 5, it is clear that the resolution of the product array is superior to that of the square-law-detected linear array for all correlation levels, although the improvement is only by about 20%. It should be remembered, however, that the comparison is made to a square-law-detected array whose resolution, for example, for uncorrelated returns is improved by 50% over a linear (coherently-detected or envelope-detected) array.

The question now arises as to the distortions produced by the two arrays considered. The present most relevant question is regarding pointing, or boresight errors, i.e. how much do the peaks of the antenna response deviate from the actual target (angular) locations. A detailed study of such errors for various target (angular) separations was carried out and is shown in Figs. 6 and 7. Since the study included small separation angles resolution did not occur for certain relative target phases. Accordingly, a fixed error is shown for all conditions (relative phase
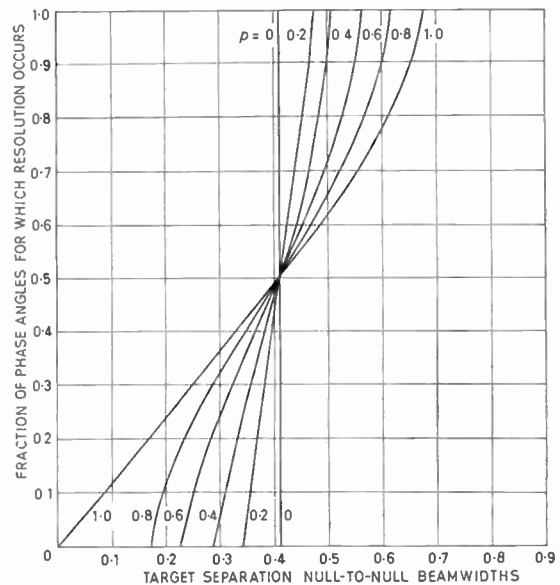

Fig. 5. Resolution of a square-law-detected linear array; two equal amplitude targets. ρ is the correlation coefficient between the target returns.
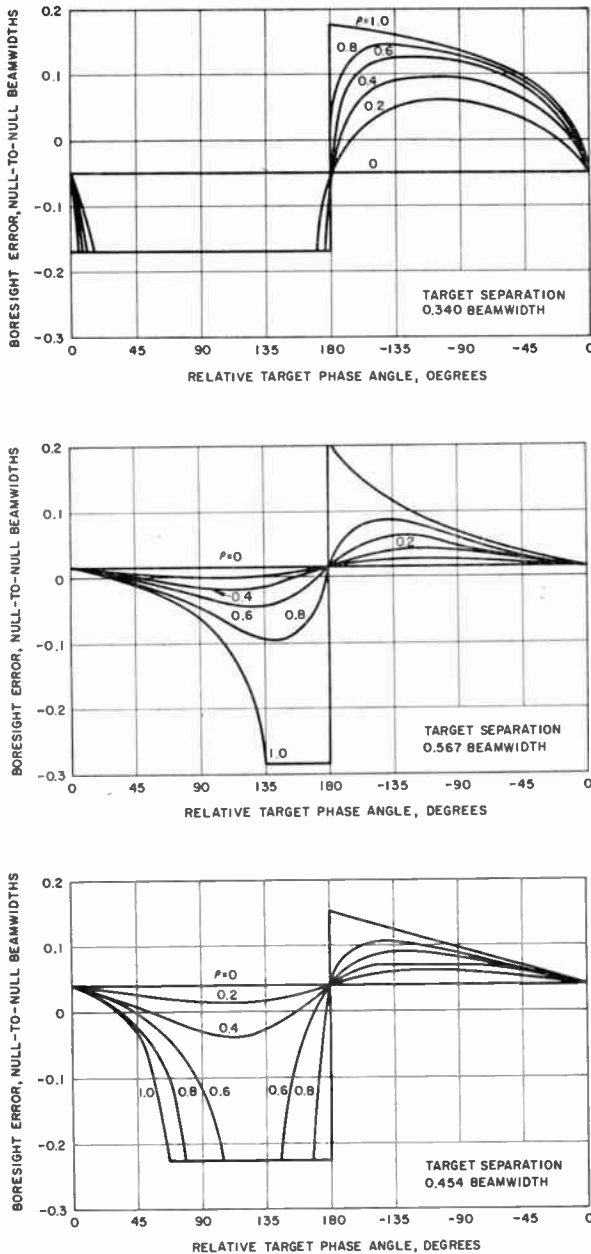
are not significantly different from the ones exhibited by the product arrays.

In fact, the errors of the square-law-detected linear array are larger on the average than these of the product array. This is due to the fact that the product array has better resolution as is evident from the comparison of the respective error curves for target separation of 0·340 beamwidths. This situation is, however, significantly changed as target separation increases. This is evident from Figs. 8 and 9. The errors of the square-law-detected linear array stay well within 0·10 beamwidth for all separations considered and may be safely assumed to be further decreased for larger target separations. On the other hand, the boresight errors of the product array for large angles of separation exhibit characteristics similar to those for small separation angles, at least for strongly correlated returns. One type of error is removed, the one due to lack of resolution, thus the

Fig. 6. Boresight errors of an antenna consisting of a product of a continuous aperture and a single end element; two equal amplitude targets. ρ is the correlation coefficient between the target returns.

and correlation) for which resolution did not occur. The pointing error was recorded as negative when target separation appeared to be smaller than the true separation, and positive when larger. Thus, when the two targets appeared as one a negative error is shown of magnitude one-half the target separation. The most interesting aspect of the curves in Figs. 6 and 7 is the fact that the errors for the linear array

Fig. 7. Boresight errors of a square-law-detected linear array; two equal amplitude targets. (Scanned about end element.) ρ is the correlation coefficient between target returns.
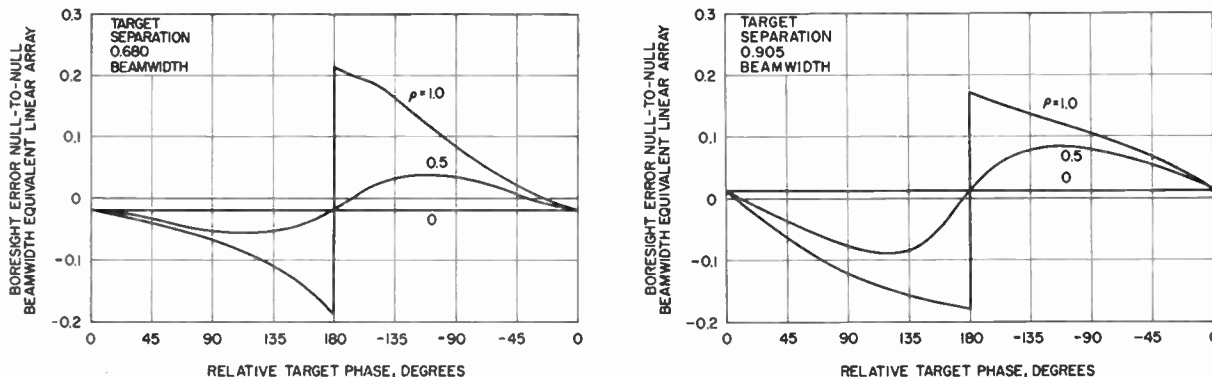
Fig. 8. Boresight error curves for linear array whose output is
multiplied by that of an end element. ρ is target correlation
coefficient. The two targets are of equal amplitude.

large negative error is missing. The positive errors
are of the same order of magnitude as for small
separation angles for $\rho = 1 \cdot 0$ and somewhat reduced
for $\rho = 0 \cdot 50$. The same behaviour may also be
expected for larger separation angles. This charac-
teristic is due to the fact that one of the two antennas
forming the product array is an isotropic element.
This lack of directivity affects the behaviour of the
cross terms which are the main contributors of bore-
sight errors for large angles of separation. This can
be seen by comparing eqns. (6) and (7). The (bore-
sight) error in locating the target at $x = 0$ is caused
by all the terms except the first in either of the two
equations. The second term (in both eqns. (6) and (7))
causes errors for small target separations, but as a
becomes comparable to π/A the contribution of this
term becomes secondary to that of the cross term.
And it is here that the difference becomes apparent
between eqns. (6) and (7). The effect of the cross
terms of the square-law-detected linear array decreases
as a increases, while for the product array one of the

cross terms is independent of a. The same pheno-
menon occurs, of course, at $x = a$. In order to ensure
that the cross terms decay for increasing target
separations it is thus essential that each one of the
antennas forming the product array be directive.
This would be essential, for example, if the array were
to operate in a multiple target environment where the
target returns are strongly correlated. A further
advantage of the use of directive elements is, of
course, an increase in gain and consequent improve-
ment in signal/noise ratio of the overall system, but
the compromise is some loss of resolution.

3. Response of a Product Array consisting of a Linear Array and an Overlapping Interferometer

In an attempt to improve the gain figure without
compromising the resolution characteristics it was
considered of interest to investigate a product array
consisting of a linear array whose output was multi-
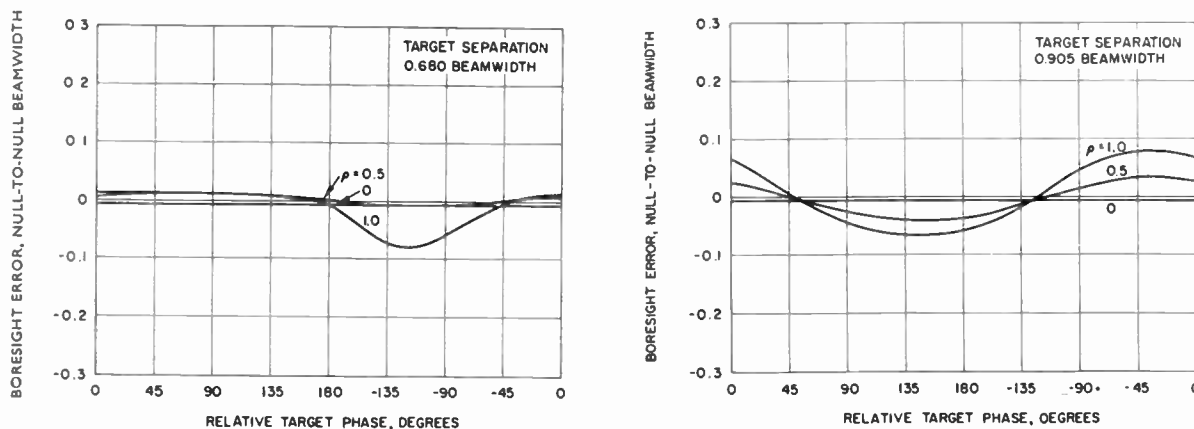plied by that of an overlapping interferometer (see

Fig. 9. Boresight errors of a square-law-detected linear array (scanned about end element); two equal amplitude targets. ρ is
the correlation coefficient between the target returns.

Fig. 10). This array has twice the gain of the previously considered linear array multiplied by an end element, and has the same resolution for uncorrelated targets.
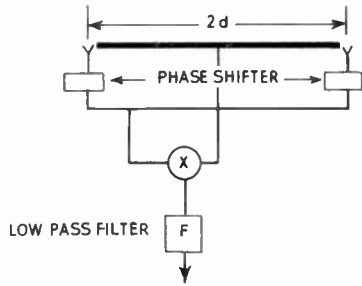

Fig. 10. Product array consisting of linear array multiplied by overlapping interferometer.

The averaged response of the array to two equal size targets is given by

$$I(x') = \frac{\sin Ax'}{Ax'} \cos Ax' + \frac{\sin A(a-x')}{A(a-x')} \cos A(a-x') +$$
$$+ \rho \cos \phi \left[\frac{\sin Ax'}{Ax'} \cos A(a-x') + \frac{\sin A(a-x')}{A(a-x')} \cos Ax' \right] \quad (8)$$

where $A = 2\pi d/\lambda$, $2d$ is the array length, $x' = \sin \theta'$ and θ' is the scan angle, ϕ is the relative target phase, one target is located at $\sin \theta = 0$ and the other at $\sin \theta = a$, both targets are of equal size, and ρ is the correlation coefficient between the returns.
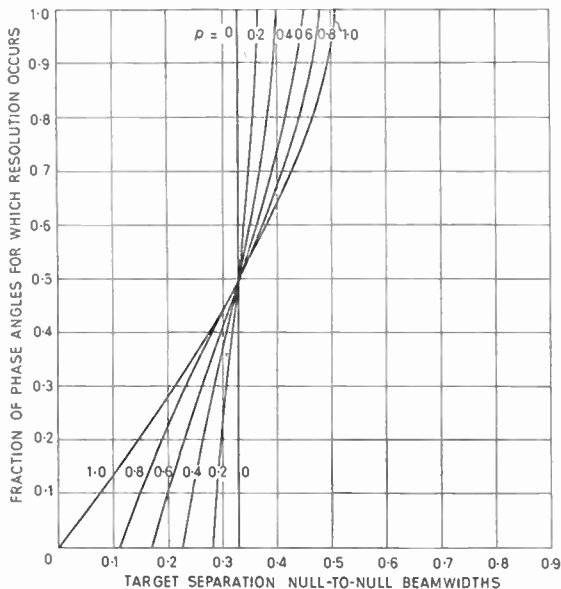
Fig. 11. Resolution of an antenna consisting of a product of a linear array and coincident interferometer; two equal amplitude targets.

This array has, as mentioned, a gain advantage over the formerly discussed linear array multiplied by an end element. It involves a little more equipment for implementation, and since its pattern is not isotropic will require scanning in synchronism with the linear array. But as seen from Fig. 11, its resolution characteristics are equal to or better than all
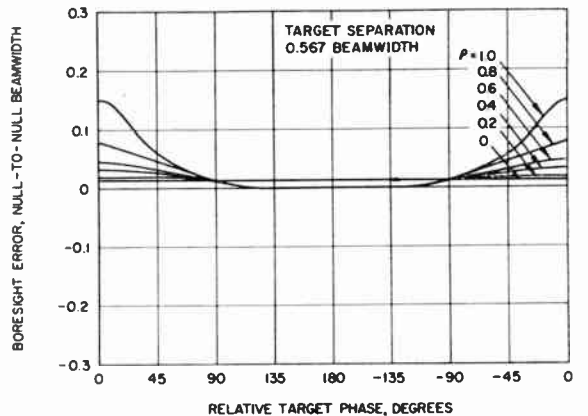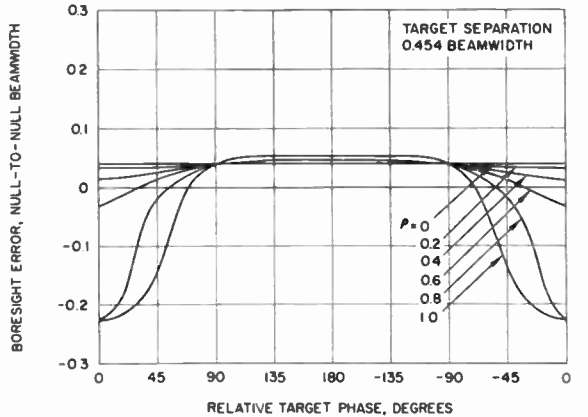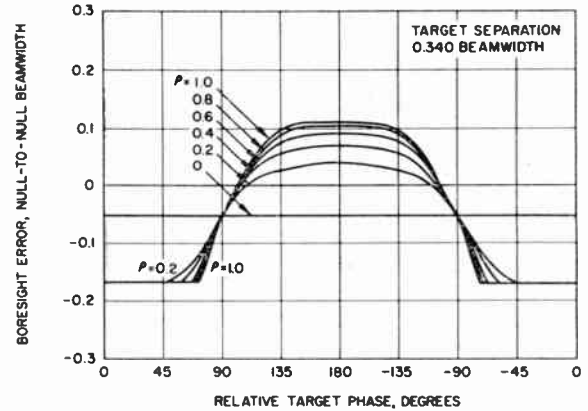

Fig. 12. Boresight errors of an antenna consisting of a product of a linear array and a coincident interferometer; two equal amplitude targets.
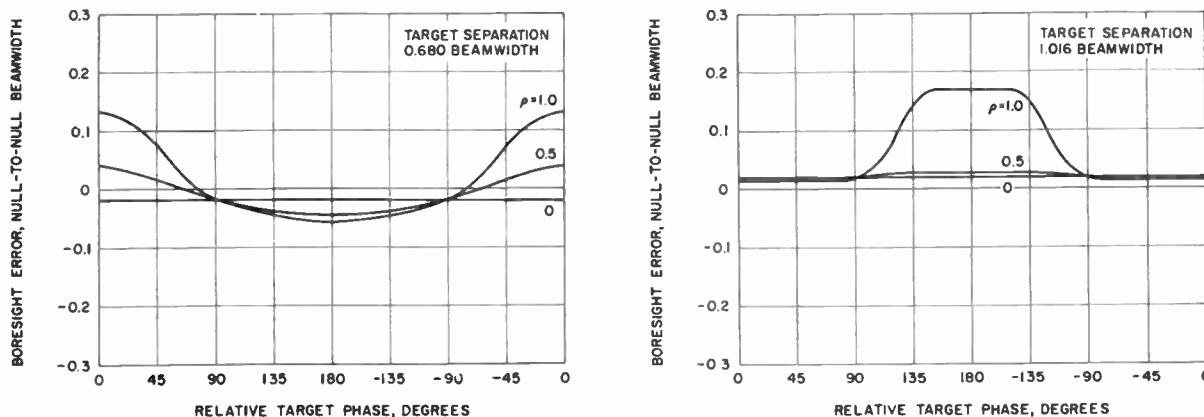
Fig. 13. Boresight errors of an antenna consisting of a product of a linear array and a coincident interferometer; two equal amplitude targets.

those previously considered. For $\rho = 0$ the resolution is, of course, identical to that of linear array times an end element, but for higher correlation levels it is superior to it. Also its boresight errors for small angles of separation are smaller, or at worst equal to other arrays previously discussed (see Fig. 12). For larger separation angles the boresight error behaves similarly to the previously considered product array (see Fig. 13) and for the same reason, i.e. lack of significant directivity. The increased directivity (beyond isotropic) reduces boresight error to a certain extent, but the presence of the spurious lobes of the interferometer does not contribute to the attenuation of the cross terms. This characteristic is also evident from the last term in eqn. (8).

From the above results (Figs. 6, 7 and 12) it appeared that boresight errors for small angles of separation were not affected significantly by a particular choice of the two component antennas forming a product. On the other hand, for larger angles of separation the boresight errors were significantly affected by the directivity of the component antennas. It thus became clear that a compromise between the resolution criterion on one hand and distortion and gain criteria on the other would be necessary if all three were to be taken into consideration. The next array considered was such a compromise between the above criteria.

4. Response of a Product Array consisting of Two Equal Sized Adjacent Linear Arrays

The last product array considered consisted of two adjacent linear arrays of equal size whose outputs were multiplied and averaged (see Fig. 14). The response of the array is given by the following equation:

$$I_4(x') = \left[\frac{\sin \frac{A}{2} x'}{\frac{A}{2} x'} \right]^2 \cos Ax' + \left[\frac{\sin \frac{A}{2}(a-x')}{\frac{A}{2}(a-x')} \right]^2 \times$$

$$\times \cos A(a-x') + 2\rho \frac{\sin \frac{A}{2} x' \sin \frac{A}{2}(a-x')}{\frac{A}{2} x' \quad \frac{A}{2}(a-x')} \times$$

$$\times \cos \left[A\left(\frac{a}{2} - x'\right) \right] \cos \phi \quad (9)$$

where the notation is the same as in the previous equations. The gain of this array is far higher than that of the first two product arrays considered, and is only 3 dB lower than the square-law-detected linear array. The resolution properties are shown in Fig. 15 and the boresight error for small and large angles of separation are presented in Figs. 16 and 17 respectively. The result of the directivity of both components is evident in eqn. (9) where the cross-term is suppressed as a function of target separation. The attenuation of the $\left(\frac{\sin x}{x}\right)$ factors in the cross terms
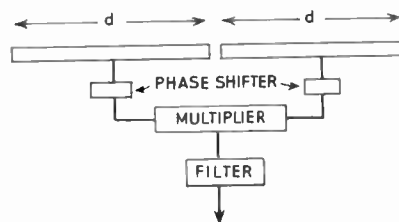

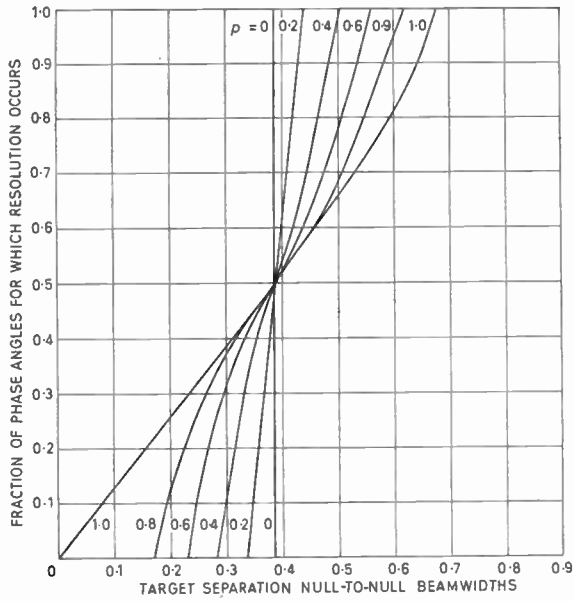Fig. 14. Non-linear array consisting of two equal adjacent linear arrays whose outputs are multiplied and averaged.

Fig. 15. Resolution of an antenna consisting of a product of two (equal) adjacent linear arrays; two equal amplitude targets. ρ is the correlation coefficient between the target returns.

is slower than that for the square-law-detected linear array, however the additional $\cos\left[A\left(\frac{a}{2}-x'\right)\right]$ factor contributes to reduce further the cross terms. The results are also clear from Fig. 17, where the boresight errors are becoming negligible for two targets a beamwidth apart, in fact they are smaller than the square-law-detected linear array. For small angles of separation the boresight errors are almost identical to the ones of the square-law-detected linear array. Regarding resolution, the characteristics of the present product array are only slightly inferior to the one consisting of a linear array multiplied by an end
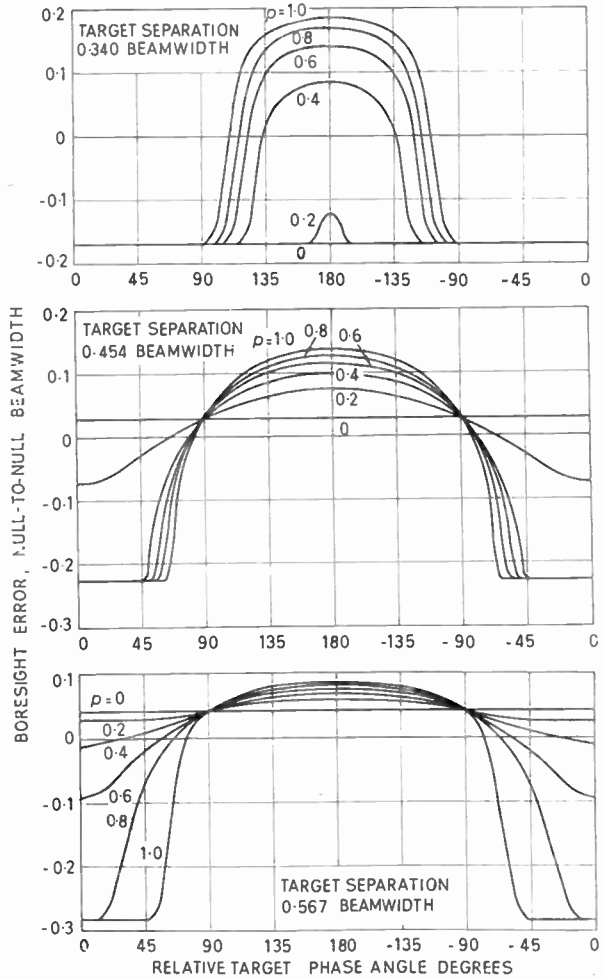

Fig. 16. Boresight errors of an antenna consisting of a product of two adjacent equal arrays; two equal amplitude targets. ρ is the correlation coefficient between the target returns.
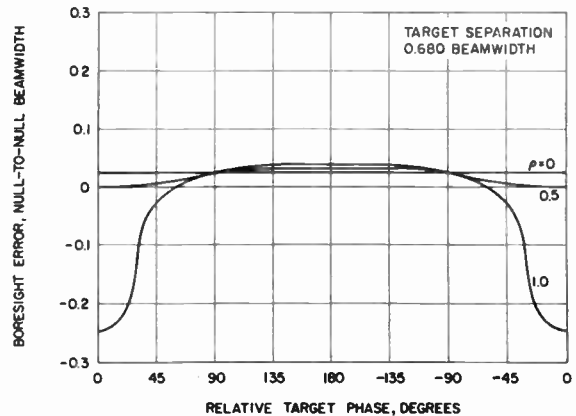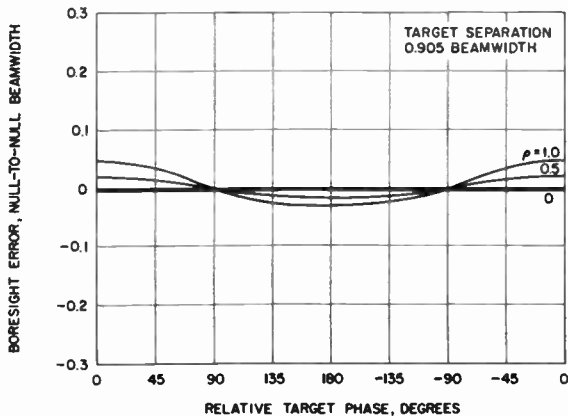

Fig. 17. Boresight errors of an antenna consisting of a product of two adjacent equal arrays; two equal amplitude targets. ρ is the correlation coefficient between the target returns.

element. For partially or perfectly correlated target returns, both the present array and the linear array multiplied by an end element are inferior to the product of a linear array and an overlapping interferometer (Fig. 11), while for totally uncorrelated returns they are all approximately equal.

5. Experimental Investigation

5.1. *Experimental Results*

As mentioned in the introduction, the purpose of the experimental programme was not only to verify the theoretical results but to test whether it is practically feasible to construct non-linear antenna systems by means of commercially available components. A product array was constructed and tested both for narrowband and wideband signals with results closely agreeing with theoretical predictions.

The specific array chosen for investigation consisted of a linear array whose output was multiplied by an isotropic end element and corresponded to the first array theoretically investigated (see Fig. 1). The

results, however, are indicative of the performance of any single correlation array.

In view of the importance of wideband signals on decorrelation of returns (see Appendix) the product antenna was operated with signal bandwidths varying between 0 and 18 Mc/s centred at 9·36 Gc/s. The results agreed quite well with computed curves (see Figs. 18–20). The particular relative target phase of 135 deg was chosen, since for this phase the cross terms have a very pronounced effect in the product array and the effect of bandwidth on the reduction of cross terms is easily seen. For a bandwidth of 18 Mc/s the returns indicated complete lack of correlation, with the relative phase having no effect at all on the response. (Several relative phases were tried with identical responses.) This bandwidth corresponds to less than 0·2% of the carrier. Note that the 0·2% bandwidth is a 3-dB bandwidth; thus, if a flat spectrum were used, decorrelation would occur for a smaller bandwidth. Also, one does not need complete decorrelation; in most cases when the correlation coefficient drops to its 3-dB point, the cross terms
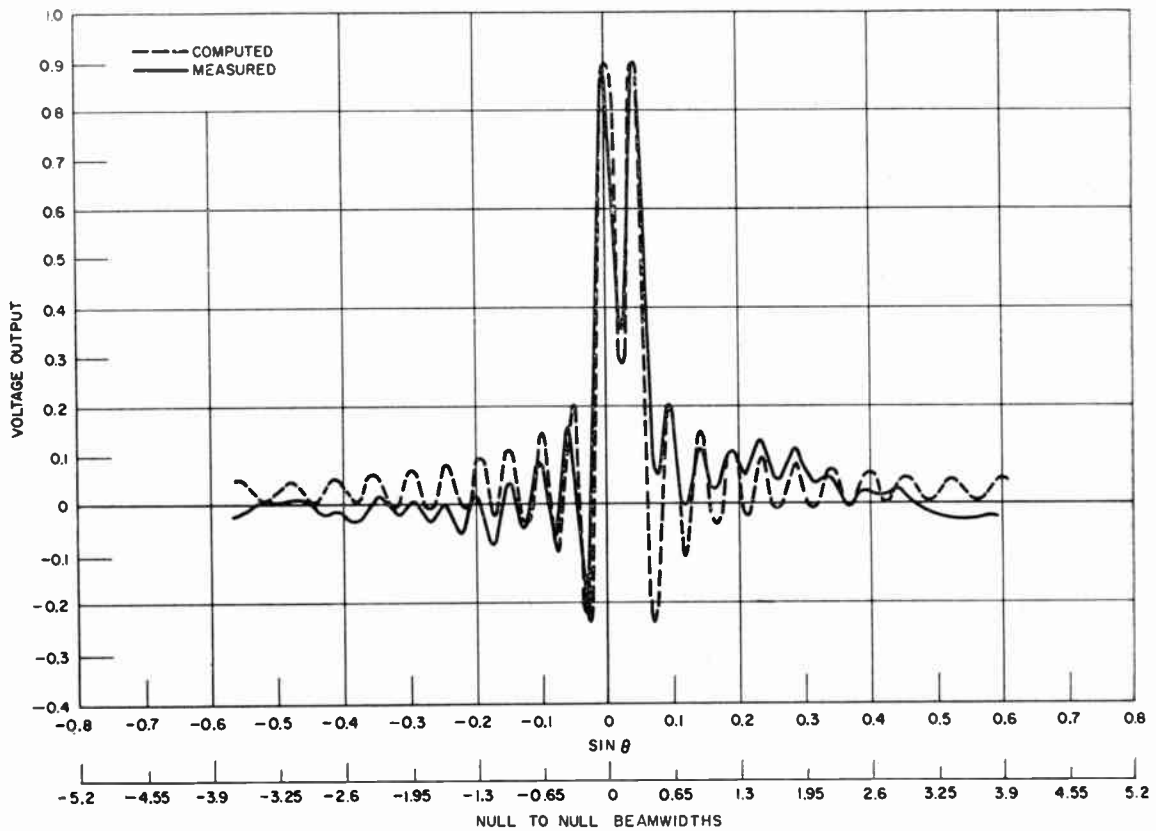

Fig. 18. Response of an antenna consisting of a product of a linear array times its end element. Target separation, 4 deg; relative strength, equal; relative phase, − 135 deg; correlation coefficient, 0, incoherent.
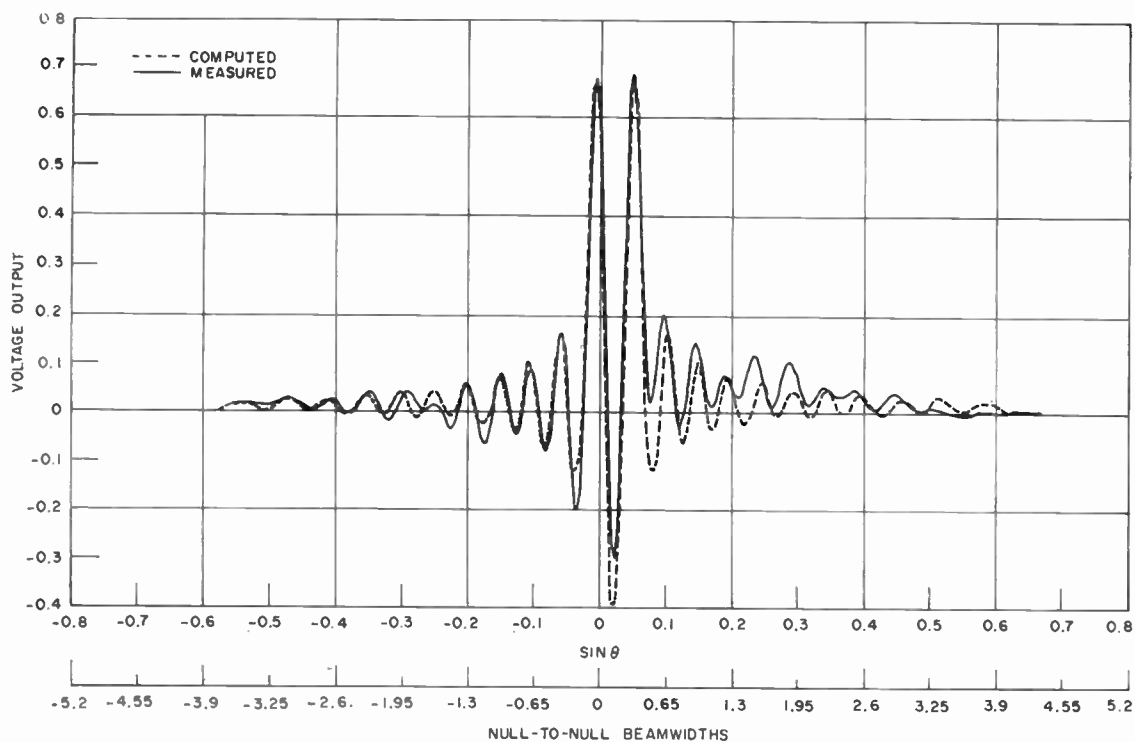
Fig. 19. Response of an antenna consisting of a product of a linear array times its end element. Target separation, 4 deg; relative strength, equal; relative phase, — 135 deg, correlation coefficient, 0·6.
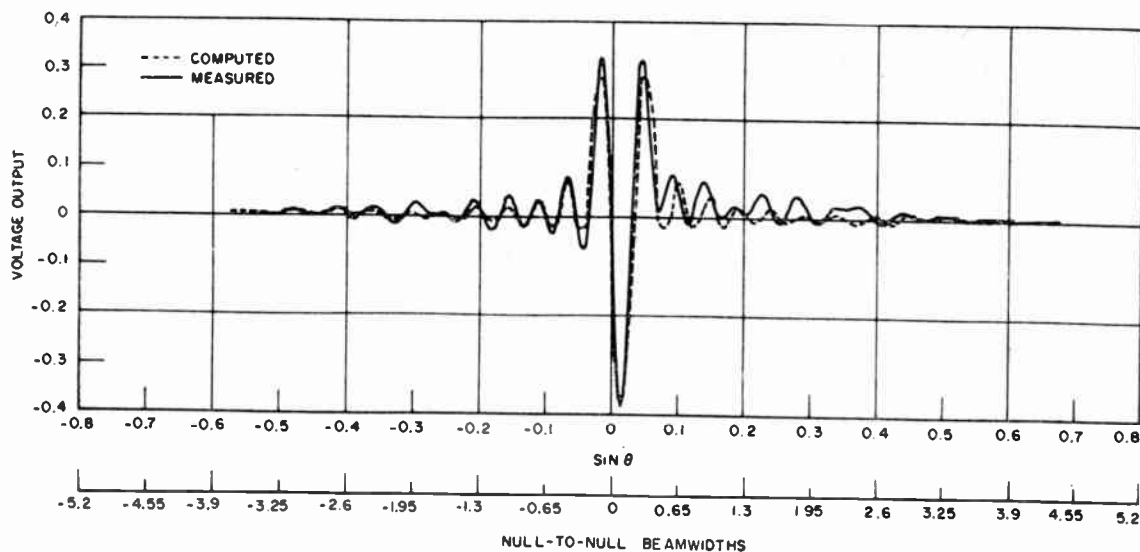

Fig. 20. Response of an antenna consisting of a product of a linear array times its end element. Target separation, 4 deg; relative strength, equal; relative phase, — 135 deg; correlation coefficient, 1, coherent.

are sufficiently attenuated to remove most of the distortion (see, for example, Fig. 19).

5.2. *Description of Equipment*

The correlation circuit used in the product array is described in Fig. 21. As can be seen, the multiplication of the two signals *A* and *B* is obtained by subtracting the squares of $(A+B)$ and $(A-B)$. The key element in this operation is the squaring device which is required to have an accurate square-law response over a wide dynamic range and have a flat frequency response over a wide band of frequencies. The square-law detector used in the above experiment satisfied the above requirements fairly well. It had good square-law response over a range from -60 to -10 dBm and a time-constant of 10^{-8} seconds. (The device is marketed by MSI under the name Bolomister Model B-160A.) The difference amplifier (Kintel Model 114A) had a bandwidth of approximately 100 c/s and thus also performed the function of a low-pass filter.

For the wide signal bandwidth experiment a random noise generator (General Radio 1390-A) was used to modulate the reflector of a klystron. Bandwidth control was achieved by controlling the amplitude of the modulating noise. This method produced satisfactory r.f. noise signals having (3 dB) bandwidths from zero to 18 Mc/s.

The experimental array used consisted of 19 end slots spaced one-half guide wavelengths apart and oriented end to end with every other one offset. The single element to be used for multiplying was mounted parallel to (above) the end (nineteenth) slot. This separate slot was two and one-half wavelengths removed from the axis of the array to reduce mutual coupling effects. Since patterns were taken in only the plane of the linear array normal to the axis of rotation this element produced the same effect as one superimposed on the end array element.

6. Conclusions

An investigation of the response of three product arrays and a square-law-detected linear array was carried out for both coherent and partially coherent targets. The results indicate that non-linear processing improves resolution, defined as the ability to separate two closely spaced targets, for all levels of correlation between the target returns. The amount of improvement beyond that of a linear array varies somewhat with the particular array configuration and, in general, depends on the sacrifice in gain, or signal/noise ratio. The magnitude of the pointing errors for closely spaced (less than half a beamwidth apart) and strongly correlated targets were found approximately the same for all antenna schemes considered. A very significant change in the amount of pointing error
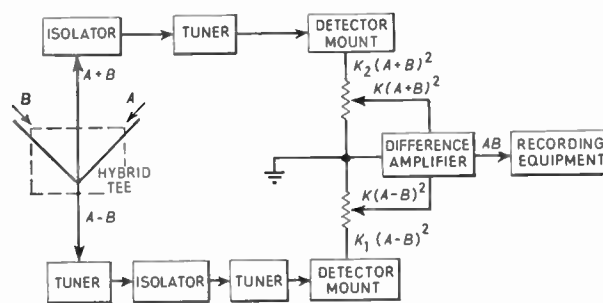

Fig. 21. Correlation circuit.

was found, however, between the various systems for large separation angles.

Here the gain, or directivity, of the individual antennas entering the product have a decisive effect. Thus, in the cases of the square-law-detected linear array and the array consisting of two adjacent linear arrays whose outputs are multiplied, the error rapidly decays with target separation to negligible magnitudes. The other two non-linear arrays considered exhibited pointing errors for large target separation angles that were of the same order of magnitude as for closely spaced targets. Such processing systems would, therefore, be unacceptable for an environment of multiple strongly correlated targets such as in ground mapping or surveillance radars. For such environments one should employ only directive elements to form the product array, although this will result in a relative loss of resolution.

The theoretical results were confirmed by experimental measurements which also provided a practical test of implementation difficulties with respect to both tolerance requirements and the commercial availability of components. The results indicate that one may implement the required processing with relative ease and good agreement with theoretical results.

7. Acknowledgments

8. References

1. B. Y. Mills and A. G. Little, "A high resolution aerial system of a new type", *Australian J. Phys.*, 6, p. 272, 1953.

2. A. E. Covington and N. W. Broten, "An interferometer for radio astronomy with a single-lobed radiation pattern", *I.R.E. Trans. on Antennas and Propagation*, AP-5, p. 247, 1957.

3. R. N. Bracewell, "Interferometry and spectral sensitivity island diagram", *I.R.E. Trans. on Antennas and Propagation*, AP-9, No. 1, p. 59, January 1961.

4. V. G. Welsby and D. G. Tucker, "Multiplicative receiving arrays", *J. Brit.I.R.E.*, 19, p. 369, June 1959.

5. V. G. Welsby, "Multiplicative receiving arrays: the angular resolution of targets in a sonar system with electronic scanning", *J. Brit.I.R.E.*, 22, pp. 5–12, July 1961.

6. M. Federici, "On the improvement of detection and precision capabilities of sonar systems", *J. Brit.I.R.E.*, 25, p. 535, June 1963.

7. A. Berman and C. S. Clay, "Theory of time-averaged product arrays", *J. Acoust. Soc. Amer.*, 29, p. 806, 1957.

8. C. J. Drane, Jr., "Phase-modulated Antennas", Air Force Cambridge Research Lab. Tech. Report No. AFCRC-TR-59-138 (AD215374), April 1959.

9. M. E. Pedinoff and A. A. Ksienski, "Multiple target response of data-processing antennas", *I.R.E. Trans. on Antennas and Propagation*, AP-10, No. 2, p. 112, March 1962.

9. Appendix

Derivation of the Response of a Correlation Array to Partially Correlated Target Returns

9.1. *Statistical Derivation*

Consider a correlation array consisting of two antennas whose gain functions are given by $G_1(x)$ and $G_2(x)$ ($x = \sin \theta$), respectively, and whose phase centres are displaced by distances D_1 and D_2 from the phase centre of the joint array. The output of the two antennas are passed through phase shifters (to provide for electronic scanning) and then multiplied and (low pass) filtered.

The response of the array (before filtering) to two point targets located at $x = x_1$ and $x = x_2$ is given by

$$I(x', t) = \{A_1 G_1(x_1 - x') \cos[\omega t + \phi_1 + D_1(x_1 - x')] + A_2 G_1(x_2 - x') \cos[\omega t + \phi_2 + \phi + D_1(x_2 - x')]\} \times$$
$$\times \{A_1 G_2(x_1 - x') \cos[\omega t + \phi_1 - D_2(x_1 - x')] + A_2 G_2(x_2 - x') \cos[\omega t + \phi_2 + \phi - D_2(x_2 - x')]\}$$

$$(10)$$

where $x' = \sin \theta'$ is the scan angle, ω is the signal frequency, ϕ_n are the phases and A_n the amplitudes of the targets and ϕ represents a fixed phase shift between the two targets due, for example, to a range difference. The correlation coefficient ρ is a measure of the correlation between $A_1 \cos \phi_1$ and $A_2 \cos \phi_2$ (or $A_1 \sin \phi_1$ and $A_2 \sin \phi_2$) where A_i assumes a Rayleigh distribution and ϕ_i is uniformly distributed over 2π. Considering the output after filtering, which rejects the double frequency terms, we obtain

$$I(x') = \frac{A_1^2}{2} G_1(x_1 - x')G_2(x_1 - x') \cos D(x_1 - x') + \frac{A_2^2}{2} G_1(x_2 - x')G_2(x_2 - x') \cos D(x_2 - x') +$$
$$+ \frac{A_1 A_2}{2} G_1(x_1 - x')G_2(x_2 - x') . \cos[\phi_1 - \phi_2 - \phi + D_1(x_1 - x') + D_2(x_2 - x')] +$$
$$+ \frac{A_1 A_2}{2} G_1(x_2 - x')G_2(x_1 - x') . \cos[\phi_2 - \phi_1 + \phi + D_1(x_2 - x') + D_2(x_1 - x')]$$

$$(11)$$

where $D_1 + D_2 = D$ the total distance between the phase centres of the two antennas. Each of the first two terms represents the autocorrelation of one of the two target returns and therefore do not involve ρ. It is the cross-product terms which depend on the correlation between the returns. Rewriting the first cross-product term (3rd term of eqn. (11)) we obtain

$$I_{c_1} = \frac{A_1 A_2}{2} G_1(x_1 - x')G_2(x_2 - x') \{\cos(\phi_1 - \phi_2) \cos[D_1(x_1 - x') + D_2(x_2 - x') - \phi] -$$
$$- \sin(\phi_1 - \phi_2) \sin[D_1(x_1 - x') + D_2(x_2 - x') - \phi]\}$$
$$= \frac{A_1 A_2}{2} G_1(x_1 - x')G_2(x_2 - x') \{(\cos \phi_1 \cos \phi_2 + \sin \phi_1 \sin \phi_2) . \cos[D_1(x_1 - x') + D_2(x_2 - x') - \phi] -$$
$$- (\sin \phi_1 \cos \phi_2 - \sin \phi_2 \cos \phi_1) . \sin[D_1(x_1 - x') + D_2(x_2 - x') - \phi]\}$$
$$= \frac{1}{2} G_1(x_1 - x')G_2(x_2 - x') \{(u_1 u_2 + v_1 v_2) \cos[D_1(x_1 - x') + D_2(x_2 - x') - \phi] -$$
$$- (u_1 v_2 - u_2 v_1) \sin[D_1(x_1 - x') + D_2(x_2 - x') - \phi]\}$$

$$(12)$$

where

$$u_1 = A_1 \cos \phi_1; \qquad u_2 = A_2 \cos \phi_2$$
$$v_1 = A_1 \sin \phi_1; \qquad v_2 = A_2 \sin \phi_2$$

Making the reasonable assumption that the probability distribution of the target amplitudes is Rayleigh and of the target phases is uniform over 2π, and that the amplitudes and phases are statistically independent, the variables u and v are Gaussian with mean zero and u_i independent of $v_j (i, j = 1, 2)$. u_1 and u_2 are the 'x' components of the returned field vectors from targets 1 and 2, respectively, and in general they are correlated with correlation coefficient ρ. Likewise, the 'y' components v_1, and v_2 are correlated with coefficient ρ, and have identically the same joint distribution as u_1 and u_2.

The total ensemble averaged† output of the array is given by

$$\overline{I(x_1')} = \frac{\overline{A_1^2}}{2} G_1(x_1 - x') G_2(x_1 - x') + \frac{\overline{A_2^2}}{2} G_1(x_2 - x') G_2(x_2 - x') +$$
$$+ \tfrac{1}{2} G_1(x_1 - x') G_2(x_2 - x') \{ \overline{(u_1 u_2 + v_1 v_2)} \cos [D_1(x_1 - x') + D_2(x_2 - x') - \phi] -$$
$$- \overline{(u_1 v_2 - u_2 v_1)} \sin [D_1(x_1 - x') + D_2(x_2 - x') - \phi] \} +$$
$$+ \tfrac{1}{2} G_1(x_2 - x') G_2(x_1 - x') \{ \overline{(u_1 u_2 + v_1 v_2)} \cos [D_1(x_2 - x') + D_2(x_1 - x') + \phi] -$$
$$- \overline{(u_1 v_2 - u_2 v_1)} \sin [D_1(x_2 - x') + D_2(x_1 - x') + \phi] \}$$

(13)

where the bar denotes ensemble average. But

$$\overline{u_i} = \overline{v_i} = 0 \qquad \sigma_{u_i}^2 = \sigma_{v_i}^2 = \sigma^2 = \overline{A_i^2} \, \overline{\cos^2 \phi_i} = \overline{A_i^2 \sin^2 \phi_i} = \frac{\overline{A_i^2}}{2} \qquad \overline{u_1 u_2} = \overline{v_1 v_2} = \rho \sigma^2 \quad (14)$$

Normalizing σ to 1 for convenience and using the above relationships we obtain

$$\overline{I(x')} = G_1(x_1 - x') G_2(x_1 - x') \cos D(x_1 - x') + G_1(x_2 - x') G_2(x_2 - x') \cos D(x_2 - x') +$$
$$+ \rho \{ G_1(x_1 - x') G_2(x_2 - x') \cos [D_1(x_1 - x') + D_2(x_2 - x') - \phi]$$
$$G_1(x_2 - x') G_2(x_1 - x') \cos [D_1(x_2 - x') + D_2(x_1 - x') + \phi] \}$$

(15)

from which the various response equations used in the text can be obtained by proper substitutions.

9.2. Time Averaging of Polychromatic Signals

Employing the same antennae as above the response to two targets reflecting a transmitted signal $S(t)$ of as yet unspecified waveform is given by

$$\mathscr{S}_1(t, x') = \int_{-1}^{1} dx \, G_1(x - x') \left[A_1 S \left(t - \frac{r_1}{c} + \frac{D_1}{2c} x \right) \delta(x - x_1) + A_2 S \left(t - \frac{r_2}{c} + \frac{D_1}{2c} x \right) \delta(x - x_2) \right]$$

$$= A_1 G_1(x_1 - x') S \left(t - \frac{r_1}{c} + \frac{D_1}{2c} x_1 \right) + A_2 G_1(x_2 - x') S \left(t - \frac{r_2}{c} + \frac{D_1}{2c} x_2 \right) \qquad \ldots\ldots(16)$$

$$\mathscr{S}_2(t, x') = \int_{-1}^{1} dx \, G_2(x - x') \left[A_1 S \left(t - \frac{r_2}{c} - \frac{D_2}{2c} x \right) \delta(x - x_1) + A_2 S \left(t - \frac{r_2}{c} - \frac{D_2}{2c} x \right) \delta(x - x_2) \right]$$

$$= A_1 G_2(x_1 - x') S \left(t - \frac{r_1}{c} - \frac{D_2}{2c} x_1 \right) + A_2 G_2(x_2 - x') S \left(t - \frac{r_2}{c} - \frac{D_2}{2c} x_2 \right) \qquad \ldots\ldots(17)$$

The signals given by eqns. (16) and (17) are then passed through delay lines multiplied and passed through a low pass filter, the output is given by

---

† The ensemble average may be well approximated by time averaging if sufficient integration time is permitted and, of course, if ϕ_n are time functions caused, for example, by scintillation. An explicit derivation for broad band signals where time averaging is used is given in Sect. 9.2 of the Appendix.

$$I(x') \simeq A_1^2 G_1(x_1 - x')G_2(x_1 - x')R_{ss}\left[\frac{D(x_1 - x')}{c}\right] +$$

$$+ A_2^2 G_1(x_2 - x')G_2(x_2 - x')R_{ss}\left[\frac{D(x_2 - x')}{c}\right] +$$

$$+ A_1 A_2 G_1(x_1 - x')G_2(x_2 - x')R_{ss}\left[\frac{D_1 x_1 + D_2 x_2 - 2Dx'}{2c} + \frac{(r_2 - r_1)}{c}\right] +$$

$$+ A_2 A_1 G_1(x_2 - x')G_2(x_1 - x')R_{ss}\left[\frac{D_1 x_2 + D_2 x_1 - 2Dx'}{2c} + \frac{(r_1 - r_2)}{c}\right] \quad (18)$$

where $D = D_1 + D_2$ and where the output of the filter (for an input $S(t)S(t-\tau)$) was approximated by the autocorrelation function of $S(t)$ for a delay τ, $R_{ss}(\tau)$. This approximation will be good if the time constant of the filter is large compared to one inverse bandwidth of $S(t)$. For example, for a signal of 100 Mc/s bandwidth a 100-kc/s filter should be adequate to provide a reasonable approximation to the autocorrelation function.

At this point we will restrict the analysis to amplitude modulated signals for illustrative purposes although, in general, such a restriction is not necessitated by physical considerations and in fact can be removed. For narrow band amplitude modulated signals, i.e. $P(t) \cos (\omega_0 t + \phi)$, the autocorrelation function can be written as follows (denoting time average by a wavy overscore):

$$R_{ss}(\tau) = \overline{P(t) \cos (\omega_0 t + \phi) P(t + \tau) \cos [\omega_0(t + \tau) + \phi]}$$

$$= \overline{\frac{P(t)P(t+\tau)}{2}} \cos \omega_0 \tau + \overline{\frac{P(t)P(t+\tau)}{2}} \cos (2\omega_0 t + \omega_0 \tau + 2\phi)$$

$$= \frac{R_{pp}(\tau)}{2} \cos \omega_0 \tau \qquad \qquad \ldots\ldots(19)$$

The second term on the right is zero because $P(t)$ is very slowly varying compared to $\cos (2\omega_0 t)$ (a consequence of the narrow band restriction) and because the cosine function has zero average value.

Introducing eqn. (19) into eqn. (18), and substituting $\lambda/2\pi$ for c/ω_0, the correlator output becomes:

$$I(x') \simeq \frac{A_1^2}{2} G_1(x_1 - x')G_2(x_1 - x') \cos \left[\frac{2\pi D(x_1 - x')}{\lambda}\right] R_{pp}\left(\frac{D(x_1 - x')}{c}\right) +$$

$$+ \frac{A_2^2}{2} G_1(x_2 - x')G_2(x_2 - x') \cos \left[\frac{2\pi D(x_2 - x')}{\lambda}\right] R_{pp}\left(\frac{D(x_2 - x')}{c}\right) +$$

$$+ \frac{A_1 A_2}{2} G_1(x_1 - x')G_2(x_2 - x') \cos \left\{\frac{2\pi}{\lambda}\left[\frac{(D_1 x_1 + D_2 x_2 - 2Dx')}{2} + (r_2 - r_1)\right]\right\} \times$$

$$\times R_{pp}\left(\frac{(D_1 x_1 + D_2 x_2 - 2Dx')}{2c} + \frac{(r_2 - r_1)}{c}\right) + \frac{A_2 A_1}{2} G_1(x_2 - x')G_2(x_1 - x') \times$$

$$\times \cos \left\{\frac{2\pi}{\lambda}\left[\frac{(D_1 x_2 + D_2 x_1 - 2Dx')}{2} + (r_2 - r_1)\right]\right\} R_{pp}\left(\frac{(D_1 x_2 + D_2 x_1 - 2Dx')}{2c} + \frac{(r_1 - r_2)}{c}\right) \quad \ldots(20)$$

Now $R_{pp}(\tau)$ being the result of an averaging process on $P(t)$, is also a slowly varying function compared to $\cos \omega_0 \tau$. Thus

$$R_{pp}\left(\frac{D(x_{1,2} - x')}{c}\right) \simeq 1$$

and

$$R_{pp}\left[\frac{D_{1,2} x_1 - D_{2,1} x_2 - 2Dx'}{2c} + \frac{(r_{1,2} - r_{2,1})}{c}\right] \simeq R_{pp}\left(\frac{r_2 - r_1}{c}\right) = \rho$$

i.e. the correlation coefficient between the returns of the two targets. It is interesting to note that the range difference $(r_2 - r_1)$ appears in both the cosine factor as well as the autocorrelation factor. Thus range differences of fractions of a wavelength can cause the cosine factors to reduce the cross terms by a significant amount. This effect reduces 'on the average' the cross terms by about 4 dB.

Radio Engineering Overseas . . .

The following abstracts are taken from Commonwealth, European and Asian journals received by the Institution's Library. Abstracts of papers published in American journals are not included because they are available in many other publications. Members who wish to consult any of the papers quoted should apply to the Librarian, giving full bibliographical details, i.e. title, author, journal and date, of the paper required. All papers are in the language of the country of origin of the journal unless otherwise stated. Translations cannot be supplied.

PULSE WIDTH MODULATION AMPLIFICATION

The general principles of d.c. and audio frequency amplification using width modulated pulses are discussed in a recent Australian paper. It is shown that by this method in which valves or transistors are operated as switches, it is possible to obtain high efficiency amplification with low distortion. The frequency spectra of the pulses are given and it is shown that there are limitations to the maximum modulation and pulse repetition frequencies that can be used in practice.

The currents in the switching elements, and the sources of loss and distortion are briefly analysed and it is shown that efficiencies in the region of 90% are obtainable. Applications of the method are to d.c. regulation and amplification, a.f. amplification, and the series modulation of r.f. amplifiers.

"High efficiency amplification using width modulated pulses", C. H. Miller. *Proceedings of The Institution of Radio and Electronics Engineers Australia,* **25,** pp. 314–23, May 1964.

PARAMETRIC FREQUENCY MULTIPLIERS

A German engineer has investigated the properties of parametric frequency multipliers which are driven by modulated signals. The considerations of this paper refer to amplitude modulation since frequency modulation and its derivatives are not affected by ideal frequency multipliers. Statements relating to the harmonic distortion factor and the intermodulation distortion factor are given for two possible modes of operation—controlled and fixed operating point. The results are to a large extent confirmed by practical results.

"The properties of parametric frequency multipliers which are driven by modulated signals", P. Birgels. *Nachrichtentechnische Zeitschrift,* **17,** No. 5, pp. 225–29, 1964.

MICROWAVE DISCRIMINATOR

A microwave discriminator which can be used in the demodulator of an 1800 channel microwave signal transmission system has been developed in Japan. The type of discriminator is called the path difference type. The principle of it is to use phase difference of a microwave signal which is divided and transmitted through long and short waveguide paths individually, and combined again before detection by crystal diodes.

Theoretical calculations and experimental results, including noise loading test, prove this type of discriminator to be satisfactory as a component of a microwave multi-channel transmission system.

"A path difference type microwave discriminator", Sadao Ito. *Review of the Electrical Communication Laboratory, NTT,* **12,** No. 1–2, pp. 191–206, March-April 1964.

TRANSISTOR TELEVISION RECEIVERS

The June 1964 issue of *L'Onde Electrique* includes the following group of papers:

"Video amplifier for transistorized television receiver", A. Sev (pp. 640–45).

"Vertical deflection circuits", R. Salvy (pp. 646–52).

"Transistorized circuits for horizontal deflection", M. Bovis (pp. 653–68).

"High power transistorized circuits for horizontal deflection", M. Guillaume (pp. 669–72).

"Development of an output transistor for a horizontal deflection circuit", J. Mercier (pp. 673–76).

"Technical requirements of transistorized u.h.f. tuners", A. Bensasson (pp. 677–84).

"Stabilization of a common-base u.h.f. transistor stage", A. Sev (pp. 685–88).

"Variations of the transition frequency f_1 as a function of the polarization current in a non-homogeneous base transistor", J. Mercier (pp. 689–93).

"Some comments on transistorized v.h.f. tuners", J. Martinon (pp. 694–700).

"A four transistor v.h.f. tuner", G. Nissen (pp. 701–03).

"Automatic gain control by simultaneous voltage/current variations", R. Roucaché (pp. 704–08).

L'Onde Electrique, **44,** No. 447, June 1964.

GENERATOR OF PULSES WITH FAST RISE-TIMES

Pulse generators with electron tubes can be synchronized to within nanoseconds, and rise-times of the current and voltage pulses of a few nanoseconds attained, if the tubes are run with the highest permitted pulse current. Starting from the quadripole theory of linear active quadripoles, a German paper investigates pulse-steepening with electron tubes. In designing pulse circuitry it is usually assumed that only a cascade of tubes in grounded-cathode configuration with high stage gain would be suitable for pulse steepening. This paper shows that pulse-steepening is possible with a cascade of several tubes in grounded-grid configuration, even when it provides no gain. With two-stage cascade of galvanically coupled tubes in grounded-grid configuration the 30 ns rise-time of the leading pulse edge that can be attained with a customary multivibrator can be reduced by up to 2 ns. The amplitude of the pulses is determined by the permissible cathode current of 800 mA of the tube chosen (E 182 CC). The pulse duration is merely limited by the permissible tube dissipation and may be up to 10 μs.

"A valve generator for producing pulses with very steep rise times", Gert Marte. *Archiv der Elektrischen Übertragung,* **18,** No. 4, pp. 211–18, April 1964.